This document is downloaded from DR-NTU (https://dr.ntu.edu.sg)
Nanyang Technological University, Singapore.

Critical flux behavior in pressure-driven and osmotic-pressure-driven membrane processes

Zou, Shan

2014

Zou, S. (2014). Critical flux behavior in pressure-driven and osmotic-pressure-driven membrane processes. Doctoral thesis, Nanyang Technological University, Singapore.

https://hdl.handle.net/10356/55370

https://doi.org/10.32657/10356/55370

Downloaded on 05 Apr 2024 13:27:28 SGT

CRITICAL FLUX BEHAVIOR IN PRESSURE/OSMOTIC -DRIVEN MEMBRANE PROCESSES ZOU SHAN 2014

NANYANG TECHNOLOGICAL UNIVERSITY

CRITICAL FLUX BEHAVIOR IN PRESSURE-DRIVEN AND OSMOTIC-PRESSURE-DRIVEN MEMBRANE PROCESSES

ZOU SHAN

SCHOOL OF CIVIL AND ENVIRONMENTAL ENGINEERING

NANYANG TECHNOLOGICAL UNIVERSITY

2014

CRITICAL FLUX BEHAVIOR IN PRESSURE-DRIVEN AND OSMOTIC-PRESSURE-DRIVEN MEMBRANE PROCESSES

ZOU SHAN

ZOU SHAN

School of Civil and Environmental Engineering

A thesis submitted to Nanyang Technological University
in partial fulfillment of the requirements for the degree of
Doctor of Philosophy

2014

Acknowledgements

I would like to gratefully and sincerely thank my advisor, Assistant Professor Tang Chuyang, for his invaluable guidance throughout my study, and my former supervisor, Associate Professor Chui Peng Cheong for offering me this cherish research opportunity. Assistant Prof. Tang, in particular gave his unwavering support and insightful supervision that enabled me complete the study. In addition to his excellent academic and professional background, he was so supportive, patient and understanding.

My special thanks to the group members, Wang Yining, She Qianhong, Gu Yangshuo, Gao Yiben, Xiao Dezhong, and late Wang Yichao.

Many thanks go to Qi Wei, Jiang Xia, Chen Soo Cheng, Loh Yee Wen, Karine Zheng Kaiyu, Loo Shu Zhen and Mr. She Qianhong, Kuang Shengli, Guo Chenghong, Wu Weiwei, for their kind help.

I also want to express my appreciation to the technicians in the environmental laboratory, especially to Mrs Phang-Tay Beng Choo, Mr Yong Fook Yew**,** and Mr Tan Han Khiang. Without their kind assistance, my work in the lab would be impossible.

I am very happy that School of Civil and Environmental Engineering, Nanyang Technological University and Environmental Engineering Research Centre to award me the research scholarship, which enable me to focus myself on the study and research.

My final acknowledgement is to my family, my wonderful parents, Zou Kangyong, Yu Guilian and my husband Wang Jianbin, for their constant support and motivation that has encouraged me all the way.

Abstract

Among the numerous topics related to membrane separation processes, flux performance study remains as the core and foundation of academic research as well as practical application. The current study focuses on the critical flux phenomena in pressure-driven (microfiltration (MF)) as well as in osmotically-driven membrane processes (forward osmosis (FO)).

For the MF system, two MF membranes (pore size of 0.1 μm and 0.2 μm, respectively) were applied to filter mixed liquor from conventional activated sludge as well as that from a membrane bioreactor (MBR). The critical flux behavior was studied by "pressure stepping "method and "pressure cycling" method under different test conditions. It was found that critical flux evaluation protocol could significantly affect the critical flux value, e.g., lower values were obtained for longer time interval used for the pressure stepping.

For the FO process for microalgae harvesting, the algae species Chlorella Sorokiniana was used in the feedwater in a cross flow mode FO system. The effect of physical parameters (flux level, membrane orientation, and cross flow) on FO fouling and flux behavior during algae separation were investigated. The impact of chemical parameters (feed water chemistry, draw solution chemistry) was explored by adding Mg^{2+} ions into the feed water and draw solution. The concept of critical flux was applied successfully in FO process. Moreover, a systematic study to investigate the effect of solute back diffusion, a unique phenomenon in FO process, on FO fouling revealed that the critical

flux can be drastically reduced as a result of the specific foulant-ion interaction induced by the diffusion of Mg^{2+} from the draw solution to the feed solution.

Depends on the semi-transparency feature of the flat-sheet FO membrane and the good visibility of algae cells through microscope, direct observation method was further applied to monitor algae deposition on FO membranes. Microscopic images were analyzed and characterized to show the process of fouling under various solution chemistry and operational conditions. The microscopic results were further compared to the flux behaviour to evaluate its potential as a critical flux determination method.

Table of contents

List of publications

Shan Zou, Yangshuo Gu, Dezhong Xiao, Chuyang Tang, 2011. "The role of physical and chemical parameters on forward osmosis membrane fouling during algae separation." Journal of Membrane Science **366**, 356-362

Shan Zou, Yi-Ning Wang, Filicia Wicaksana, Theingi Aung, Philip Chuen Yung Wong, Anthony G. Fane, Chuyang Y. Tang, 2013 "Direct Microscopic Observation of Forward Osmosis Membrane Fouling by Microalgae: Critical Flux and the Role of Operational Conditions." Journal of Membrane Science **436**, 174-185

List of figures

List of tables

List of symbols

Symbol	*Description*
A	Water permeability coefficient of the membrane
B	Solute permeability coefficient of the membrane
C_b	Concentration at bulk
C_{ds}	Solute concentration in draw solution
$C_{support}$	Solute concentration in the porous support layer
F_{drag}	Hydrodynamic drag force
$F_{barrier}$	Barrier force
$F_{barrier}^{f-m}$	$F_{barrier}$ resulting from foulant-membrane interaction
$F_{barrier}^{f-f}$	$F_{barrier}$ resulting from foulant-deposited-foulant interaction
J_{ci}	Critical flux caused by irreversible fouling
J_{cs}	Strong form critical flux
J_{cw}	Weak form critical flux
J_L	Limiting flux
J_c	Critical flux
Jci	Critical flux for irreversibility sustainable flux
J_{CS}	Strong from critical flux
J_{cw}	Weak form critical flux
J_o	Initial flux
J_m	Mixed liquor flux
J_s	Solute flux

Symbol	*Description*

J_{sus}	Sustainable flux
J_w	Secondary water flux
J_v	Water flux
L	Length of the MF module submerged in the liquor
m_c	Cake load/area of membrane
R_{ads}	Resistance caused by adsorption
R_c	Cake resistance
R_c	Resistance of concentration polarization
R_f	Resistance of membrane fouling
Rh	Characteristic hydrodynamic radius of humic acid molecules
R_{irrev}	Resistance of irreversible membrane fouling
R_m	Resistance of membrane material
R_{rev}	Resistance caused by reversible membrane fouling
ΔP	Applied pressure
Greek letters	
α	Specific cake resistance
β	Van Hoff's coefficient
$\Delta\pi$	Osmotic pressure difference across the active layer of membrane
μ	Solution viscosity
σ	Reflection coefficient

List of abbreviations

Abbreviation	*Description*
BOD	Biological oxygen demand
BSA	Bovine serum albumin
COD	Chemical oxygen demand
CFV	Cross-flow velocity
DS	Draw solution of the FO process
ECP	External concentration polarization
EPS	Extracellular polymeric substances
FO	Forward osmosis
FW	Feed water of the FO process
ICP	Internal concentration polarization
MBR	Membrane bioreactor
MF	Microfiltration
MLSS	Mixed liquor suspended solid concentration
NF	Nanofiltration
OD	Capillary outside diameter of the MF fiber
PS	Polysulfone
PVDF	Polyvinylidene fluoride
UF	Ultrafiltration
RO	Reverse osmosis
SRT	Sludge retention time
Abbreviation	*Description*
SS	Suspended solids

TOC	Total organic carbon
TMP	Transmembrane pressure
WERF	Water environment research foundation

Chapter 1 Introduction

1.1 Background

Over the last 40 years, membrane technology has been successfully applied in various industrial processes. Pressure-driven membrane processes such as microfiltration (MF), ultrafiltration (UF), nanofiltration (NF) and reverse osmosis (RO) are used for water treatment, reclamation, and desalination at different scales (Fane et al., 2011). There have also been significant developments in membrane-based separation for industrial applications, such as metal plating, paper and pulp, leather, oil refinery. In parallel, osmotically-driven forward osmosis (FO) has also been gaining increasing attention for its potential applications in water and wastewater treatment and desalination (Cath et al. 2006).

Membrane fouling, however, is still a formidable obstacle in membrane processes (Fane et al., 2006; Goosen et al., 2004; Tang et al., 2011). Fouling refers to the reduction in membrane permeability as a result of the foulants (such as inorganic scaling, colloids, organics, or biofilm) attachment to the membrane. This leads to reduced membrane productivity, increased energy consumption, and sometimes deteriorated product quality. One potential strategy to control fouling is operating the membrane below the critical flux (Bacchin et al. 2006).

The critical flux concept, which has been stated as a threshold flux below

which fouling is negligible and above which fouling tends to be severe, has been successfully applied to pressure-driven membranes processes (Bacchin et al. 2006). Nevertheless, there is an apparent need to standardize the protocol for critical flux measurement. Compared to pressure-driven membrane processes, the fouling behaviour of osmotically-driven FO process is much less understood (Cath et al. 2006). While the critical flux concept is presumably also applicable to FO, fouling in FO can be considerably more complicated compared to that in RO, UF or MF, which diverse further attention from membrane researchers (Mi and Elimelech 2008, Mi and Elimelech 2010, Tang et al., 2010).

1.2 Objectives and scope

The main objective of this research was to study the membrane fouling for both microfiltration and forward osmosis membranes. The microfiltration tests were performed in a bench-scale submerged system using mixed liquor from both conventional activated sludge process and that from a membrane bioreactor (MBR) system. The forward osmosis experiments were performed in a bench-scale cross flow FO setup using microalgae containing feed solutions. In both systems, the membrane fouling and the critical flux behaviour were studied. The specific aims of this research included:

1) To understand the effect of different testing conditions and experiment protocols on critical flux determination;

2) To explore FO fouling behavior during microcell (microalgae) harvesting and to demonstrate the existence of critical flux in FO;

3) To investigate the effect of solution chemistry as well as hydrodynamic conditions of FO operational system on FO fouling and the critical flux.

1.3 Thesis organization

This thesis contains six chapters and an appendix. Chapter 1, 2 and 6 presents the introduction, literature review and conclusions. The appendix shows a preliminary simulation of the MF flux performance. Chapter 4 has been accepted for publication in the Journal of Membrane Science, Chapter 3 and Chapter 5 have been submitted for potential publication. The contents each chapter are summarized briefly as shown below:

Chapter 1 provides an overview of the thesis. It discusses the importance of filtration flux behaviour study for both of the pressure-driven (MF) and osmotically-driven (FO) membranes to advanced fouling control understanding.

Chapter 2 briefly presents the current research status of membrane fouling study for MF and FO membrane respectively. Critical and limiting flux phenomenon as the newly developed threshold flux concept is described.

Chapter 3 presents the experimental details of MF filtration study and

discusses the effect of evaluation protocol on critical flux and limiting flux. Longer time interval or filtration history applied during determination would provide a lower critical flux value. This chapter also demonstrates the existence of limiting flux for MF filtration and discusses the conceptional mechanism behind it. The foulant-membrane interaction was believed to play a significant role in critical flux phenomenon, but limiting flux was most possibly contributed by foulant-foulant interaction.

Chapter 4 states the effect of hydrodynamic parameters (such as orientation, initial flux) and solution chemistry (pH and Mg^{2+}) on FO flux and microalgae fouling performance. Critical flux could be found for FO process as well, though its value depended strongly on the type of draw solution (DS). Active layer (AL)-facing-feed water (DS) orientation created more stable water flux but generated a much lower initial flux compared to AL-facing-DS orientation. $MgCl_2$ as DS induced a higher permeate water flux compared with using NaCl, but the existence of Mg^{2+} in FW or DS (salt back diffusion from DS to FW) deteriorated membrane fouling severely.

Chapter 5 discusses the effectiveness of microscopic observation in exploring membrane fouling and flux reduction phenomenon during algae harvesting by FO process using "osmosis stepping" method (increase DS concentration step by step). Critical flux was found to be applicable to FO process as well. The integrated analysis based on the microscopic images combined with flux data showed that the fouling resulted by particle deposition was prior to the organic fouling. The surface coverage analysis directly proved the deteriorative effect

of Mg^{2+} ions on algae fouling.

Chapter 2 Literature Review

2.1 Pressure-driven membrane processes

A membrane process separates a feed stream into a concentrate and a permeate fractions. Membrane processes can be classified based on their separation principles or mechanisms (Mulder, 1996). Pressure-driven membrane processes use a pressure difference between the feed and the permeate as the driving force to induce permeation of the solvent (e.g., water) through a semi-permeable membrane. Suspended particles and dissolved components are retained based on properties such as size, shape and charge (Fane et al., 2011; Mulder, 1996).

Pressure-driven membrane processes can be classified into microfiltration (MF), ultrafiltration (UF), nanofiltration (NF) and reverse osmosis (RO). As shown in Table 2.1 (Van Der Bruggen et al., 2003), these membrane processes distinguish with each other based on several criteria: the characteristic of the membrane (pore size), the operating pressure, the size and charge of the retained components.

MF and UF are usually applied for the removal of particulate and microbial contaminants and are frequently used as pretreatment for advanced NF and RO filtration. The pore size of NF membranes is typically about 1 nm. NF removes most of nature organic matter, viruses and a range of salts. It is often used to soften hard water. RO membranes have a nominal pore size less than 0.5 nm which enables the removal of monovalent ions. RO is mostly utilized for

extremely pure water production and desalination.

Table 2-1. Specifications of pressure driven membrane processes (Van Der Bruggen et al., 2003)

Membrane processes	Pore Size (nm)	Pressure (bars)	Rejection	Separation mechanism
Microfiltration (MF)	100 – 10,000	< 2	Particles	Sieving
Ultrafiltration (UF)	2 – 100	1 – 5	Multivalent ions; macromolecules; particles	Sieving
Nanofiltration (NF)	0.5 – 2	5 - 20	Multivalent ions; small organic compounds; macromolecules; particles	Sieving; charge effects
Reverse Osmosis (RO)	< 0.5	20 – 120	Monovalent ions; multivalent ions; small organic compounds; macromolecules; particles	Solution – Diffusion

With the growing academic interests and expanding industrial applications, researchers have achieved considerable improvements in this technology. For

instance, further development on membrane materials for higher selectivity and permeability (Belfort et al., 1994; Zeman and Zydney, 1996), efficient module design (Belfort et al., 1994; van der Waal and Racz, 1989; Zeman and Zydney, 1996) and several improvements in peripheral technologies (Belfort et al., 1994; van der Waal and Racz, 1989; Van Reis et al., 1997; Zeman and Zydney, 1996) have sparked widespread adoption of this process in chemical processing, environmental control, pharmaceutical and biomedical industrial applications.

2.1.1 Membrane material and structure

Conventional materials for MF are the poly-organic materials such as hydrophobic polyvinylidene fluoride (PVDF) and the hydrophilic polysulfone (PS) (Van Der Bruggen et al., 2003). PVDF membranes are typically applied in the wastewater pretreatment, oil/water separations surface water bacteria removal which is the best choice for very low pressure and high flux application. The PS membranes are usually used for ultrapure water post-treatment, suspended solids removal and process stream clarification such as sugar solutions purification. The inorganic ceramic materials are also utilized as they have superior chemical, thermal and mechanical stability. For the application requiring better resistance to high temperatures and corrosive environments, metallic membranes have been introduced as well and are expected to have a longer lifespan than others because of the robustness(Leiknes et al., 2004).

MF application development can be partly contributed by the invention of asymmetric membrane structure. It consists of a thin selective layer which

determines a high permeability and a thick supporting layer which provides sufficient mechanical strength (Mulder, 1991).

2.1.2 Microfiltration application in water treatment: Membrane Bioreactor (MBR)

Within the pressure-driven membranes, MF and UF membranes are considered as porous membranes and have relatively high water permeability. With a sieving mechanism, suspended solids, colloids and bacteria that are larger than the membrane pore size will be rejected. These membranes have been widely used in MBRs (Fane et al., 2011). MBR process is an integration of membrane filtration process and activated sludge bioreactor. By using micro- or ultrafiltration membrane technology, MBR systems combine membrane process with biodegradation, allowing a complete physical rejection of bacterial flocs and substantially all suspended solids within the bioreactor (Figure 2-1). Subsequently, the MBR systems have many advantages compared with conventional wastewater treatment processes. For instance, MBR could achieve higher mixed liquor volatile suspended solids (MLVSS) concentration, longer sludge age, and thus smaller footprint and reactor requirements, better disinfection capability, higher effluent quality, less sludge production and higher volumetric loading (Judd, 2006; Judd, 2004).

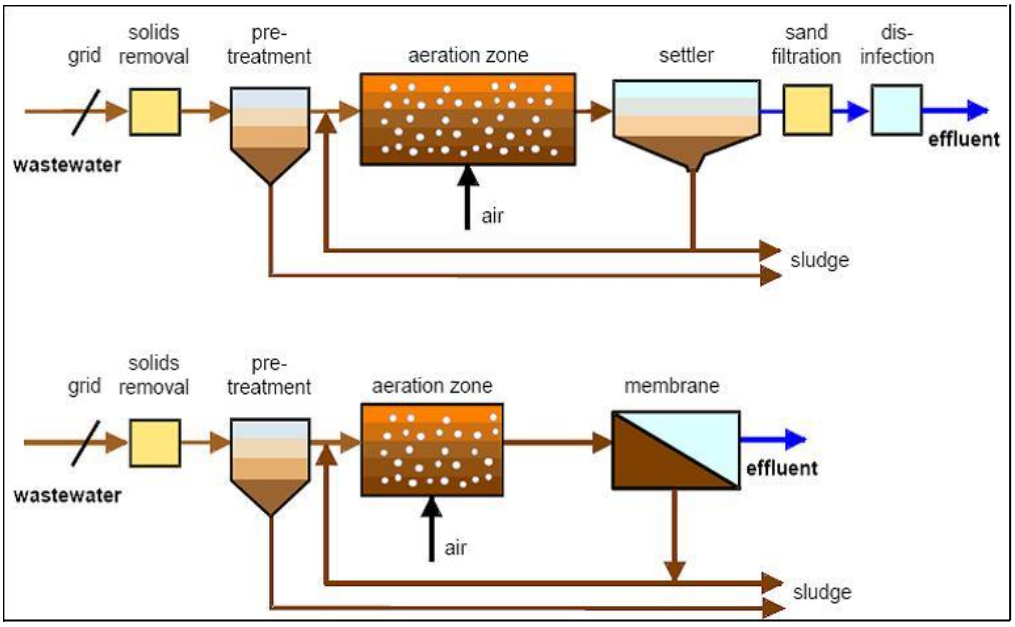

Figure 2-1. Schematic of conventional activated sludge process (top) and external (sidestream) MBR (bottom) (http://en.wikipedia.org/wiki/Membrane_bioreactor)

When UF and MF membranes became commercially available in a large scale, the MBR process was introduced to the market in the late 1960s. Dorr-Olivier Inc. united an activated sludge bioreactor with a flat-sheet membrane process in a crossflow mode (Smith et al., 1969). The polymeric membrane's pore size ranged from 0.003 to 0.01μm (Enegess et al., 2003). Unfortunately, with the high membrane cost, poor tertiary permeate quality and the noticeable fouling-caused flux decline, this original process did not get widely accepted except in niche areas. In 1988, MBRs were modified by submerging membrane in the reactor and operating at high transmembrane pressure (TMP) to maintain filtration (Yamamoto et al., 1989). In the recent MBR development, modest fluxes, and the idea to use two-phase bubbly flow to control fouling were introduced (Cui et al. 2003). Gradually, the lower operating cost obtained with the submerged configuration along with the steady decrease in the membrane

cost, encouraged exponentially increasing applications from the mid-1990s. Since then, further improvements in the MBR design and operation have been introduced and incorporated into larger plants (Yang et al., 2006). While early MBRs were operated at solids retention time (SRT) as high as 100 days with mixed liquor suspended solids (MLSS) up to 30 g/l, the recent trend is to apply a lower SRT (around 10–20 days), resulting in more manageable MLSS levels (10–15 g/l). Thanks to these new operating conditions, the fouling propensity in the MBR has tended to decrease and overall maintenance has been simplified as less frequent membrane cleaning is necessary (Yang et al., 2006). Currently there are many MBR systems commercially available (most of them in submerged form). With regard to membrane configurations, both hollow fiber and flat sheet membranes have been applied for MBR applications (Stephenson et al., 2000).

The economic viability of the current generation of MBRs depends on the achievable permeate flux, mainly controlled by effective fouling control with modest energy input (typically $\leq$1 kWh/m^3 product) (Yang et al., 2006). More efficient fouling mitigation methods can be implemented only when the fouling phenomena are better understood. It is expected that the application scale and number of MBRs will continue to grow rapidly (Yang et al., 2006).

2.1.3 MBR fouling

The membrane permeability inevitably decreases with filtration time as a result of fouling. Fouling is due to the deposition of soluble and particulate materials onto the membrane surface and/or into the membrane pores. This major drawback and process limitation have been widely studied since the early

research for the MBRs, and remain as one of the most difficult challenges facing further MBR develop (Cui et al., 2003).

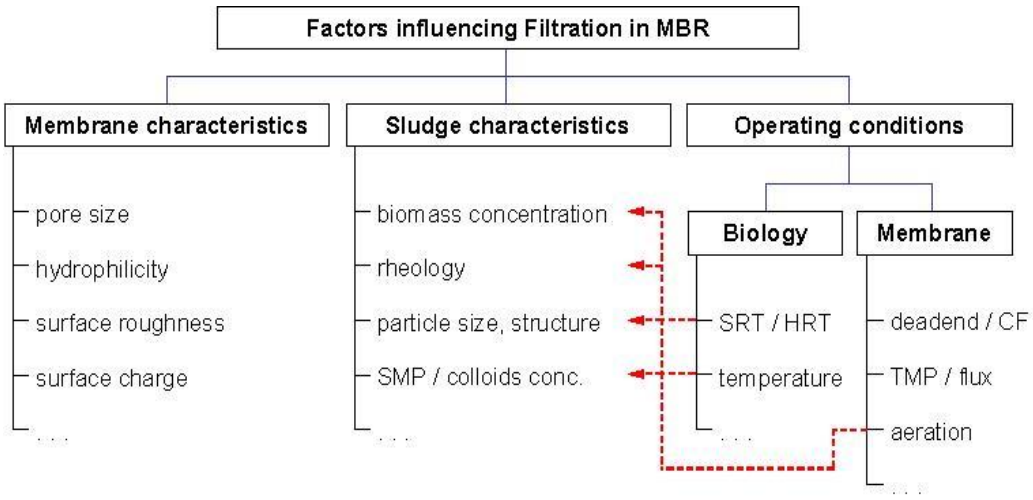

Figure 2-2. Factors influencing filtration in MBR (Chang et al., 2002).

Membrane fouling is caused by interaction between the membrane material and the activated sludge liquor components, which may include biological flocs consisting of a wide range of living or dead microorganisms along with soluble and colloidal particles. The suspended biomass composition varies both with feed water composition and MBR operating conditions employed. In the past, many research works on identifying, investigating, controlling and modelling of membrane fouling have been published. The diversity of operating conditions, the feed water components matrices, and the different analytical methods in most studies on biomass composition have made the study of MBR fouling a challenge task. Polarization layer and cake layer formation were believed to be the main reasons for the increased total resistance in MBR process (Chudacek and Fane, 1984; Park et al., 1999; Pillay and Buckley, 1992). Nevertheless, it has been generally accepted that MBR

fouling are strongly affected by three groups of parameters: ①biomass characteristics, ② membrane characteristics and ③ operating conditions (Figure.2-2, (Chang et al., 2002)).

2.1.3.1 The main foulants in MBR

The conclusions regarding the effects of foulants for MBR process among different research groups are inconsistent. By using dead-end filtration Wisniewski et al. (1998) found that half of the total resistance could be induced by dissolved molecules. Other researchers reported that compared with the resistance caused by suspended solids (SS) (65%) and colloids (30%), the contribution of soluble compounds to the fouling were only 5% (Defrance et al., 2000). The effect of physiological states of sludge on fouling was studied by Chang et al. (1998). They claimed that extracellular polymeric substances (EPS) played the most important role among various foulants. Colloids were considered as the major foulants resulting colloid-caused resistance by Bouhabila et al. (2001). Lee et al. (2003) concluded that the contribution of supernatant containing colloids and solutes to the total resistance were around 33%, while SS was near 68%.

2.1.3.2 Particles transport and membrane fouling

The formation of cake layer indicating that the particles shape into a stagnant, consolidated and aggregated structure that is slow to break-up and re-disperse is also as known as depolarization. Generally, the cake layer permeability can be affected by flux, electrostatic interactions and particle size. According to the study by Petsev et al. (1993), it decreased with (a) the increase in

electrolyte concentration; (b) the increase in permeate flux level; (c) the decrease in the particle surface potential below a certain value; (d) the increase in particle size. Fane et al. (1983) attributed the same behaviour to Brownian diffusion and hydrodynamic particle migration. Bacchin et al. (2006) summarized that the major depolarization mechanisms included Brownian diffusion, surface interaction, shear-induced diffusion and lateral migration, where the Brownian diffusion dominated for smaller particles (size << 100 nm) and shear-induced diffusion and lateral migration dominated for larger particles (size >> 100 nm). For particles in the intermediate size range, the surface interaction might be the most possible explanation for the depolarization process (Bacchin et al. 2006, Tang et al. 2011).

2.1.3.3 The effect of foulant properties

The effect of MLSS concentration

Within MBR system, activated sludge acts as a media for biological decomposition reaction to occur. Activated sludge is a complex heterogenous suspension without well-defined composition. It contains compounds from feed water, metabolites produced during the biological degradation, as well as the biomass itself. In addition to the large amount of suspended solids, the dissolved polymers such as extracellular polymeric substances (EPS) can also contribute to membrane fouling (Gao et al., 2010).

MLSS concentration is often considered at the first sight as the main parameter for fouling potential. Since the early stages of MBR development, many researchers have paid much attention on the effect of this parameter on

membrane fouling. An increase in MLSS concentration seemed to have a comparative negative impact on MBR performances that membrane resistance increased approximately linearly with MLSS concentration(Fane, 1981). Similar results were also reported by Chang and Kim (2005). The WERF (Water Environment Research Foundation) study (WERF, 2006) concluded the following findings: (1) a decrease in MLSS concentration seemed to decrease fouling at low MLSS concentration of 5g/L, (2) severe fouling occurred when the MLSS concentration was above 15g/L, and (3) the effect of MLSS concentration appeared negligible ranging from 8 to 12g/L. However, a recent study (Rosenberger et al., 2005) observed a contradictory trend that an increase of MLSS concentration (<6g/L) tended to mitigate the membrane fouling, which underlined the complexity of the mechanisms involved in MBR fouling.

Based on the conventional cake filtration theory, the cake resistance R_c (m^{-1}) can be expressed as (Chang et al., 2001; Le-Clech et al., 2006; Shimizu et al., 1993):

$$R_c = \alpha \cdot \nu \cdot C_b = \alpha \cdot m_c \qquad 2.1$$

where α is specific cake resistance ($m \cdot kg^{-1}$); ν is permeate volume per unit area (m); C_b is bulk MLSS concentration ($kg \cdot m^{-3}$); m_c is the cake load/area of membrane which generally increases along with the MLSS concentration. The flux decline was observed with an increase of MLSS concentration though the fouling rate was lower than the model test(Bin et al.,

2004). A possible explanation was that the formation of the initial fouling cake layer at high MLSS concentration served as a prefilter to the membrane pores. While for a lower MLSS concentration, colloids and particles posed a dominant role to block the pores gradually.

The effect of foulant composition

According to the research of colloid filtration by Visvanathan and Ben Aim (1989) as well as the protein filtration by Bowen and his co-workers (1995), the process of the typical membrane pores blocking and cake layer formation was described as four consecutive steps: 1) blockage of the finest pores; 2) coverage of the larger pores' inner surface; 3) superimposition of particles and direct blockage of larger pores; 4) formation of the cake layer (Le-Clech et al., 2006). For MBR effluents and other complex fluids containing complicated mixtures of foulants, macromolecules to penetrate into the membrane pores or absorb on its surface. In some cases, a colloidal cake layer was considered as a prefilter. To elucidate this phenomenon, Davis and co-workers carried out a serial of microfiltration work using yeast and protein mixtures (Arora and Davis, 1994; Güell et al., 1999; Kuberkar and Davis, 1999). They found that the formation of yeast cake layer on the membrane surface helped capture the micro-scale aggregated bovin serum albumin (BSA) particles and thus prevented them from adsorbing or clogging the membrane pores. As a result, the prefilter of the yeast layer alleviated the membrane fouling and maintained the water flux stability. Recent studies by Ye et al. (2005) showed that the reversibility of the deposits formed in the mixtures of yeast and BSA was substantially reduced compared with that of yeast solution alone, indicating that the macromolecules played a role in binding the yeast particulates

together. In the research using alginate (a microbial polysaccharide), the specific resistance increased with time, possibly suggesting a continuous infiltration of small fractions of the alginates trapped earlier during the filtration, resulting in a consolidation effect on the cake layer structure. When both alginate and protein were present, the transmission of mixed components was reduced while the compressibility of the mixed deposit was increased. Thus the permeability and compressibility varied with the chemical parameters of the extracellular components matrix in MBR.

The impact of the particles presented in complex fluids on flux behaviour during the membrane filtration also came into notice. Timmer et al. (1997) showed the presence of silicates though in small quantities would completely determine the flux behaviour in the crossflow microfiltration of β-lactoglobulin solutions. Causserand et al. (2001) found that protein adsorption could cause the permeability to change in clay cake. On the isoelectric point of the clay–protein matrix, a threshold minimum limiting flux was found. Interestingly, the mixture behaviour was similar to protein at higher pH values, whereas below pH 4.5, the threshold flux was similar to that of clay suspensions alone. Causserand et al. (1997) optimized the electrostatic interactions between proteins and an adsorptive surface like clay. The formation of those clay particles layer on top of the original particles helped improve protein rejection and decrease membrane fouling by the protein.

The effect of large particles on the fouling process cannot be judged easily. Researchers suggested that, for UF of organic molecules such as polysaccharides and proteins, fouling can be controlled by adding suspended

solids. Panpanit and Visvanathan (2001) found that bentonite addition in the ultrafiltration for oil/water emulsions dramatically decreased membrane fouling, which was attributed to the adsorption of oil onto bentonite and the formation of larger particles. However, the flux improvement gradually declined as the bentonite concentration increased beyond a limiting value, possibly due to the formation of compressed cake layer of the particles on the membrane surface. In some recent studies of constant flux microfiltration using bentonite and alginate mixtures, a bentonite cake layer was found on the membrane surface and the alginate formed a viscous layer on top of the benitonite layer. The velocities of particles passing through this viscous layer reduced steadily with filtration time, indicating a consolidation of the viscous gel layer. This may provide insights into the cohesive and transport characteristics of such complex cake layer structure. In contrast, when the cake build-up was sufficient to create high shear stress caused by crossflow (McDonogh et al., 1992), the foulant layer consisting of compact cellular or particulate cakes which formed onto the swollen macromolecular layer may disengage spontaneously.

2.2 Forward osmosis membrane process

2.2.1 Introduction

Recently, forward osmosis (FO) has emerged as a promising alternative membrane separation technology. In water treatment, RO process is generally a more popularly used process than FO. RO uses hydraulic pressure as the

driving force for separation, which serves to counteract the osmotic pressure gradient that would otherwise favor water flux from the permeate to the feed. A shown in figure 2-3, in contrast, the driving force for FO is the osmotic pressure gradient across the membrane. Pressure-retarded osmosis (PRO) was viewed as an intermediate process between FO and RO, where hydraulic pressure is applied similar to RO. Forward Osmosis uses selectively permeable membrane to allow separation of water from dissolved solutes. Without any external pressure applied, a pure water flux is induced spontaneously across the FO membrane from a low concentration feed water (FW) to a high concentration draw solution (DS), thus effectively separating the feed water from its solutes.

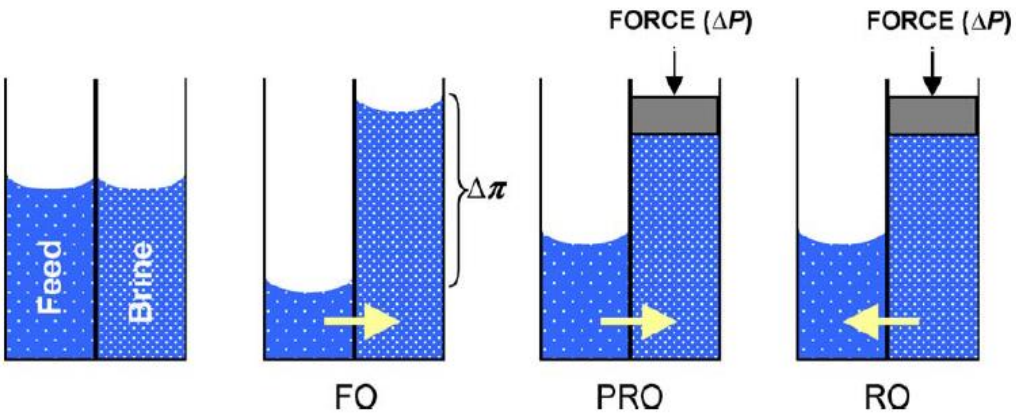

Figure 2-3 Solvent flows in FO, PRO and RO (Cath et al., 2006).

The relationship between osmotic and hydraulic pressures and water flux can be described as (Lee et al., 1981):

$$J_v = A(\sigma\Delta\pi - \Delta P) \qquad 2.2$$

where J_v is water flux, A is water permeability constant of the membrane, σ is reflection coefficient, $\Delta\pi$ is osmotic pressure difference across the active layer of membrane, and ΔP is applied pressure. For FO process, ΔP is zero since there is no hydraulic pressure employed.

Compared to pressure-driven MF and UF processes, FO offers many advantages including 1) wider range of contaminants removal and better separation efficiency attributed by its nonporous rejection layer (Packer, 2009); 2) potentially lower power consumption (e.g., in the case where a high osmotic pressure DS, such as seawater, is naturally available) and possibly lower fouling propensity (Achilli et al., 2009; Cornelissen et al., 2008). Consequently, FO may have many potential applications in water and wastewater treatment (Achilli et al., 2009; Cornelissen et al., 2008)， desalination (McCutcheon et al., 2006)，food processing (Petrotos et al., 1998)，and electricity production (i.e., osmotic power harvesting using a derivative pressure retarded osmosis process) (Lee et al., 1981; Loeb, 2002; Xu et al., 2010).

However, a significant challenge in FO applications is concentration polarization (CP) and membrane fouling (Cath et al. 2006). Despite that FO may potentially have lower fouling propensity compared to pressure-driven membranes, drastic flux loss can occur under certain unfavorable conditions such as high draw solution concentrations and high flux levels (Lay et al., 2010; Mi and Elimelech, 2008; Tang et al., 2010). In addition, the solute back diffusion from the high concentration DS to the feed water, a unique phenomenon in the concentration-driven FO process (Tang et al., 2010), may also have critical impact on FO fouling.

2.2.2 Concentration Polarization

Equation 2.2 described the water flux in osmotic-driven membrane process. In FO process, the osmotic pressure difference across the active layer of the membrane is much lower than the theoretical value between the bulk feed water and draw solution. This caused an accordingly much lower water flux than expected (theoretical value) (McCutcheon et al., 2006) as a result of both external concentration polarization (ECP) and internal concentration polarization (ICP).

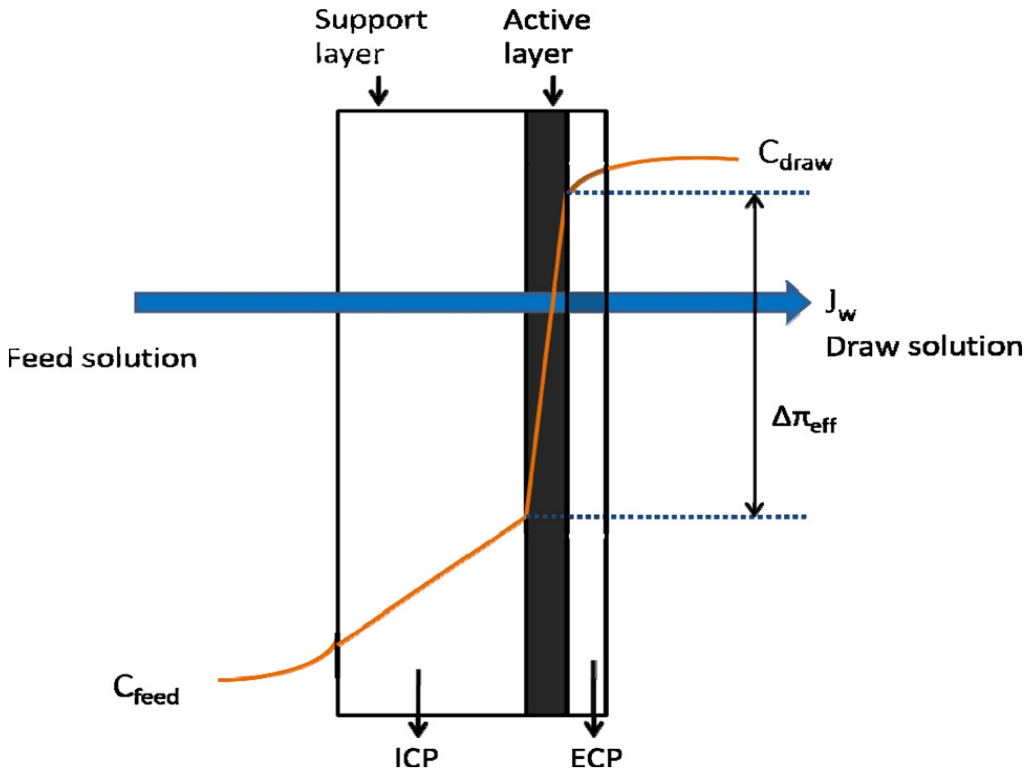

Figure 2-4 Illustration of both internal concentration polarization and external concentration polarization through an asymmetric FO membrane (Zhao et al., 2012).

2.2.2.1 External concentration polarization

Referred to FO process with a AL-facing-DS orientation as shown in Figure 2-4, on the DS side, along with the permeate water passed through the membrane from FW to DS side, the concentration of solutes at DS side adjacent to the membrane surface is lower than in the bulk DS. This is generally called dilutive external polarization (Cath et al. 2006). Similarly to that, with an AL-facing-FW orientation, as the pure water continuously penetrating the membrane while the solutes in FW were rejected and aggregated by the membrane, the concentration at FW side near the membrane is concentrated, which is called concentrative external CP (Cath et al. 2006). Both of the two external CP posed an adverse effect on the effective osmotic pressure resulting in a decreased driving force and thus a reduced water flux. To minimize the negative effect of CP, higher crossflow velocity and/or greater turbulence near the membrane can be used. However, many researches had shown that ECP had a relatively milder effect on FO flux compared to ICP (Cath et al., 2006; McCutcheon et al., 2006).

2.2.2.2 Internal concentration polarization

A typical FO membrane is asymmetric, consisting of a selective active layer which is very thin and a thick porous supportive layer. Under the membrane orientation of AL-facing-DS and the porous support layer facing FW (Figure 2-5), as pure water infiltrated through the membrane while solutes come into the support layer but retained by the dense active layer, hence a concentrative polarized layer formed inside the porous support layer (McCutcheon and Elimelech 2006). As a result, concentrative internal CP cannot be minimized

by increased crossflow. When the active layer facing feed water (Figure 2-5), as water passing through the active layer into the support layer, the diluted ICP occurs since the concentration inside of porous layer is diluted (McCutcheon and Elimelech 2006).

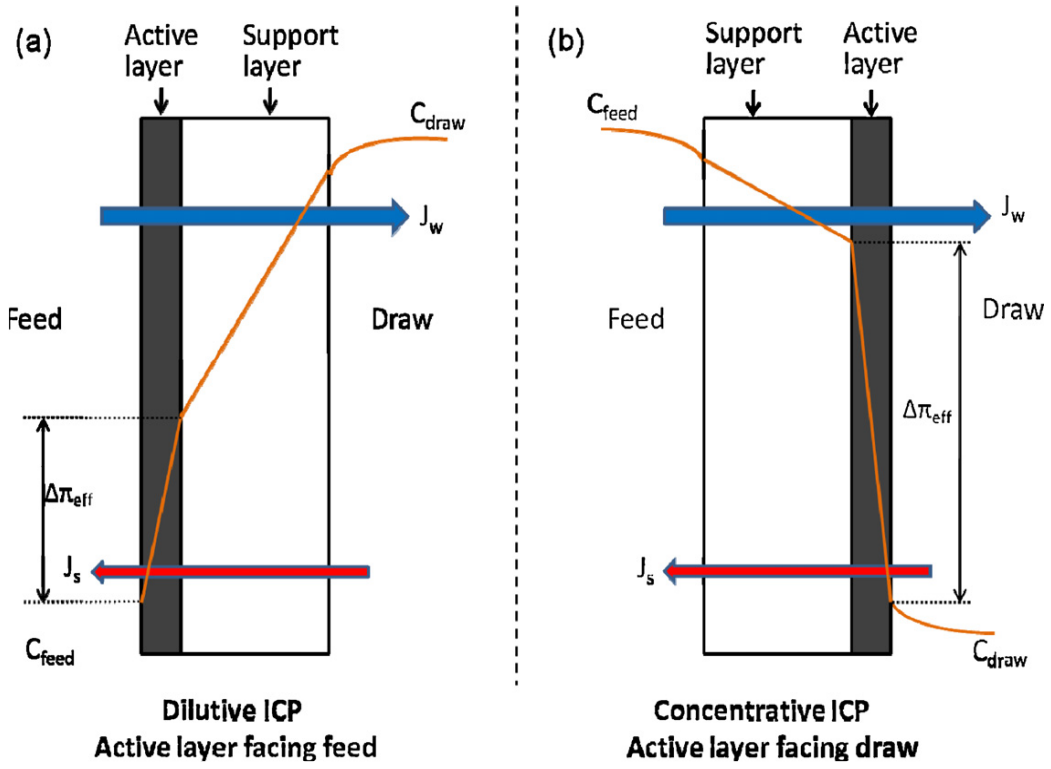

Figure 2-5 Illustration of concentrative ICP and dilutive ICP (Zhao et al., 2012).

2.2.3 FO flux models

2.2.3.1 FO Water Flux

The classical solution-diffusion model combined with diffusion-convection transport in the membrane support layer was used to mathematically describe the solute and water transport in a forward osmosis process by Tang and his

coworkers (2010). With the AL-facing-DS orientation, the solution-diffusion model to the selective layer was applied:

$$J_v = A(\pi_{draw} - \pi_{support}) \quad 2.3$$

$$J_s = B(C_{draw} - C_{support}) \quad 2.4$$

where A and B are the transport coefficients for water and solute, J_v is the volumetric flux of water; J_s is the mass flux of solute; C_{draw} and π_{draw} are the solute concentration and osmotic pressure of the draw solution; and $C_{support}$ and $\pi_{support}$ are the solute concentration and osmotic pressure at the interface of FO support layer and rejection layer.

For the solute transport in the supporting layer:

$$J_v C + J_s = D_{eff} \frac{dC}{dx} \quad 2.5$$

where D_{eff} is the effective diffusion coefficient of solute in the porous backing layer; C is the solute concentration in the porous support layer at a distance x away from the interface between the rejection layer and the supporting layer.

Equations 2.3-2.5 was solved to yield the following result (Tang et al., 2010):

$$J_v = K_m \ln\left(\frac{A\pi_{draw} - J_v + B}{A\pi_{feed} + B}\right) \quad \text{(AL-facing-DS)} \quad 2.6$$

where K_m is the mass transfer coefficient.

The flux equation for the AL-facing-FW configuration was similarly determined by Tang et al.(2010):

$$J_v = K_m \ln\left(\frac{A\pi_{draw} + B}{A\pi_{feed} + J_v + B}\right) \qquad \text{(AL-facing-FW)} \qquad 2.7$$

2.2.3.2 FO Solute Flux

Tang et al. derived the FO solute flux from Equations 2.1 and 2.2:

$$\frac{J_s}{J_v} = \frac{B(C_{draw} - C_{support})}{A(\pi_{draw} - \pi_{support})} \qquad 2.8$$

By applying the van't Hoff equation, they got

$$J_s = \frac{B}{A \cdot \beta R_g T} J_v \qquad 2.9$$

2.2.4 FO application for algae harvesting

Microalgae are prokaryotic or eukaryotic photosynthetic microorganisms with a unicellular or simple multicellular structure. They are present in all existing ecosystem but particular in aquatic environment. During the past decades extensive studies of microalgae have been created due to the promising future of the applications in industrial implementation and environmental protection (Amin, 2009). Microalgae are considered as an alternative power resource providing feedstock for several different renewable fuels such as biodiesel

(Figure 2-6), methane, hydrogen, and ethanol. The utilization of microalgae for biofuels production can also serve to remove CO, CO_2 from industrial flue gases (Packer, 2009) and the nutrients compounds during cultivation. Microalgae sometimes serve adverse impacts on surface water environment that seasonal algal bloom released toxin and unpleasant color and odor (Henderson et al., 2008; Karner et al., 2001)

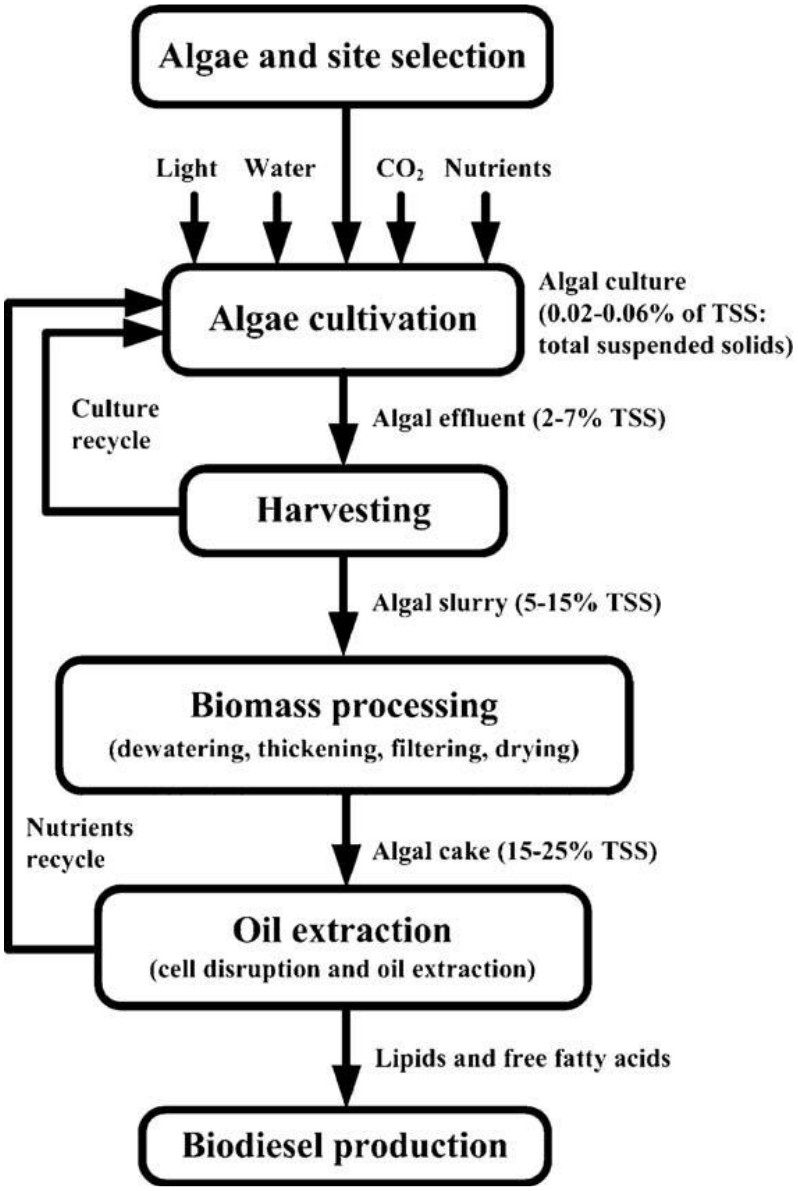

Figure 2-6 Microalgae biodiesel value chain stages (Mata et al., 2010).

In these processes, the separation of microalgae cells from source water is a critical problem. Algal harvesting consists of biomass recovery contributing to about 25% of the total biomass production cost (Molina Grima et al., 2003) Conventional methods, such as coagulation, flocculation, floatation and centrifugation, may involve one or more steps including several physical, chemical and/or biological interactions. Meanwhile, algae removal by

membrane filtration, e.g., MF and UF, becomes an active research topic due to its high separation efficiency and good suitability for fragile cells and small scale production processes. Zhang et al. (2010b) used a crossflow UF process to harvest and dewater algal cells. In their study, air-assisted backwash were used to maintain a high permeate flux. However, these pressure-driven membrane filtration processes are more expensive especially because of the need for fouled membrane replacement and pumping. Experience has shown that an appropriate and economical harvesting method is still a popular topic.

The national Aeronautics and Space Administration (NASA) of the United States has reported the new invention of an algae photo-bioreactor using FO membrane which is called Offshore Membrane Enclosure for Growing Algae (OMEGA) (Marlaire, 2009b). According to the description, algae feed on the CO_2 and nutrients from municipal wastewater influent by photosynthesis to produce biomass and oxygen. By using the semi-permeable FO membrane, the interception of the nutrients and algae biomass is achieved, and the filtered clean water is released through the FO membrane by the high osmotic pressure of seawater. Since the primary objective of the OMEGA project is for algae biomass harvesting and naturally abundant seawater is used as the draw solution, the difficult task of draw solution regeneration (i.e., separation of FO permeate water from and re-concentration of the draw solution) is avoided.

2.3 Critical flux

2.3.1 Critical flux concept

Bacchin *et al*. (1994; 1995) established a theoretical model that accounted for the balance of surface interaction, diffusion and convection. Among these transport phenomenon, surface interaction plays a dominant role in preventing particle deposition onto membranes for particle size between 10 nm and 10μm. Based on the models conducted in their studies, "critical flux" was defined as "the threshold operating flux below which no fouling occurs". This gives a physical explanation for the existence of critical flux: the critical flux is the minimum flux required to counteract the repulsion force between particles, which leads to the particles coagulation on the surface.

Field et al. (1995) experimentally observed a critical flux as "a flux below which a decline of flux with time does not occur; above it fouling is observed". As shown in Figure 2-6 (Field et al., 1995), the strong form critical flux is the flux at which the TMP starts to deviate from the linear pure water flux, while the weak form critical flux is the point at which the flux-TMP relationship becomes non-linear. The weak form critical flux might be explained by the assumption that membrane got fouled very rapidly during the start-up phase of the filtration causing the flux-TMP data line located below the pure water data line.

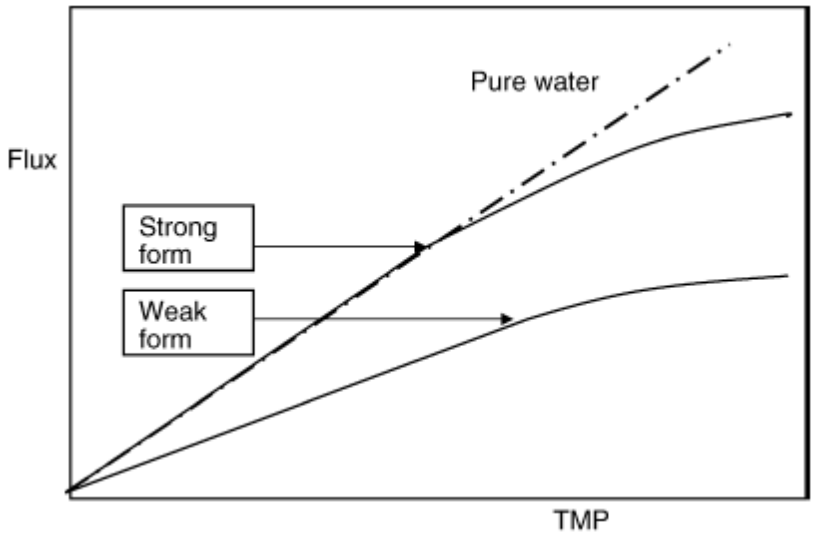

Figure 2-7 Forms of critical flux (Field et al., 1995).

Generally, critical flux was used either for the phenomenon that the permeate flux–TMP curve started to deviate from linearity, or that the irreversible fouling started to occur. Some definitions have been given from a deterministic standpoint focusing on the flux level leading to the approaching of the foulant close to and then depositing upon the membrane, while others are from an experimental standpoint concerning the first deviation from a linear variation of flux with TMP.

2.3.2 Methods of critical flux measurement

2.3.2.1 Flux stepping and flux cycling

The critical flux can be determined using flux–pressure experiments by setting flux values and recording the pressures or by setting pressures and recording the flux values. Initially, some researchers conducted a serial of increasing pressure steps followed by a set of decreasing steps (Chen et al., 1997). By

using this method, Chen et al. found that there was a serious hysteretic effect on critical flux but the first deviation from linearity was not clear. The stepwise filtration procedure has been used for different suspensions by many researchers such as Gesan-Guiziou et al. (2000), Kwon et al. (2000), Manttari and Nystrom (2000) and becomes a commonly accepted method for critical flux determination.

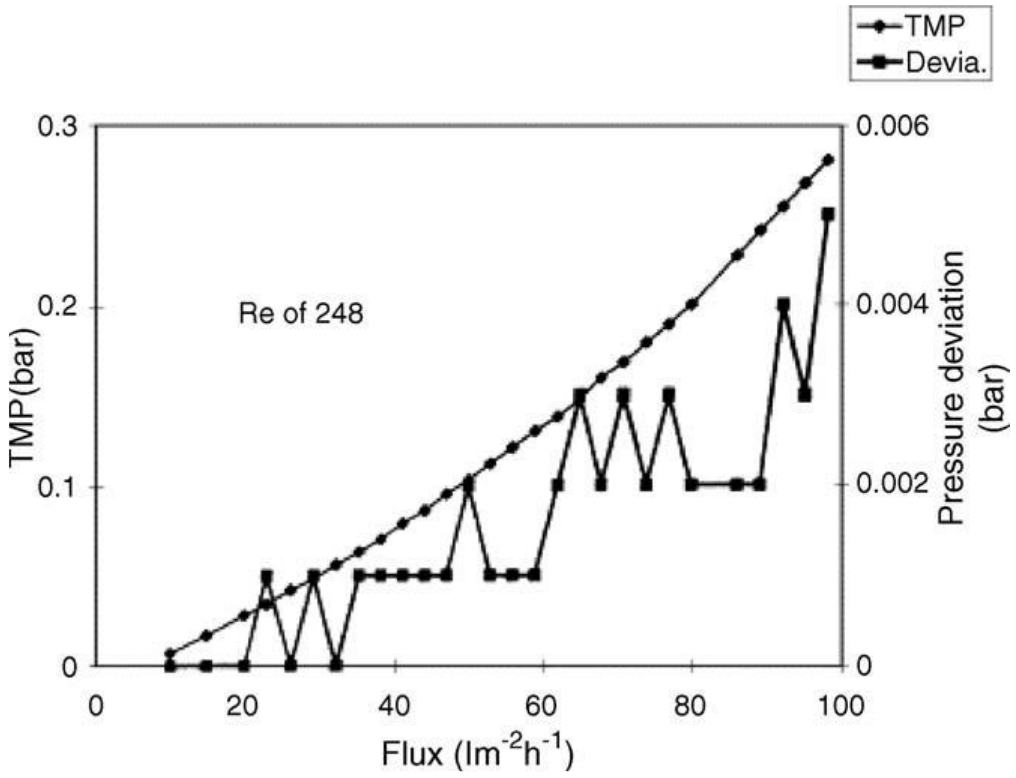

Figure 2-8 Illustration of flux cycling method for critical flux determination(Wu et al., 1999).

Wu et al. (1999) used the previously mentioned stepping method concept but adjusted the stepping strategy on flux. This new filtration experiment involved a set of up-and-down flux steps which was a serial of flux cycles. At step 1 (Figure 2-7), flux was set as designed value J_1 , and the TMP was measured as

TMP_1 when the system arrived at a steady state. For the second step, the flux was then increased a little higher as J_2 and the TMP_2 was again measured. At step 3, the flux was not set forward as the normal flux stepping method but set back to J_1 and the TMP value during this stage was recorded as TMP'_1. If the deviation between the two values TMP_1 and TMP'_1 equalled zero, they assumed that no fouling occurred. Then the flux was cycled again by setting forward to J_3 followed by setting backward to J_2. The deviation between TMP_2 and TMP'_2 was checked once more to obtain the information whether fouling had occurred. With the same suspension, the critical flux measured by flux cycling was slightly lower than the value determined by flux stepping method, indicating that the former is more sensitive to some trace amount fouling during the experiment.

2.3.2.2 Pressure stepping and cycling

Critical flux can be determined more accurately by analysing the fouling reversibility for each step of pressure or flux. The procedure of filtration for this determination method consists of “up” and “down” pressure initially designed by Wu et al. (1999) and then developed by Espinasse et al. (2002). The standard filtration procedure proposed is to alternate positive and negative pressure changes, as shown schematically in Figure. 2-8. When the pressure is set to any different value, the flux is monitored to achieve steady state over time. The pressure can then be set a new value. By comparing the stabilized flux value at steps 1 and 4 (in Figure 2-8), whether a lower-than-expect flux value at step 3 is related to an irreversible fouling or to reversible phenomena (polarization layer) can be deduced. For example, if the flux at step 4 is on

point b which is below the step 1 flux (point a), fouling induced by step 3 is definitely irreversible, and, if the flux is on point a indicating no flux deduction, fouling is totally reversible; therefore, a fraction of reversibility can be suggested according to the flux value at step 4.

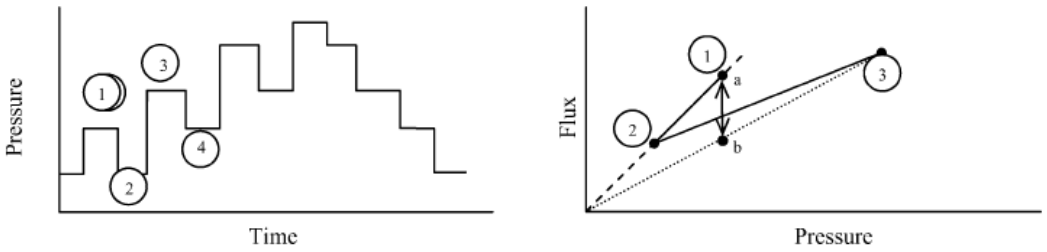

Figure 2-9 Pressure step used for an accurate determination of critical flux. Comparison of permeate flux/pressure obtained in steps 4 and 1 permits conclusion as to degree of fouling irreversibility in pressure step 3 (Espinasse et al., 2002).

2.3.2.3 Direct observation through the membrane

The flux–pressure relationship sometime may be insensitive to indicate the starting of membrane fouling, especially if the membrane used has a large hydraulic resistance (e.g., NF, RO, and FO membranes). In such cases, direct microscopic observation can be useful to study the fouling behaviour and to determine the critical flux value. Fane and co-workers (Li et al., 1998, 2000) developed a direct observation through membranes (DOTM) technique, where a microscope is used to look through an transparent membrane. Deposition or absence of particles on the membrane surface can be observed. These authors have used this technique and shown that the DOTM technique can be more sensitive compared to flux-pressure measurement on critical flux

determination. The DOTM is restricted to transparent membranes and modules with a transparent section on the permeate side. Other microscopic observation method has also been recently developed (Kang et al., 2004) which does not require the use of transparent membranes. In all cases, these direct observation methods are applicable only for relatively large particles (> 1 μm in diameter).

2.3.2.4 Other methods for critical flux determination

Other methods for critical flux determination may involve the use of non-invasive monitoring techniques, such as the use of ultrasound detection (Chong et al., 2007), electrical impedance spectroscopy (Freger, 2005), etc. In addition, foulant mass may be used if the amount of membrane area tested is sufficiently large (Bacchin et al. 2006).

2.3.3 Factors influencing the critical flux

2.3.3.1 Effect of suspension properties

Suspension stability

Surface interaction has intrigued numerous academic interests to investigate its effect on critical flux as soon as it was highlighted as the main reason causing critical flux phenomenon for colloidal suspensions (Bacchin et al., 1995). The studies principally focused on the impact of pH and ionic strength, which respectively changes the solute charge and surface repulsion through charge screening. Generally, critical flux increases with an increased pH value which is above the isoelectric point (IEP). Consistently, it has been observed (Youravong et al., 2002) that an increase in pH gives an increase in critical

flux for both protein suspensions with whey protein concentrate and sodium caseinate suspensions.

With regard to ionic strength, an increase in ionic strength below the threshold coagulation concentration would decrease the critical flux for both of the clays suspension (Bacchin et al., 1996) and the latex particles (Espinasse et al., 2002; Kwon et al., 2000). They emphasized again the role of suspension stability in critical flux concept.

The mechanism of precipitation or crystallisation of a solute can be explained as a result of the solute stability decreased to a certain value. For example, critical flux was significantly decreased by increasing the solution pH beyond a threshold value in a membrane bioreactor used for denitrification purpose (Ognier et al., 2002). Because the carbonate calcium started to precipitate if the pH value was high enough and then the precipitation deposited on the membrane. This again revealed a significant decrease in critical flux resulted from suspension instability.

Suspension concentration

Many studies showed a trend that the critical flux was likely decreased by arising the suspension concentration. Gesan-Guiziou et al. (2002), for example, obtained a rapidly reduced critical flux with a higher concentration of suspensions of latex. Kwon et al. (2000) found the same trend for latex suspensions filtration. However, the relationship between the permeate flux and the logarithm of the concentration was not linear which means film model cannot be applied in this case. Consequently, membrane fouling caused by

particles deposition cannot be explained by either film model or gel model. Other factors like diffusion or viscosity (Aimar and Sanchez, 1986) and the presence of surface interaction (Bacchin et al., 1995) might contribute to the mass accumulation. The effect of concentration in a complex suspension, e.g. activated sludge concentration, can exhibit similar behaviour. Referring to some works for complex suspension such as the activated sludge in MBR (Madaeni et al., 1999), the suspension concentration as well had an effect on critical flux. Meanwhile, there are other observations that increasing bacterial cells concentration in fermentation broth (Persson et al., 2001) only decreased the critical flux slightly.

Suspension size

To determine the effect of the suspension size on the critical flux, we need to prepare suspension with different particle size but the same surface properties. This requirement suggested the difficulties of the research. Kwon and his co-workers (Kwon et al., 2000) had explored the particle size effect using polystyrene latex particles with seven different sizes ranging from 0.1 to 10 μm. It is observed that critical flux value for 0.2 μm particles is higher for particles of 0.1mm. Harmant and Aimar (1998) theoretically proved this tendency that a minimal critical flux value was obtained with the particles size around 100nm. Results of studies by Li et al. (2000) have a good consistency with the conclusion that the critical flux for larger particle size seemed to be higher than that for smaller ones.

2.3.3.2 Effect of solution hydrodynamics

Hydrodynamic effect

Some researchers tried to use a power law of the Reynolds number to represent the effect of tangential flow at the membrane surface on critical flux. All works focusing on the effect of the cross-flow velocity on critical flux have a consistency result but it cannot be concluded firmly yet based on these studies. It has to be noted that if there is a substantial pressure applied on membrane, even a larger cross-flow velocity can only induce a slight increase in critical flux (Madaeni et al., 1999).

Analogy in dead end filtration

Without the presence of tangential flow at the membrane surface, e.g. in a dead-end mode filtration, the impact of shear force on critical flux cannot be observed clearly (if the shear force prevails among the factors). There is a threshold filtered volume (Bacchin et al., 2002; Harmant and Aimar, 1998) found for dead-end filtration of some certain suspensions. In fact, for dead end mode operation treating colloidal suspension or natural water (Bessiere et al., 2005), the deposition of foulant on membrane surface did not appear until a certain amount of filtered volume achieved. Such a "critical" volume phenomenon represents the same concept with the "critical" flux which is observed in cross-flow filtration, both indicating the formation of an irreversible fouling deposition onto the membrane surface has occurred. Subsequently, the dead end filtration is proved to be linked with cross-flow filtration for some colloidal suspension as there is a critical state inducing initial fouling for both filtration operation modes.

2.3.3.3 Effect of membrane properties

It has been experimentally investigated that the geometric structure of the membrane has a significant impact on critical flux. Wu *et al*. (1999) observed that for PES membranes with higher cut-off properties, it tends to have a decreased critical flux. Wu and his co-workers presumed that the reduced critical flux could be contributed by the surface properties change, however, may also be explained by the difference in the local porosity and thus the local permeate flux. Typically, local porosity could have an impact on the balance point of the various forces such as drag force and surface interaction, the resultant of which may determine the level of critical flux. This effect gains much attention particularly for macromolecules. A recent work found that during the ultrafiltration of colloidal latex suspension using tubular ceramic membranes, the critical flux was hardly affected by initial membrane permeability (Gésan-Guiziou et al., 2002). However, a significant decrease in critical flux was observed when the membrane was pre-coated with an irreversible deposit.

Kuiper et al. (2000) observed that with circular pores microsieves, porosity can strongly affect the formation and the growing of the cake layer on membrane surface. As for high porosity of microsieves where the distance between pores is very small, there is a steric hindrance stress among the particles preventing from coagulation and deposition on the overall membrane surface. In this case, regarding to the fouling status on the whole membrane surface, the cake layer cannot form even if critical flux is surpassed. Such a system could still have a

critical flux for irreversible fouling, expressed by term J_{ci}, in excess of conventional strong form critical flux J_{cs} or weak form critical flux J_{cw}.

A higher porosity mostly leads to a better overall flux on the porous surface which is lower than the maximum local flux and thus plays an important role in the increased global critical flux.

2.3.4 Critical flux modelling

Generally, flux reduction for constant pressure operation or pressure increment for constant flux operation are related to a filtration law. Thus the combination of different fouling mechanisms can be modelled by Darcy law:

$$J = \frac{\Delta P - \Delta \pi}{\mu(R_m + R_{ads} + R_{rev} + R_{irrev})} \qquad 2.10$$

Where $\Delta \pi$ is osmotic pressure which has a negative effect on the efficiency of the transmembrane pressure. Additionally, classification of various hydraulic resistances R are taken into account, including the surface or pore adsorption term R_{ads}, a reversible membrane fouling R_{rev} possibly caused by pore blinding or cake deposition, and irreversible fouling R_{irrev} possibly induced by cake deposition or gel formation.

This model makes the differentiating of the fouling mechanisms possible. It can be used typically to distinguish the fouling which is independent of solvent

filtration through the membrane from that introduced by the applied pressure and flux. Fouling caused by adsorption could be irreversible (R_{irrev}) when the pressure is very low or reversible (R_{rev}) if the pressure is high enough.

The strong form of critical flux J_{cs} was applied to better discriminate no fouling conditions (where R_m is the only resistance in Equation (2.10)) from fouling where other types of resistances also exist. When the critical flux is not exceeded, the TMP-flux curve is still plotted in a linear line, which means the osmotic pressure is negligible:

$$\text{for} \quad J < J_{cs} : J = \frac{\Delta P}{\mu R_m} \tag{2.11}$$

$$\text{for} \quad J > J_{cs} : J = \frac{\Delta P}{\mu(R_m + (R_{rev} + R_{irrev}))} \tag{2.12}$$

where at least one of R_{rev} or R_{irrev} is non-zero when R_{ads} is considered as negligible.

The weak form of critical flux, J_{cw}, has been developed to discriminate the status below and above the critical point at which initial fouling phenomena occurred and driven by the solvent penetrating through the membrane. Firstly, only adsorption present at the beginning of the test was taken into account as the additional term (Field et al., 1995). It was further developed by Wu *et al.* (1999) that a very low fouling condition could be differentiated from more

significant ones, by using J_{cs} and J_{cw} to mark the boundary of the intermediate region.

$$\text{for} \quad J < J_{cs} : J = \frac{\Delta P}{\mu(R_m + R_{ads})} \tag{2.13}$$

$$\text{for } J > J_{cs} : \quad J = \frac{\Delta P}{\mu(R_m + R_{ads} + R_{rev} + R_{irrev})} \tag{2.14}$$

where at least one of R_{rev} or R_{irrev} is non-zero.

A new term "critical flux for irreversibility" was defined by Bacchin et al., (1995), as J_{ci}, to provide the information with regard to its irreversibility. Below the critical flux for irreversibility (Figure 2-13), there is only a concentration polarization layer presents on the membrane surface and for some cases another monolayer of adsorption added, however, above this critical flux, there are also layers of irreversible foulant deposited on the membrane. When macromolecules or colloidal suspension was used as feed water, this critical flux is linked to the starting point of particles coagulation getting close to the membrane surface, followed by deposition upon it.

The irreversible form of the critical flux can be expressed as:

$$\text{for} \quad J < J_{cs} : J = \frac{\Delta P - \Delta \pi}{\mu(R_m + R_{ads} + R_{rev})} \tag{2.15}$$

$$\text{for} \quad J > J_{cs} : J = \frac{\Delta P - \Delta \pi}{\mu(R_m + R_{ads} + R_{rev} + R_{irrev})} \qquad 2.16$$

where R_{ads} might include in-pore fouling or monolayer adsorption.

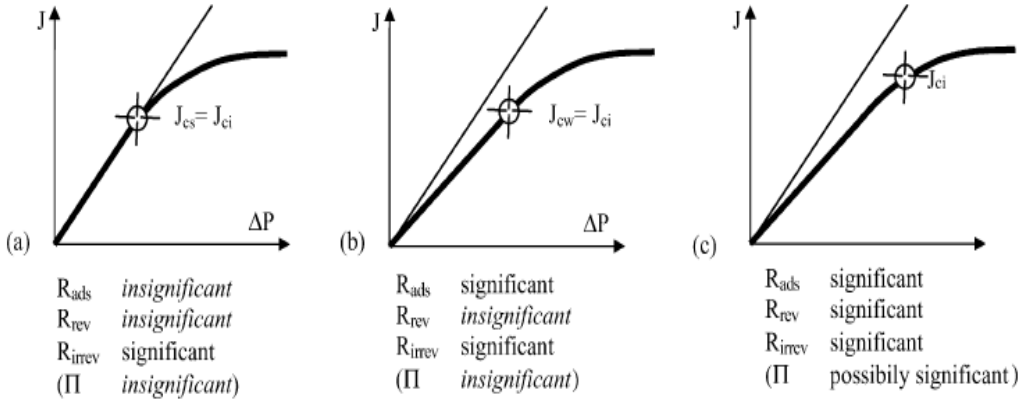

Figure 2-10 Relationships between different critical flux definitions for three types of fouling behaviors (Bacchin et al., 2006).

2.4 Summary

In order to understand the potential interaction effect between permeate flux level and membrane fouling behaviour for both microfiltration and forward osmosis, the relevant literature has been reviewed.

A significant amount of research to date has examined the influence on flux performance exerted by membrane fouling unidirectionally only. As the decrease in flux during the filtration indicates a change in hydrodynamic conditions, which inevitably affect further fouling growing. The relationship between flux level and membrane fouling is still yet to be established. So how different flux levels will impact on membrane fouling?

For MF, some literature on critical flux phenomenon shows certain nexus between flux levels and membrane fouling. But the value of critical flux derived from different determination methodology varies. Therefore the operating strategy which is predominantly informed by critical flux value will also depend on what determination methodology being used. Then how do experiment protocols affect critical flux value? As only limited information is available on this topic and thus a systematic study is needed to answer this research question.

FO filtration is believed to have less fouling propensity compared with pressure-driven membrane process owning to its low flux operation under no external pressure. The research on the potential application of FO technology in conventional separating industrials such as algae harvesting will be highly valuable. For FO, there are numerous studies focusing on concentration

polarization but the information on FO membrane fouling is very limited. What are the mechanisms dictate the drastic flux loss in FO? What is the effect of different physical (flux level, membrane orientation, and cross flow) and chemical parameters (feed and draw solution chemistry) on FO fouling during algae separation? Although the filtration principle of osmotically driven membrane process (FO) is different from that of pressure driven membrane process (MF), is there any common phenomenon shared between the two types of filtration? In particular, can the concept of critical flux in MF be applied to FO? Last but not least, whether the advanced imaging technology can be used in FO membrane fouling studies? Unfortunately, there is so far no literature on the systematic application of direct microscopic observation method for FO critical flux determination.

The work presented here attempts to answer these questions.

Chapter 3 Characterization of Critical and Limiting Flux for MF Membranes in MBR Process

3.1 Introduction

Membrane bioreactor (MBR) has been widely used in treating domestic and industrial wastewaters (Yang et al. 2006). Compared to conventional activated sludge processes, MBR enjoys many advantages such as smaller foot print, better and more consistent product quality, etc. (Yang et al. 2006). However, membrane fouling remains as one of the major challenges (Chang et al. 2002). Severe fouling can lead to reduced productivity, increased energy consumption, increased chemical usage for cleaning, and reduced membrane life span.

An important concept in membrane fouling is the critical flux concept. According to Field et al. (1995), severe fouling occurs when the membrane flux exceeds a threshold value (i.e., the critical flux). Below the critical flux, the membrane flux tends to be more stable. Experimentally, the critical flux can be evaluated by plotting the flux versus trans-membrane pressure (TMP) curve for given feed water. The flux at which the curve starts to deviate from the pure water flux line is the strong form of critical flux (Bacchin et al., 2006). The strong form of critical flux, below which there is no membrane fouling, may not always exist. For example, a membrane's permeability can be severely reduced due to the adsorption of organic matter even at zero flux conditions (Brites and Depinho, 1993; Clark et al., 1991). In this case, a weak

form of critical flux may be defined as the flux below which the flux increases linearly with the TMP (Bacchin et al., 2006).

The flux (or pressure) stepping method is commonly employed for critical flux determination (Bacchin et al., 2006). For example, in pressure stepping, the TMP is increased in small steps at given time interval. Within each step, the pressure is maintained constant while the flux behaviour is monitored. Presumably, the experimental critical flux value will depend on the step size (dP, the increase in pressure between steps), the step duration (dt), and the time scale needed for foulant deposition. Other critical flux measurement methods, such as pressure cycling, have also been reported in the literature (Bacchin et al. 2006). The influence of measurement protocols on the critical flux determination has not yet been systematically investigated.

The aim of the research was to investigate the effect of measurement conditions (step size, step interval, stepping vs. cycling, etc.) on the critical flux value. This may provide a basis for developing more reliable critical flux measurement.

3.2 MATERIALS AND METHODS

3.2.1 Materials

3.2.1.1 Chemicals

Unless specified otherwise, all reagents and chemicals are analytical grade with purity over 99%. Purified water was supplied in-house from a MilliQ

water system (Millipore, Billerica, MA) with a resistivity of 18.2 Mohm-cm. Ethanol, 2% glutaraldehyde solution and sodium cacodylate buffer were used for scanning electron microscopy (SEM) pretreatment.

3.2.1.2 Activated sludge

Two types of sludge were used in this study. The Activated Sludge (Sludge A) was collected from a conventional activated sludge process in Ulu Pandan Water Reclamation Plant (UPWRP, Singapore). The MBR Sludge (Sludge B) was obtained from an MBR pilot plant located in UPWRP. These sludges were collected weekly from the plant, and their compositions are given in Table 3-1.

Table 3-1 Characteristics of Activated Sludge and MBR Sludge

Concentration (mg L^{-1})	Activated	MBR Sludge
Total organic carbon (TOC)	810 - 860	1530-1570
Mixed liquor suspended solids (MLSS)	2160 - 2240	3760-3850
Mixed liquor volatile suspended solids (MLVSS)	1740 - 1820	3210 – 3300
pH	7.0-7.2	6.9-7.2

3.2.1.3 Microfiltration (MF) Membrane Module

Two types of hollow fiber MF membranes were used, MIF503 with a pore size of 0.1 μm and MOF503 with a pore size of 0.2 μm. These membranes were purchased from Tianjin Motian Membrane Eng. & Tech. Co. Ltd. (China). Table 3-2 shows the specification of MIF and MOF membranes. Both membrane types are of polyvinylidene difluoride (PVDF). All the membranes

were stored in MilliQ water bath immediately upon receiving following manufacturer's advice.

Table 3-2 Membrane module specification

		MOF503	MIF503
Specification	Module Configuration	Hollow fiber Microfiltration	Hollow fiber Microfiltration
	Module Length (mm)	90-110	90-110
	Capillary I.D. / O.D. (mm)	0.5 / 0.8	0.8 / 1.4
	Pore Size (μm)	0.2	0.1
	Effective Membrane Area ($10^{-3}m^2$)	2.2608 - 2.2732*	3.9564 - 3.9781*
Operating Conditions	Maximum Operating Pressure (MPa)	< 0.15	< 0.12
	pH Range	2 - 10	2 - 10
Material		Polyvinylidene	Polyvinylidene

*: independent modules were studied.

In the current study, membrane modules (Figure 3-1) were made by assembling hollow fibers (10 fibers, length ~ 10 cm). The effect membrane area in each module is given by:

$$A = \pi \times OD \times L \times No. \quad 3.1$$

Where OD is the capillary outside diameter of the fiber;

L is the length of the module contacting with liquor;

No. is the number of fibers in one module (No.=10).

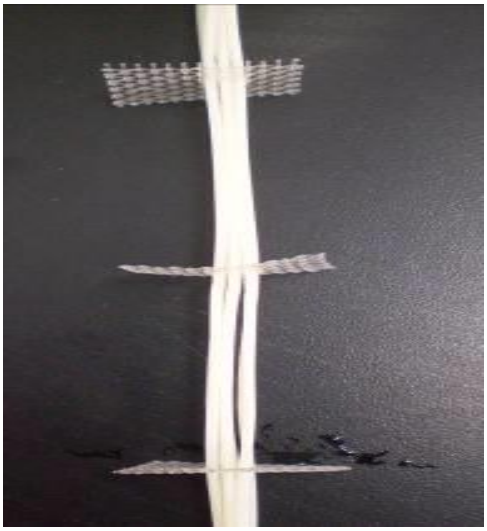

Figure 3-1 Handmade membrane module

3.2.2 Experimental setup

The experiments and controls for the filtration tests were performed in batch scale using different membranes (MOF and MIF) and complex fluids (sludge A and B) as described above.

The bench-scale filtration system was operated in a constant pressure mode (Figure 3-2). The trans-membrane pressure was maintained by the compressed

air. Valves were installed at various locations to regulate the TMP. A digital pressure sensor (CKD ppx-r01h, Japan) was used to monitor the pressure in the feed container. A magnetic stirrer was placed under the reactor to prevent the activated sludge from stratification or settling down. A peristaltic pump was used to pump water back to the reactor to make up the permeate water that was pumped out so as to maintain a constant mixed liquor concentration and a stable liquid level as well. An electronic balance was used to measure the mass of the permeate water at predetermined time interval and the results were recorded by a computer data logging system.

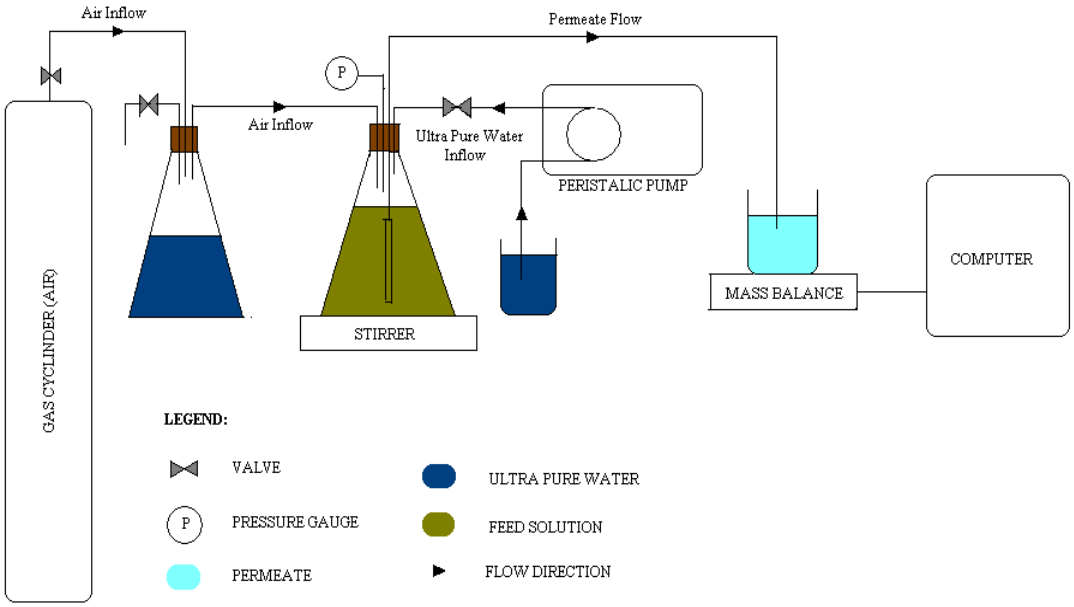

Figure 3-2 Pressure-Constant MBR System Diagram

3.2.3 Chemical analysis

Mixed liquor suspended solids (MLSS) and volatile suspended solids (MLVSS)

The organic fraction of the mixed liquor suspended solids, volatile solids, was determined according to established method (Clesceri, 1998). For the determination of MLSS and MLVSS, 1 ml of each sample was transferred to the glass fibre filter paper and filtered to dry by vacuum. The weights of aluminium dish and filter paper for each sample were predetermined after drying at $500\,^{\circ}C$ for one hour. After filtering through glass fibre filter paper, samples were dried at $103\,^{\circ}C$ for one hour. The dry weights of samples on dish and filter paper were then measured to determine MLSS. The samples were further burned at $500\,^{\circ}C$ for twenty minutes, and the corresponding weight loss was used in the calculation of MLVSS.

Total organic carbon (TOC)

Total organic carbon was determined by a TOC analyzer (Shimadzu C-Vcsh, Japan). The following steps were carried out for TOC analysis:

- Samples were centrifuged and filtered through 0.45μm membrane filter.

- Filtered samples are diluted to 20ml volume.

- Samples were put in TOC analyser.

- Actual TOC = (20ml / sample volume) × TOC reading

Particle size distribution analysis

Particle size analysis of the activated sludge was conducted by using the Malvern Mastersizer 2000. The analyzer measures particle size based on the principle of laser diffraction in the range of 0.02 to 2000μm of particulate materials which include powders, suspensions and emulsions by wet and dry measurements.

pH

The pH of the sludge samples were measured by EUTECH pH/ion/ conductivity/ DO meter (Cyberscan PCD 6500) after calibration.

3.3 RESULTS

3.3.1 Pressure stepping and cycling

In order to observe the effect of measurement methods on the critical flux value, the same mixed liquor (diluted conventional sludge by 2 times), membrane type (MOF) and the same TMP stepping size and interval (0.3 kPa at 10 minutes interval) were applied.

Method 1 : Pressure stepping

As described in Section 2.3.2, the pressure stepping method was applied to measure the critical flux for activated sludge. The data obtained by pressure

stepping method (Table 3-3) was shown in Figure 3-3, which are presented in terms of stationary flux (the average of the last 9 measurements on each pressure step corresponding to 9 min) vs. Pressure. For comparison, the pure water flux is also presented in the same figure. The flux-TMP curve for the mixed liquor was below the clean water flux line for the entire range of pressure evaluated (0.6 – 3.0 kPa), which suggests that the strong form of critical flux did not exist for the current case likely due to adsorption and pore constriction. Instead, a weak form of critical flux was observed during the pressure stepping measurement. The corresponding critical flux value was estimated to be ~17.2 $L/m^2.h$ using the pressure stepping method.

Table 3-3 Pressure stepping with time

Time(min)	0-10	11-20	21-30	311-40	41-50	51-60	61-70	71-80	81-90
TMP(kPa)	0.6	0.9	1.2	1.5	1.8	2.1	2.4	2.7	3.0

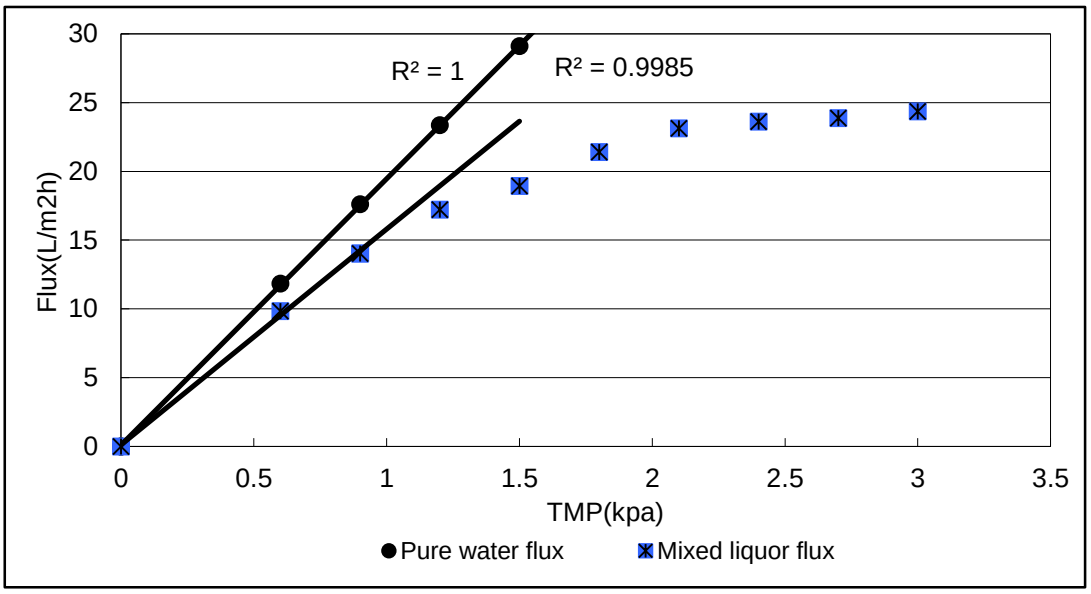

Figure 3-3 The critical flux measurement by pressure stepping method (TMP stepping interval = 0.3kPa) using MOF membrane in diluted conventional sludge.

Method 2: Pressure cycling

The general process of pressure cycling method was introduced in section 2.3.2. In the current study, the detailed pressure cycling program shown in Figure 3-4(a), and the resulting flux versus time plot is shown in Figure 3-4(b). The stationary flux at each pressure step is further plotted against the corresponding pressure in Figure 3-5. The flux value of step (60~70min) was below that of step (30~40min), despite the same pressure of 1.5 kPa was applied in both cases. This indicates some irreversible fouling occurred during the pressure step between 50~60min (TMP = 1.8 kPa). The irreversible critical flux lied between the stationary fluxes of the step (30~40min) and step

(50~60min), 15.2~17.2 L/m^2.h. And an average value of the two fluxes could be used to approximate the critical flux, 16.2 L/m^2.h.

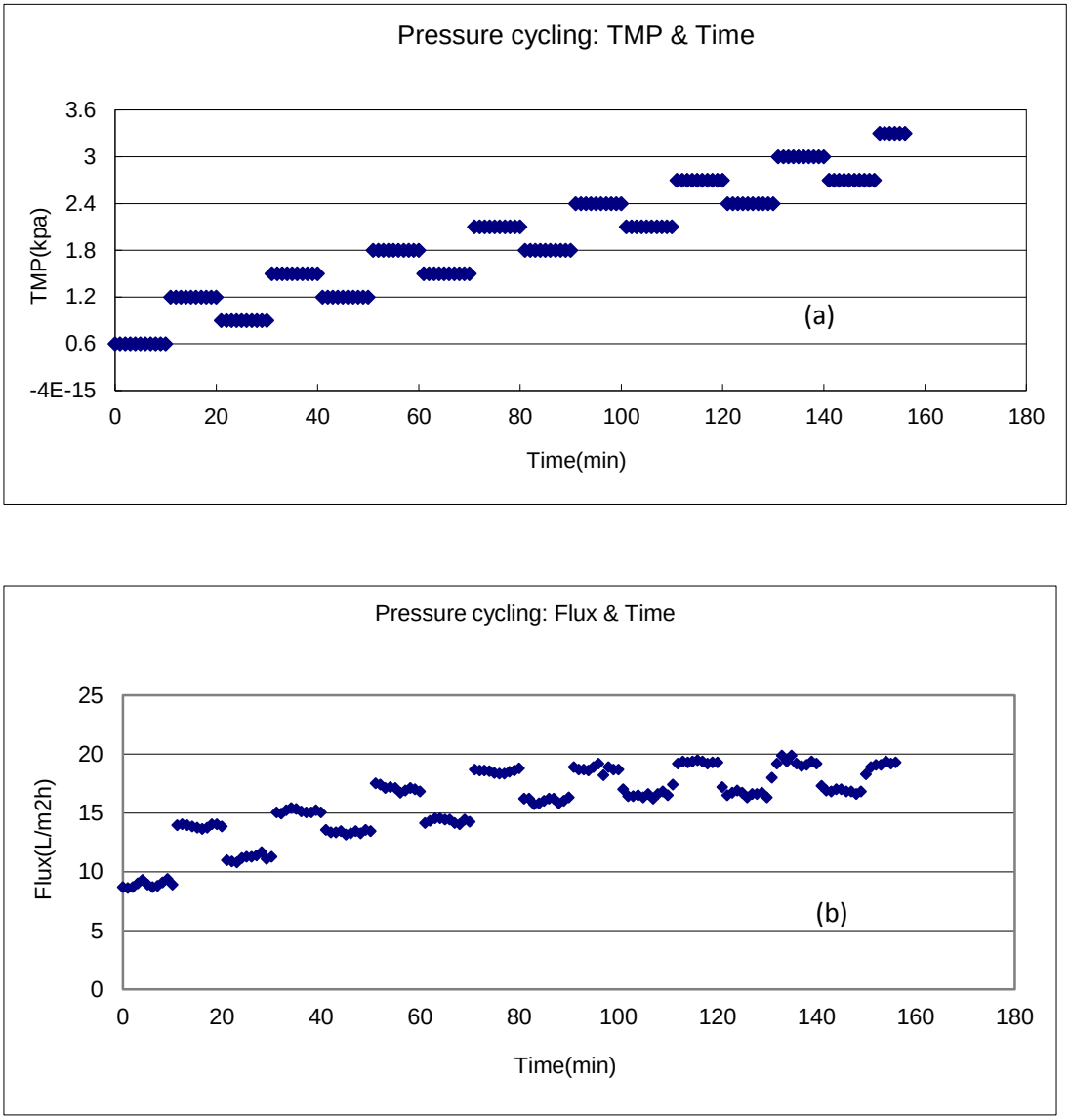

Figure 3-4 (a) Pressure & time in pressure cycling; (b) Flux & time in pressure cycling.

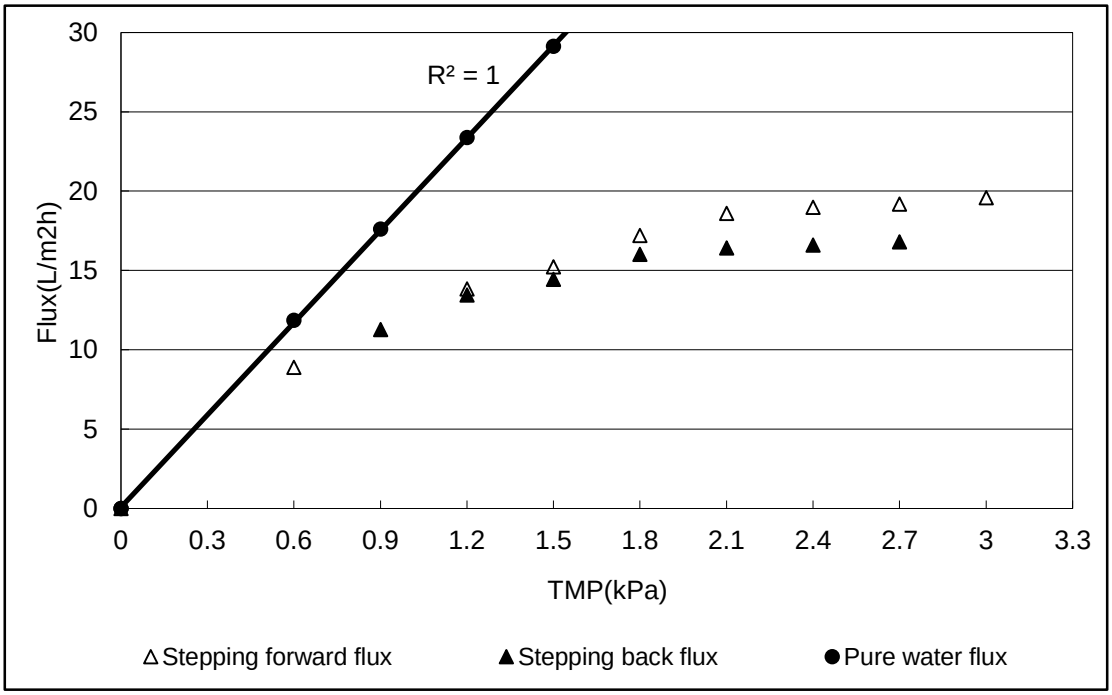

Figure 3-5 Relationship between applied flux and TMP plotted as flux vs. TMP (TMP stepping interval=0.3kPa, using MOF membrane in diluted conventional sludge).

The difference between the initial flux of mixed liquor and pure water flux at the same pressure will be discussed in section 3.3.3.

3.3.2 Pressure stepping using different timescales

Pure water flux for every single module was tested before filtering mixed liquor. The purpose of this was to avoid errors caused by the differences between the membrane modules themselves. Both the activated sludge and MBR sludge were tested in this series of experiments using membrane MIF. The critical flux was measured using simple pressure stepping method with different timescales.

The flux-TMP curves for the activated sludge at stepping intervals of 10 and 30 minutes are presented in Figure 3-6. For a step interval of 10 min, the flux-TMP curve started to deviate from linearity at 6 kPa, corresponding to a flux of 7.40 L/m^2.h. In comparison, such deviate occurred at a lower TMP of 4 kPa when the stepping interval was 30 min (critical flux ~6.28 L/m^2.h). This seems to suggest that the critical flux value was affected by the time interval used for the critical flux determination. Similar effect was also observed using the MBR sludge as the feed (Figure 3-7), where the critical flux corresponding to the 5-min interval was ~ 5 L/m^2.h, compared to ~ 3.5 L/m^2.h for 30-min and 10-min intervals. At shorter time intervals, the amount of foulant accumulating on the membrane may be limited even if fouling had occurred. As the linearity check (which is used to determine critical flux) depends on the sensitivity of flux/pressure measurement, enough time is needed to sense the fouling of the membrane. Therefore, the use of a short stepping duration may lead to a higher measured critical flux.

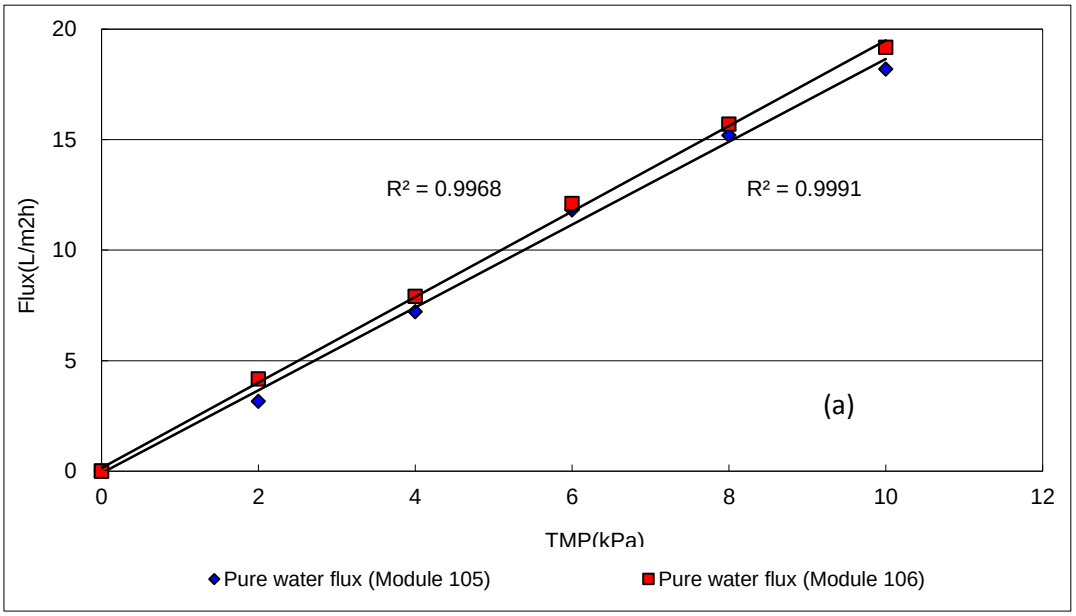

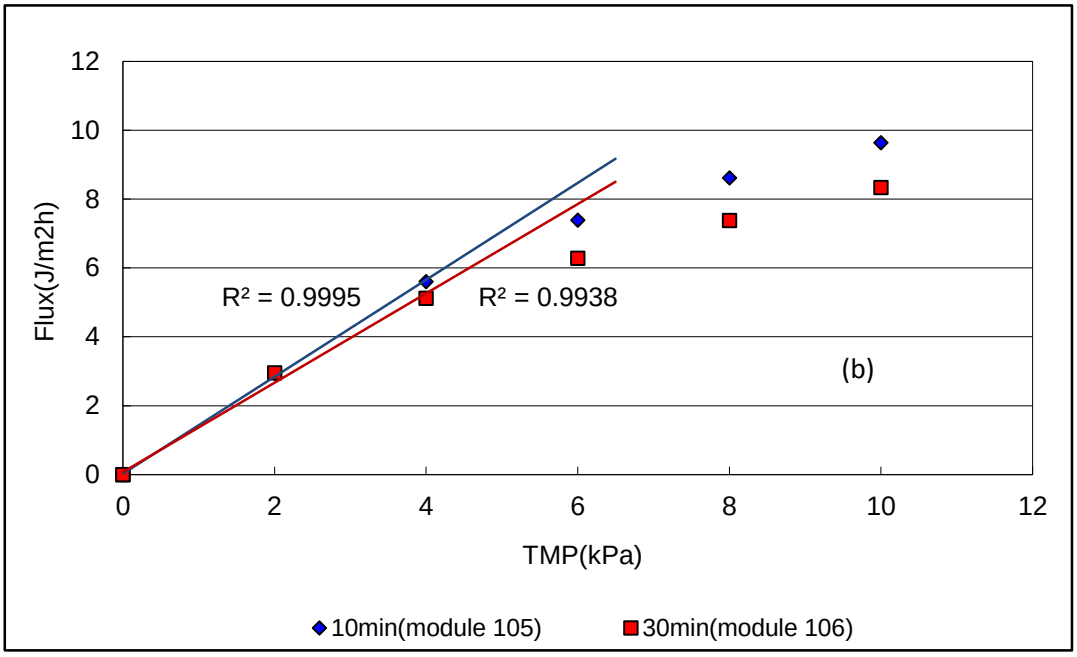

Figure 3-6 Effect of time interval on the critical flux measurement for activated sludge using MIF membrane. (a) Pure water flux for the two membrane modules used in next stage mixed liquor tests; (b) Flux & TMP using different timescales in pressure stepping procedure: 30 min interval during each step for the membrane module 106; 10 min interval for module 105.

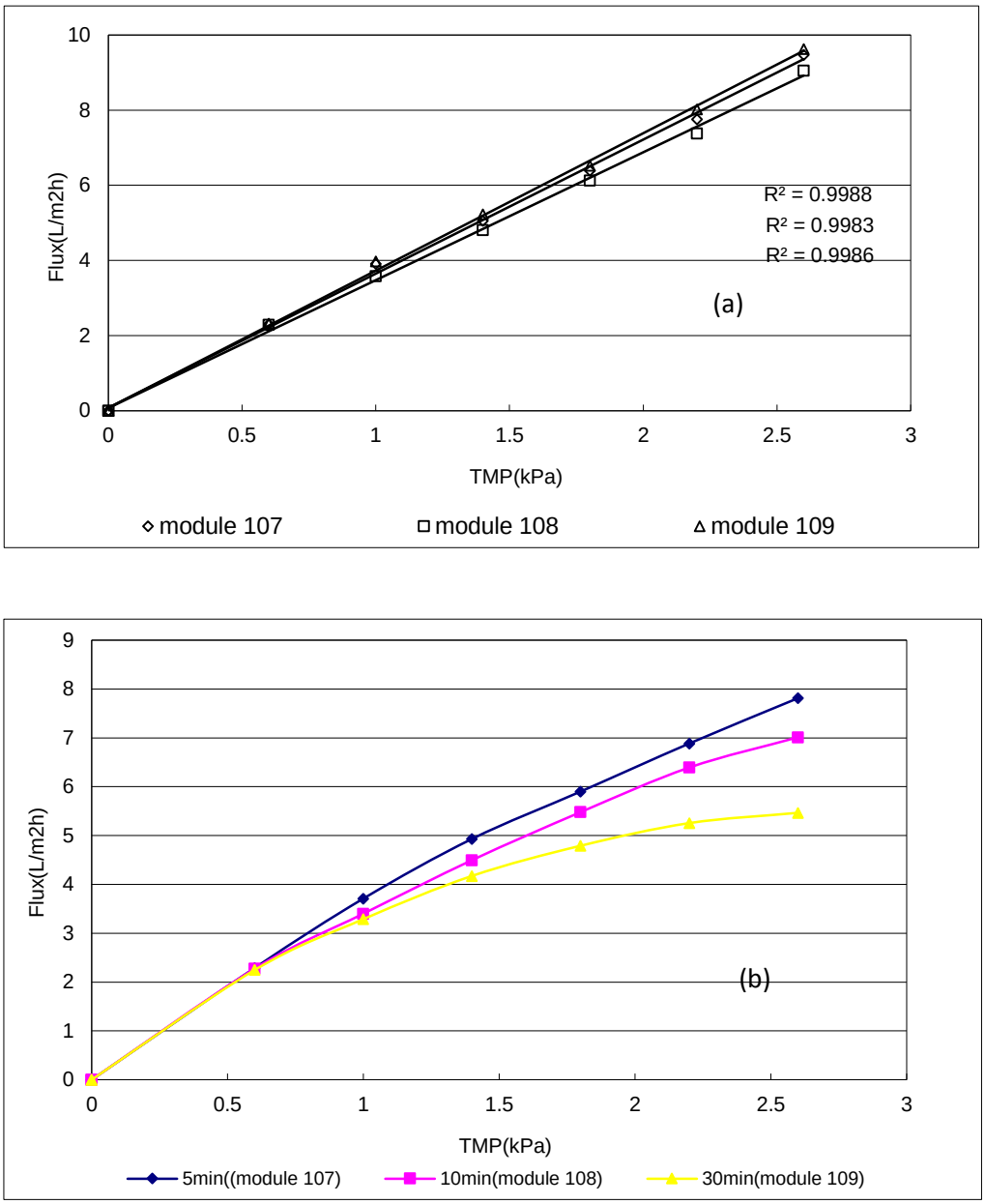

Figure 3-7 Effect of time interval on the critical flux measurement for MBR sludge using MIF membrane. (a) Pure water flux for the three membrane modules used in next stage mixed liquor test; (b) Flux & TMP using different timescales in pressure stepping procedure: 5min interval during each step for the membrane module 107; 10min interval for module 108; 30min interval for module 109.

3.3.3 Pressure stepping in pure water followed by mixed liquor

A difference is observed even between the initial flux of mixed liquor and pure water flux at the same pressure. This could be attributed to several possible reasons: (1) concentration polarization, or (2) adsorption and pore constriction. Additional experiments were performed to gain better understanding by performing pressure stepping experiments for the mixed liquors. However, different from that in Sections 3.1 and 3.2, the clean flux was also measured at the end of each pressure step, before the pressure was stepped up for the next test step. The purpose of the clean water measurement was to check the membrane resistance purely arising from the foulant deposition, but not from concentration polarization.

As illustrated in Figure 3-8, even for the first a few steps during which the fluxes were below the weak form of critical flux (3.7 $L/m^2.h$ for conventional sludge and 3.5 $L/m^2.h$ for MBR sludge), the pure water flux after the membrane (secondary water flux) exposure to sludge was already below the original pure water flux. This difference could only be caused by foulant deposition, since there shall be no concentration polarization using a pure water as the feed. Thus, the weak form of critical flux behaviour in the current study is attributed to membrane adsorption and pore closure. A simple mathematical analysis was conducted in Appendix Section A.

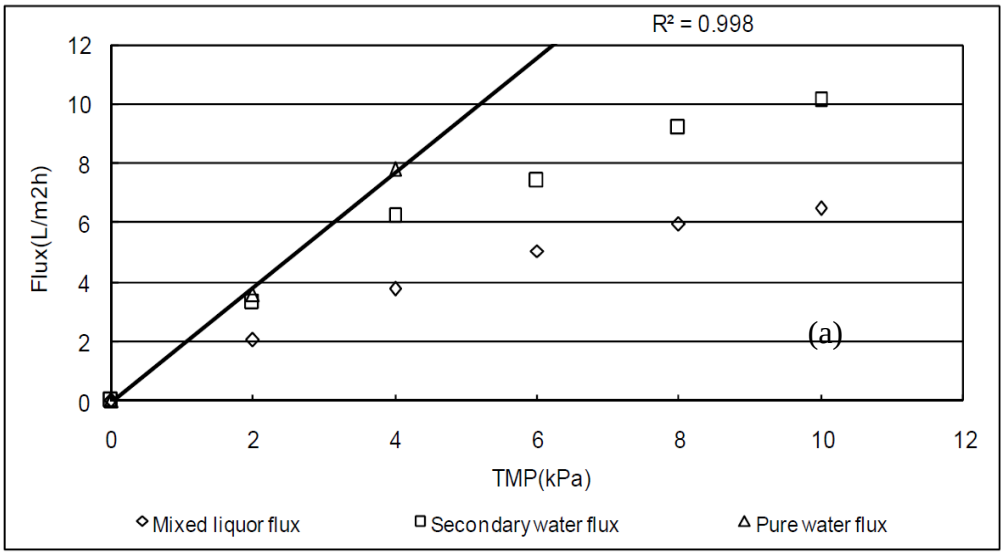

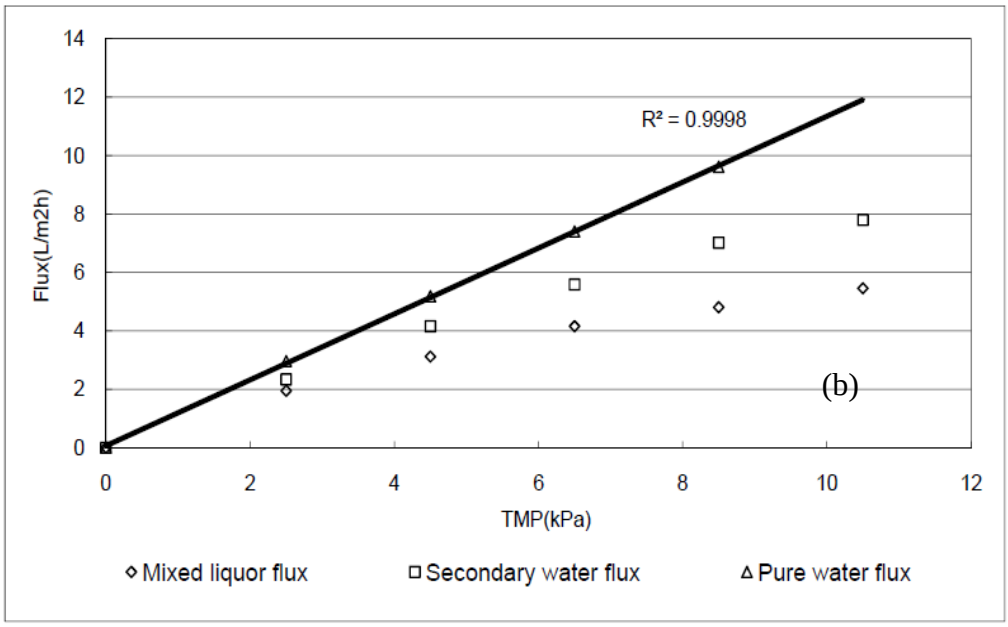

Figure 3-8 Mixed liquor flux and secondary water flux on MOF membrane by pressure stepping method. (a) Conventional sludge was used as mixed liquor; (b) MBR sludge was used as mixed liquor.

3.3.4 Existence of limiting flux

Figure 3-10 shows the flux performance of MIF membrane during 3-6 hours fouling test. The applied pressure ranged from 15 to 50kPa. Clearly, the initial flux was greater at higher transmembrane pressure. However, membrane samples with elevated initial fluxes ($>4\,L\cdot(m^2\cdot h)^{-1}$) were significantly fouled during the test, and their fluxes declined continuously. The rate of flux decline was greater for samples with greater initial fluxes. In addition, the rate of flux decline under a given pressure was greatly reduced at longer filtration time when the flux became much lower than the corresponding initial flux. Near the end of the 6 hours period, further changes in permeate fluxes for all the membrane samples became very slow (rate of flux decline $<0.005\ \ L\cdot(m^2\cdot h)^{-1}$ over a 30 minutes duration), and the fluxes are considered pseudo stable. Interestingly, membrane samples with high initial fluxes ($>4\,L\cdot(m^2\cdot h)^{-1}$) ended up with almost identical pseudo stable fluxes. On the other hand, samples with low initial fluxes ($<4\,L\cdot(m^2\cdot h)^{-1}$) had neglectable flux decline. Similar results have been reported by Tang et al. (2007) for RO and NF membranes fouled by humic acid, who suggested that the greater flux reduction at higher initial flux is probably due to the increased hydrodynamic drag force on humic molecules, in addition to concentration polarization.

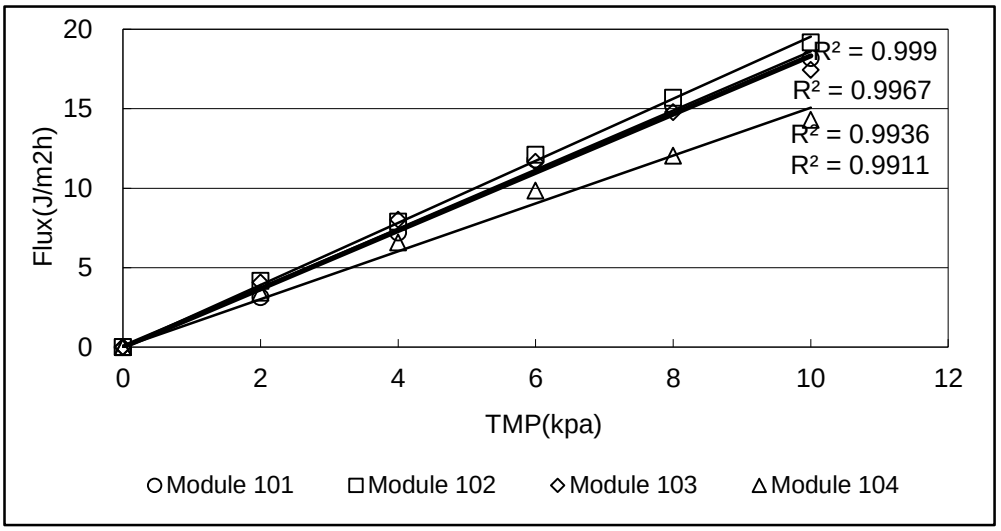

Figure 3-9 Pure water flux for MIF membrane modules (101-104).

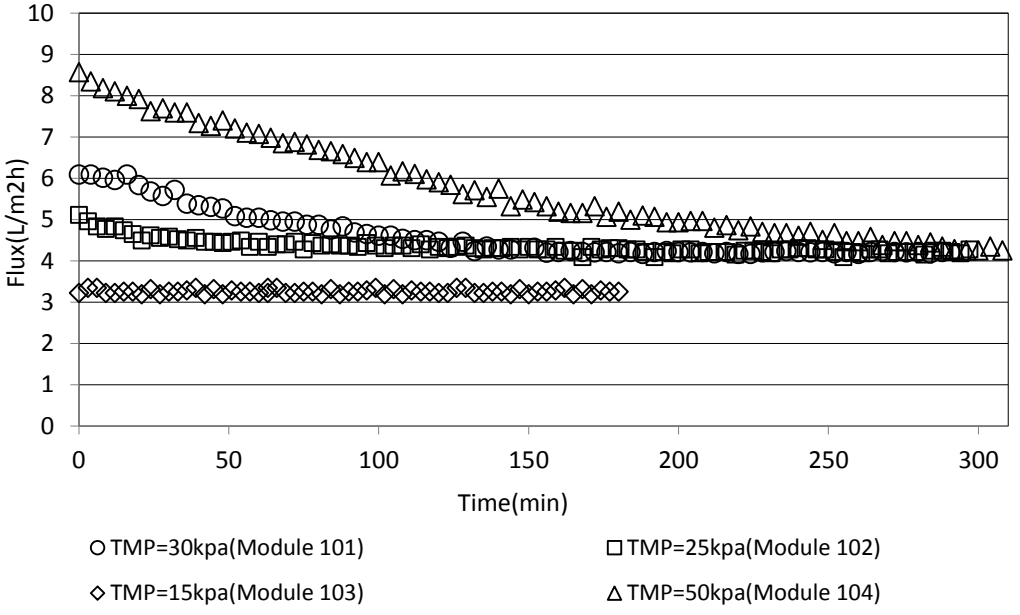

Figure 3-10 The existence of limiting flux for MBR sludge using MIF.

3.3.5 Limiting flux measurement using membranes with different pore size

Figure 3-11 plots the initial flux and pseudo stable flux against applied pressure. The initial flux for the first three points increased almost linearly with applied pressure over 0-30 kPa, in good agreement with Darcy's law. At an applied pressure of 40 kPa, however, the initial flux was lower than expected, which may be attributed to membrane compaction or rapid initial fouling. On the other hand, the pseudo stable flux was nearly identical at TMP > 20 kPa. The corresponding limiting flux was ~ 4 L/m^2.h.

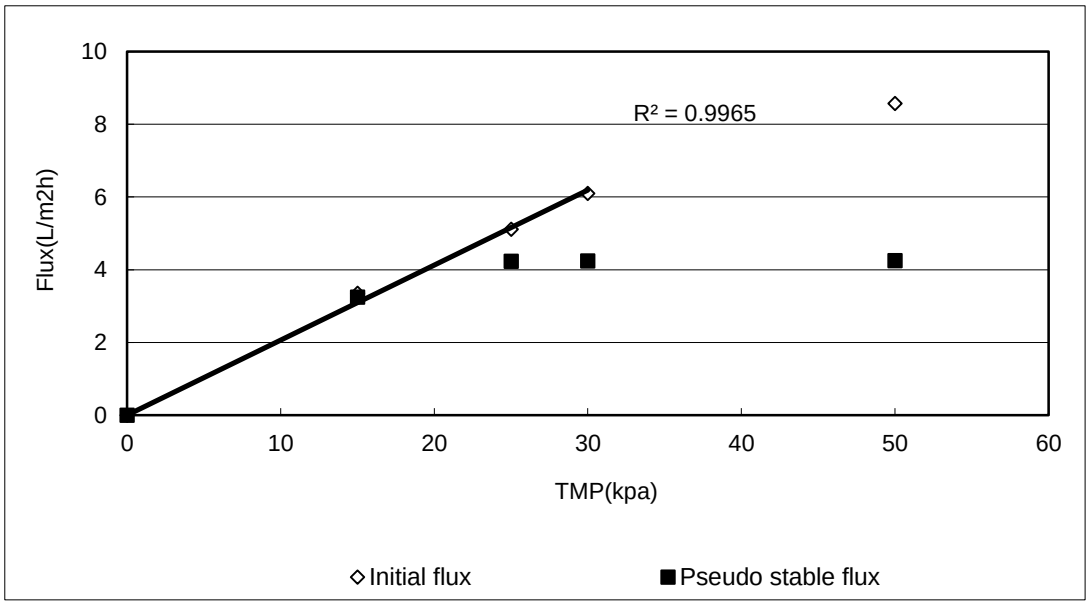

Figure 3-11 Initial flux and pseudo stable flux vs. applied pressure.

Figure 3-12 shows the flux performance of membranes with different pore size (MOF membrane-0.2μm; MIF membrane-0.1μm) under the same given pressure of 25 kPa. The values of pseudo stable flux at the end of the 4 hours

filtration test for two membrane types are equal to each other under the same constant pressure operation condition. This result suggests that the limiting flux is likely independent of membrane properties even for porous membranes. Previous studies by Tang and co-workers (Tang et al., 2007; Tang et al., 2009) observed that the limiting flux value is not affected by membrane properties based on the evaluation of 11 RO and NF membranes.

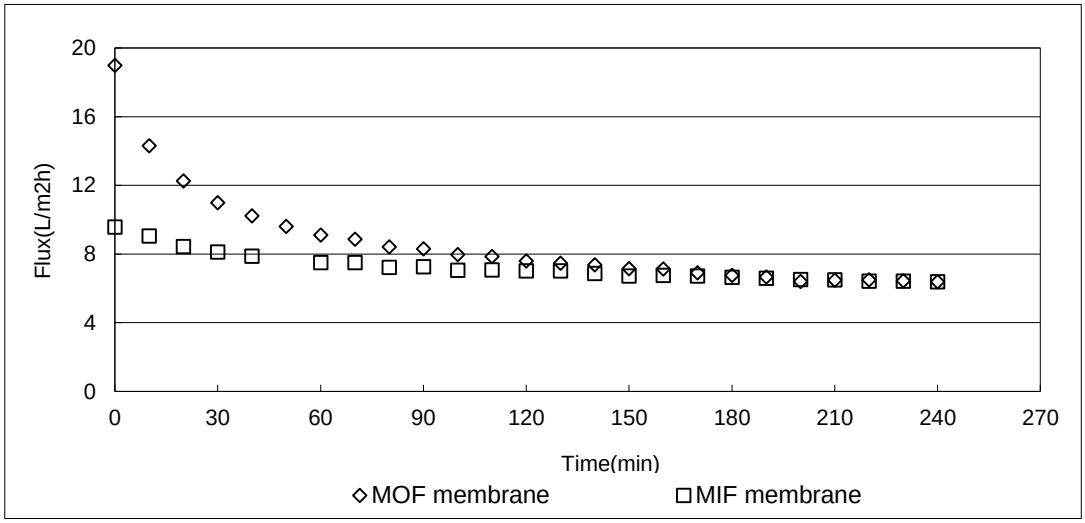

Figure 3-12 The independence of membrane pore size on limiting flux (MOF membrane-0.2μm; MIF membrane-0.1μm) under the same constant TMP of 25kPa.

3.3.6 Limiting flux tests using different types of mixed liquor

The same experimental procedure as depicted in section 3.3.4 was carried out in determination of limiting flux for different mixed liquor (sludge A, MLSS ~ 2180 mg/L), conventional sludge and MBR sludge (sludge B, MLSS ~ 3840 mg/L).

Figure 3-10 and Figure 3-13 show the flux performance of MIF membrane in conventional and MBR sludge, respectively. With an increment of MLSS value, the limiting flux for sludge B (4 L/m^2.h) was significantly lower than that for sludge A (7 L/m^2.h).

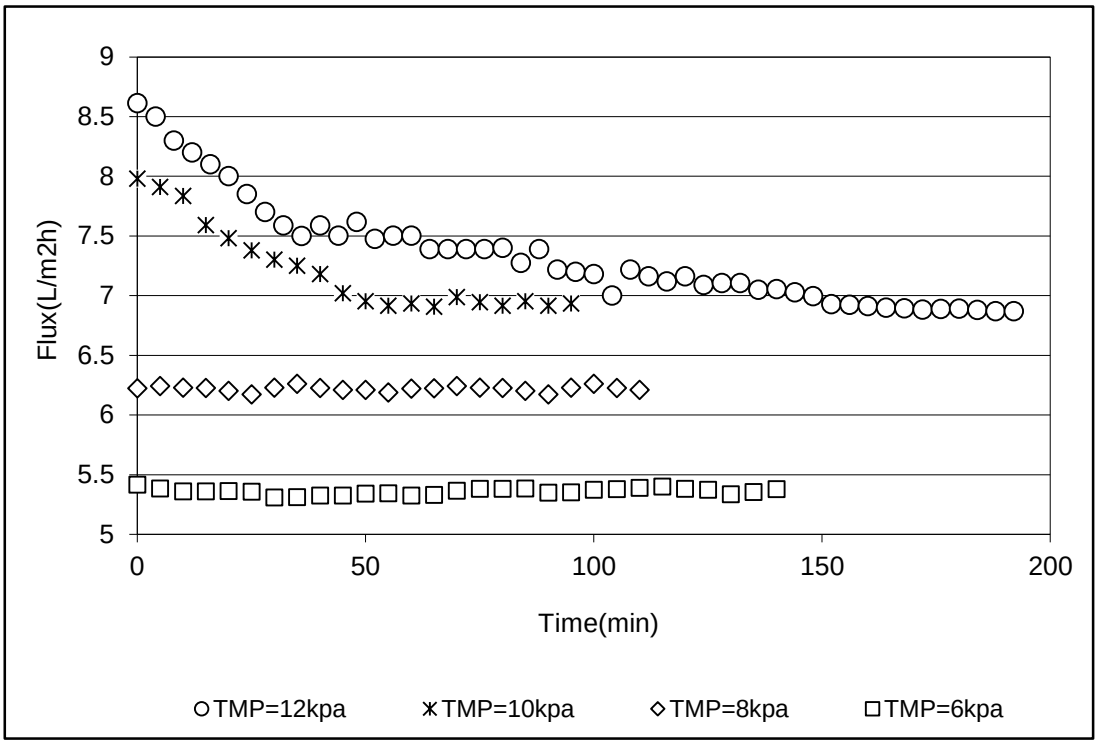

Figure 3-13 The existence of limiting flux for activated sludge using MIF.

3.4 Discussion

3.4.1 Comparison of different measurement methods for critical flux determination

As illustrated by Wu et al. (1999), the transition from reversible fouling to irreversible fouling occurs either at the same point as the deviation from linearity or it occurs at a higher flux. Clearly a check of reversibility is required. Compared with simple pressure stepping method and pressure cycling method allows a continuous quantification of fouling reversibility to determine the two critical fluxes: the "critical flux for irreversibility", J_{ci} as well as the strong form of critical flux, J_{cs}.

On the other hand, the different measurement procedures also influenced the critical flux value determination. As illustrated in Figure 3-14, for simply pressure stepping or pressure cycling methods, with the same pressure step interval and time interval, the latter one will go through a longer filtration period when achieving the same higher pressure step.

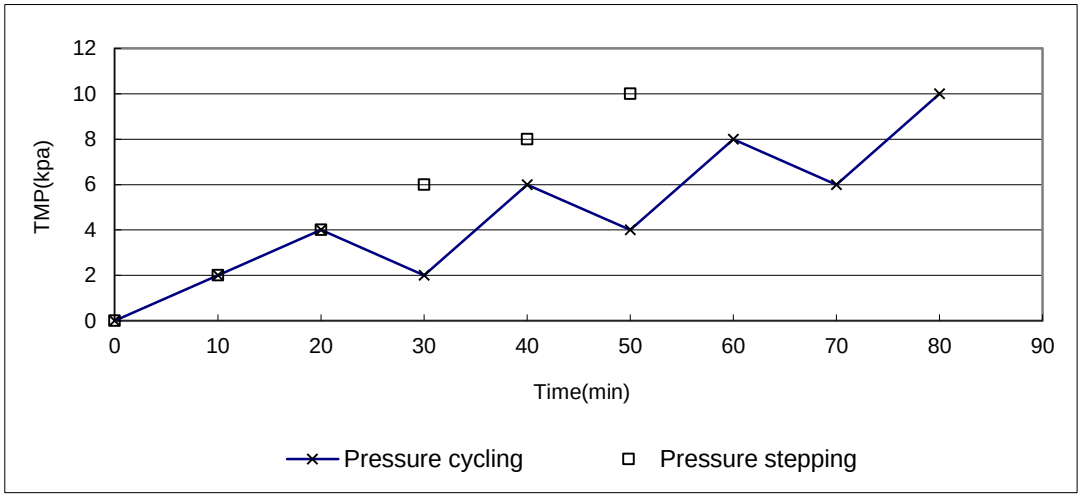

Figure 3-14 An example of experimental procedures for pressure cycling and stepping methods for critical flux determination.

3.4.2 Effect of timescales on critical flux measurement

Timescales of measurement are important if membrane fouling is slow. The amount of foulant deposition (and thus the additional hydraulic resistance due to fouling) relative to the membrane resistance determines if the effect of fouling (the deviation from a linear flux-TMP behaviour) can be experimentally determined. Thus, the critical flux value will be strongly affected by the step interval used for the measurement, with a longer time interval giving a lower (but more realistic) critical flux value. In contrast, if membrane fouling occurs very rapidly, the effect of timescales might be negligible. As a result, the difference of critical flux obtained using different timescales should be in an acceptable range.

3.4.3 Limiting flux

The current study demonstrated a limiting flux behaviour during sludge filtration by MF membranes. Furthermore, the limiting flux did not depend on the membrane pore size. This observation is consistent with previous studies by Tang and co-workers (Tang et al., 2007; Tang et al., 2009). Based on the discussion and experimental results by these authors, the permeate flux will get to a steady state when the hydrodynamic drag force is quite close to the forces of foulant-membrane and/or foulant- foulant interaction. As a result, the threshold limiting flux is probably contributed only by the interaction forces between the foulants, but has no relationship with the initial flux or membrane material. The gained data showed in Section 3.3.4 showed that the independence of membrane porosity on limiting flux tally closely with the conception.

Many studies show a decrease in the critical flux when the suspension concentration rises. A similar trend between MLSS concentration and limiting flux was observed in current study that a higher MLSS mixed liquor environment resulted in a lower limiting flux.

3.5 Conclusions

Some basic properties of critical and limiting flux in batch scale mixed liquor culture tests were investigated. Results from this study shows:

- The effects of determination methods and timescales of the measurement on critical flux investigated in the study are in good agreement with the former results by some researchers (Bacchin et al., 2006). The pressure cycling method could be considered as a more accurate measurement to determine the strong form and the weak form critical flux. With the regard of timescale, a proper time interval should be chosen to avoid any ignorance of irreversible fouling since some macro-fouling could only be observed to a certain extent of accumulation.

- The existence of limiting flux for complex suspensions and its independence of membrane porosity and the dependence of MLSS value were investigated as well. The data obtained in the study is consistent with the former conceptual limiting flux model (Tang and Leckie, 2007).

Chapter 4 Membrane Fouling and Flux Reduction during Algae Separation

4.1 Introduction

Separation of microalgae cells from source water has gained a resurgence of research interest in recent years (Amin, 2009). Microalgae convert carbon dioxide and sunlight into algal biomass - a promising biofuel source (Clarens et al., 2010; Mata et al., 2010). Engineered algae photobioreactors may also be used for carbon dioxide removal and thus reducing greenhouse gas emission (e.g., flue gas from coal fired power plants) (Brune et al., 2009; Clarens et al., 2010; Packer, 2009) as well as for wastewater treatment (de-Bashan et al., 2008a; Muñoz and Guieysse, 2006). In these applications, algal biomass separation is a critical aspect for subsequent biofuel production as well as for maintaining a stable reactor operation. In parallel, it is also well known that seasonal algal bloom can have severe adverse impacts on surface water qualities. In some severe cases, the release of algal toxin and the production of unpleasant color and odor can even make the water unsuitable as a drinking water source (Henderson et al., 2008; Karner et al., 2001). Once again, microalgae removal is important from drinking water production perspective.

Conventional methods, such as coagulation, flocculation, flotation and centrifugation, have been traditionally used for algae separation. In parallel, membrane filtration (e.g., microfiltration (MF) and ultrafiltration (UF)) has received increased attention due to its high separation efficiency and easy

operation (Kwon et al., 2005; Zhang et al., 2010a). For example, Zhang et al. (Zhang et al., 2010a) used a UF process to harvest and dewater algal cells, where cross-flow filtration and air-assisted backwash were used to maintain a high water flux. Unfortunately, these pressure-driven MF and UF membrane processes are prone to fouling and are relatively energy intensive. The search for an ideal algae separation technology with high separation efficiency and low energy input is an ongoing research topic.

Recently, forward osmosis (FO) has emerged as a promising alternative membrane separation technology (Cath et al., 2006). Driving by the concentration difference across a solute-rejecting dense membrane, FO does not require an external applied pressure. A pure water flux is established spontaneously across the FO membrane from a low concentration feed water (FW) to a high concentration draw solution (DS) under the chemical potential gradient (Cath et al., 2006). Compared to pressure-driven MF and UF processes, FO offers many advantages including 1) better separation efficiency thanks to its nonporous rejection layer (Achilli et al., 2009) and 2) potentially lower power consumption (e.g., in the case where a high osmotic pressure DS, such as seawater, is naturally available). Consequently, FO may have many potential applications in water and wastewater treatment (Achilli et al., 2009; Cornelissen et al., 2008), desalination (McCutcheon et al., 2006), food processing (Petrotos et al., 1998), and electricity production (i.e., osmotic power harvesting using a derivative pressure retarded osmosis process) (Lee et al., 1981; Loeb, 2002; Xu et al., 2010). The National Aeronautics and Space Administration (NASA) of the United States has further proposed to

implement FO in an algae photobioreactor that receives sewage for algae cultivation and subsequently biofuel production in a project named Offshore Membrane Enclosure for Growing Algae (OMEGA) (Marlaire, 2009a; Soderman, 2010). In this project, the semi-permeable FO membrane is used to retain algal biomass as well as the nutrients required for their growth, while the contaminant-free water is extracted through the FO membrane by the high osmotic pressure seawater.

A significant challenge in FO applications is membrane fouling. Despite that FO may potentially have lower fouling propensity compared to pressure-driven membranes (Achilli et al., 2009; Cornelissen et al., 2008; Mi and Elimelech, 2010), drastic flux loss can occur under certain unfavorable conditions such as high draw solution concentrations and high flux levels (C. Y. Tang et al., 2010; Mi and Elimelech, 2008; W. C. L. Lay et al., 2010). In addition, the solute back diffusion from the high concentration DS to the feed water, a unique phenomenon in the concentration-driven FO process (C. Y. Tang et al., 2010), may also have critical impact on FO fouling.

The objective of the current study was to investigate the effect of physical (flux level, membrane orientation, and cross flow) and chemical parameters (feed water chemistry as well as draw solution chemistry) on concentration-driven FO fouling phenomenon and flux behavior during algae separation. To our best knowledge, this is the first systematic study on 1) algal fouling of FO membranes and 2) the effect of solute back diffusion on FO fouling.

4.2 Materials and methods

4.2.1 Chemicals and materials

All the reagents and solutions were prepared with analytical grade chemicals and ultrapure water (ELGA water purification system, UK) unless stated otherwise. The microalgae species Chlorella Sorokiniana (C.S) was used as the model algae. C.S is unicellular green algae with an average cell diameter of ~5 µm. C.S species grows rapidly even under extreme conditions, and it has been widely used for wastewater treatment as well as for biodiesel production (de-Bashan et al., 2008a; Mata et al., 2010). The microalgae were cultivated with the synthetic medium mixture of BG 11 following the method described by Bordel et al. (2009).

The flat-sheet FO membrane used in the current study was obtained from Hydration Technology Inc. (Hydrowell Filter, HTI, Albany, OR). The membrane properties have been reported by several previous studies (C. Y. Tang et al., 2010; Cath et al., 2006; Gray et al., 2006; McCutcheon and Elimelech, 2006). Briefly, the membrane is made of cellulose triacetate (CTA) with an embedded polyester mesh for mechanical support (C. Y. Tang et al., 2010; Cath et al., 2006). Compared to typical thin film composite RO membranes, the HTI membrane has a much thinner cross-section (< 50 µm), which is presumably designed to minimize internal concentration polarization (ICP) in the porous support layer (C. Y. Tang et al., 2010; Cath et al., 2006). The water permeability and solute rejection of the membrane shows some slight batch-dependent variations (C. Y. Tang et al., 2010; Gray et al., 2006). In

the current study, all the FO membrane coupons were obtained from the same batch, and they were tested in a cross flow reverse osmosis setup to measure its water flux and solute rejection over an applied pressure range of 0 to 17 bar (Figure 4-1(a)) in order to determine their separation properties (C. Y. Tang et al., 2010).

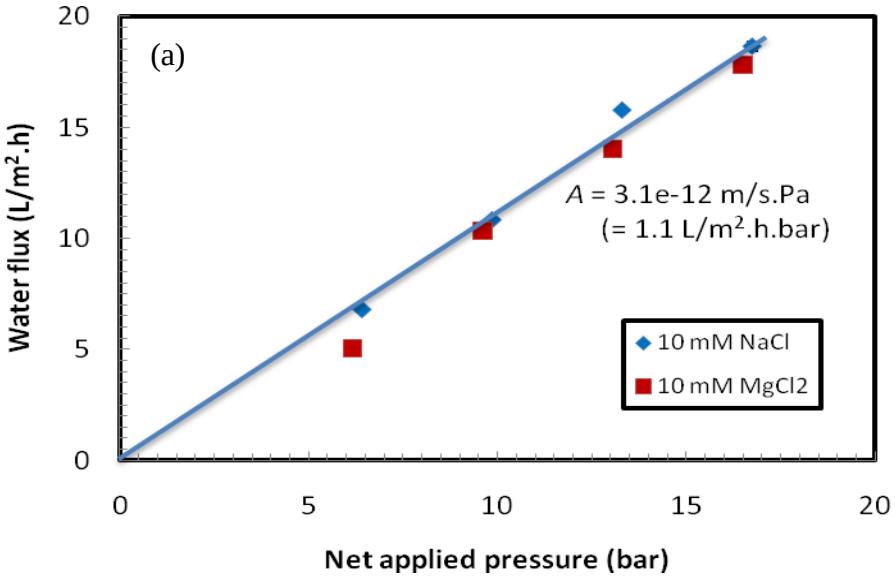

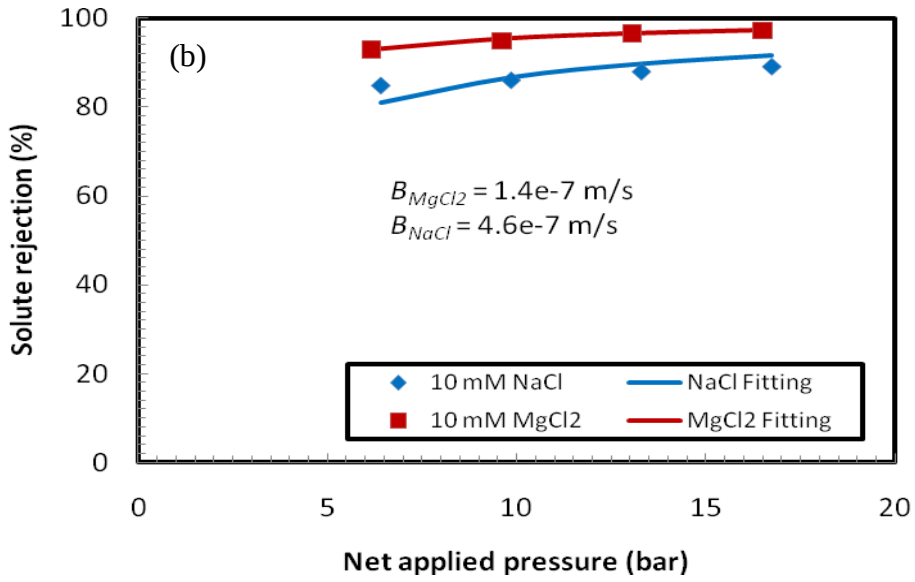

Figure 4-1 ater flux (a) and solute rejection (b) as a function of applied pressure for the HTI membrane tested in RO mode. The feed water contained either 10 mM NaCl or 10 mM $MgCl_2$.

The water permeability coefficient A was obtained from the water flux vs. applied pressure plot, while the solute permeability coefficient B was evaluated by fitting the rejection vs. pressure curve based on the following equation (C. Y. Tang et al., 2010):

$$R = \left(1 + \frac{B}{A(\Delta P - \Delta\pi)}\right)^{-1} \qquad 4.1$$

where R is the measured solute rejection; ΔP and $\Delta\pi$ are the hydraulic pressure difference and osmotic pressure difference across the membrane, respectively. Based on Figure 4.1(b), the following separation properties were determined:

A = 3.1 x 10^{-12} m/s.Pa = 1.1 L/m^2.h.bar

B_{NaCl} (for sodium chloride) = 4.6 x 10^{-7} m/s

B_{MgCl2} (for magnesium chloride) = 1.4 x 10^{-7} m/s

4.2.2 FO experiments

FO experiments were performed using a bench-scale cross flow FO setup according to the studies (Ref. (C. Y. Tang et al., 2010) and Figure 4-2). For each test, a clean FO membrane coupon (~ 60 cm^2 active membrane area) was used in the cross flow test cell. Diamond-patterned spacers were placed in both the feed water and draw solution flow channels. Variable speed peristaltic pumps were used to maintain the desired cross flow velocities for both the feed water and the draw solution, respectively. The draw solution tank contained concentrated sodium chloride (0.3 - 5M) or magnesium chloride (0.5 and 2 M) solutions, while Chlorella sorokiniana was added to the feed tank as model foulant. The feed water tank was placed on a digital balance that was connected to a computer data logging system, and the mass of the feed tank was recorded at regular time intervals to determine the permeate water flux through the FO membrane. In addition, the feed water conductivity was also monitored in order to determine the solute back diffusion from the draw solution to the feed water. Where $MgCl_2$ was used as draw solution, samples were also taken from the feed tank at predetermined intervals for subsequent measurement of magnesium concentrations using inductively coupled plasma

mass spectrometry (ICP/MS, PerkinElmer Optima 2000DV).

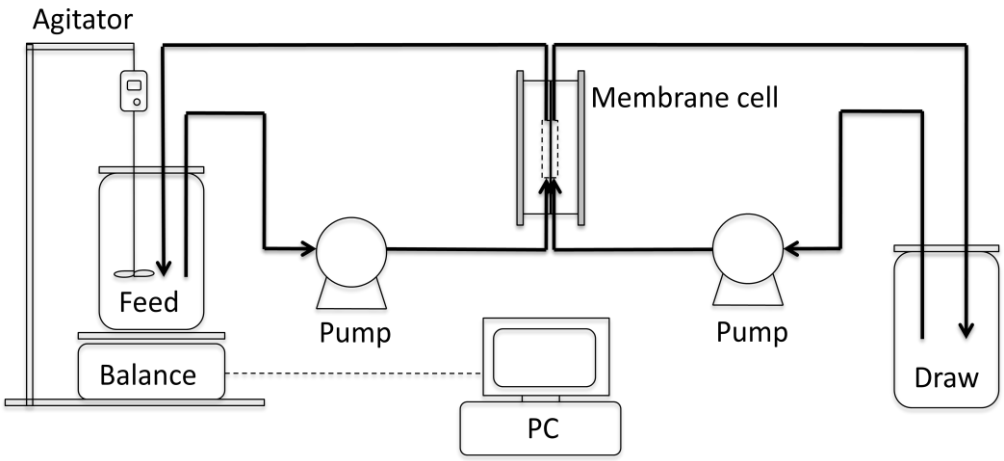

Figure 4-2 Schematic diagram of the bench-scale forward osmosis (FO) test setup.

For a typical FO experiment, the FO membrane coupon was first equilibrated with the draw solution and foulant-free feed water for 30 minutes to achieve a stable water flux. Algae stock solution was then added to the feed water to initiate the membrane fouling, and the fouling test was continued for another 4 hours. The pH of the feed water was adjusted by addition of hydrochloric acid and/or sodium hydroxide, and its value was relatively stable throughout the equilibration and fouling stages (targeted pH value +/- 0.1). The effect of various physical (flux level, membrane orientation, and cross flow velocity) and chemical parameters (pH and magnesium concentration in the feed water, and draw solution type) on FO fouling by algae was investigated by varying one parameter each time. Unless otherwise stated, the following reference testing conditions were adopted:

Feed water: 100 mg/L algae in 10 mM NaCl at pH 5.8

Draw solution: concentrated NaCl solution (0.3 – 5.0 M)

Membrane active layer facing the draw solution (AL-facing-DS orientation)

Cross flow velocity for both FW and DS: 22.5cm/s

Temperature of 22 ± 1 ℃

Since FO flux may also be affected by factors other than fouling, such as the dilution of draw solution (C. Y. Tang et al., 2010; Xu et al., 2010) and internal concentration polarization (C. Y. Tang et al., 2010), baseline tests were also conducted. Each baseline was performed under conditions identical to the corresponding fouling test, except no algae biomass was introduced to the feed water. The extent of membrane fouling can be determined by comparing the water flux in a fouling test to the corresponding baseline flux. Similar methodology was adopted in prior studies (C. Y. Tang et al., 2010; Mi and Elimelech, 2008).

4.3 Results and discussion

4.3.1 FO baseline behavior

Baseline tests were conducted to determine the FO performance in the absence of membrane fouling, and the FO water flux (J_v) and solute flux (J_s) are

presented in Table 4-1.

Both the active-layer-facing-the-draw-solution (AL-facing-DS) and the active-layer-facing-the-feed-water (AL-facing-FW) membrane orientations were evaluated. For both orientations, it is clear that the FO water flux increased with increasing draw solution concentrations (C_{ds}) as a result of the greater apparent driving force across the membrane (i.e., the concentration difference between the DS and FW). However, while the classical solution-diffusion model predicts a linear J_v versus C_{ds} relationship, the experimental water flux was highly non-linear with respect to the DS concentration. Consider the AL-facing-DS orientation using NaCl as the draw solution, the water flux was only increased by ~ 60% when C_{ds} was doubled from 0.5 M to 1.0 M. Further increasing the DS concentration was even less effective to increase the water flux (35% increase in water flux when C_{ds} increased from 1 M to 2 M, and 32% increase corresponding to 2 M → 4 M). Such reduced effectiveness of draw solution concentration has been reported previously by several research groups and has been attributed to ICP, i.e., the accumulation (or dilution) of solutes in the porous support layer of the FO membrane (C. Y. Tang et al., 2010; Gray et al., 2006; Lee et al., 1981; McCutcheon and Elimelech, 2006; Xu et al., 2010). In the AL-facing-DS orientation, the ICP phenomenon is caused by 1) the accumulation of the solutes from the feed water that are retained by the FO

Table 4-1 FO water flux (J_v) and solute flux (J_s) under baseline conditions where no foulant was added to the feed water.

Draw Solution	Membrane Orientation	Draw Solution Concentration (M)	J_v (L/m^2.h)	J_s (mole/m^2.h)	J_s/J_v (M)	$B/(A.\beta R_g T)$ (M)
NaCl	AL-facing-DS	0.5	16.9	0.52	0.0307	0.031
		1.0	26.8	0.83	0.0310	
		2.0	36.3	1.17	0.0323	
		4.0	48.1	1.52	0.0316	
	AL-facing-FW	0.5	10.1	0.34	0.0338	
		1.0	15.8	0.53	0.0335	
		2.0	22.9	0.81	0.0353	
		4.0	28.8	1.02	0.0353	
$MgCl_2$	AL-facing-DS	0.5	22.3	0.13	0.0059	0.0063
		2.0	55.4	0.37	0.0066	

rejection layer, and 2) the back-diffused solutes across the FO membrane from the high concentration DS (C. Y. Tang et al., 2010). As a result of such solutes accumulation inside the support layer (the concentrative ICP (McCutcheon and Elimelech, 2006)), the effective driving force for FO (i.e., the concentration difference across the rejection layer of the membrane) is significantly less than the apparent driving force (i.e., the concentration difference between the DS and FW), which explains the FO water flux inefficiency as well as its non-linearity (C. Y. Tang et al., 2010; Cath et al., 2006). Furthermore, ICP becomes more severe at greater C_{ds} due to the higher water flux level (C. Y. Tang et al., 2010; Cath et al., 2006), which is responsible for the experimental observation that water flux enhancement by increasing C_{ds} became marginal at higher DS concentrations. Compared to the AL-facing-DS orientation, the FO water flux in the AL-facing-FW orientation was significantly lower under otherwise identical experimental conditions (Table 4-1). In the latter orientation, the solute concentration inside the porous support layer ($C_{support}$) can be drastically diluted by the FO permeate water [the dilutive ICP (McCutcheon and Elimelech, 2006)], causing $C_{support} << C_{ds}$. In general, the dilutive ICP is more severe than the concentrative ICP (C. Y. Tang et al., 2010; Cath et al., 2006; McCutcheon and Elimelech, 2006; Wang et al., 2010a), consistent with the lower water flux observed in AL-facing-FW orientation in the current study.

The solute flux J_s (Table 4-1) had a similar dependence on the DS concentration such that 1) J_s increased at greater C_{ds}, and 2) the increase in J_s became less effective at higher C_{ds}. Indeed, the ratio of the solute flux to the water flux (J_s/J_v) was nearly constant, which suggests that the solute flux may also be affected by ICP. While the FO water flux has been extensively studied

(C. Y. Tang et al., 2010; Gray et al., 2006; Lee et al., 1981; McCutcheon and Elimelech, 2006; Wang et al., 2010a), there have been only a handful studies on solute back diffusion in FO (C. Y. Tang et al., 2010; Wang et al., 2010a). Tang et al. (C. Y. Tang et al., 2010) suggested that ICP can significantly reduce the solute back diffusion since J_s is directly proportional to the concentration difference across the FO rejection layer (which is reduced at more severe ICP). According to their model, the J_s/J_v ratio is given by

$$\frac{J_s}{J_v} = \frac{B}{A \cdot \beta R_g T} \qquad 4.2$$

where β is the van't Hoff coefficient, A and B are defined in Eq 4.1, R_g is the universal gas constant, and T is the absolute temperature. For the case of using NaCl as draw solution, Equation 4.2 predicts a constant J_s/J_v ratio of 0.031 M regardless of the membrane orientation and the DS concentration, which is in good agreement with the experimental results (Table 4-1). It is worthwhile to note that the J_s/J_v ratio carries a concentration unit, and this ratio may be regarded as the effective concentration of solutes leaking through the membrane from the draw solution. A high J_s/J_v ratio is highly undesirable, as this may adversely affect the FO process (e.g., the solute back diffusion contributes to the ICP inside the support layer as well as increasing the bulk feed water concentration in an FO reactor). In addition, the J_s/J_v ratio also represents a loss term for the draw solutes per unit of permeate water produced. Where draw solution recovery is necessary, the replenishment of draw solutes may require additional operational cost to run an FO process.

Magnesium chloride draw solutions resulted in higher water flux and lower

solute flux when compared to NaCl draw solutions at equal molar concentration (Table 4-1). The reduced solute back diffusion can be attributed to the significantly better rejection of $MgCl_2$ ($B_{MgCl2} << B_{NaCl}$ for the HTI FO membrane used in the current study). The predicted J_s/J_v is 0.0063 M using $MgCl_2$ as DS (Equation 4.2), which once again agrees very well with the experimental measurements. Meanwhile, the higher water flux for $MgCl_2$ DS may be partly explained by the higher osmotic pressure of $MgCl_2$ solutions compared to NaCl DS at equal molar concentration (Cath et al., 2006). In addition, the reduced J_s for $MgCl_2$ means reduced ICP, which also helps to enhance the FO flux. Therefore, compared to NaCl, $MgCl_2$ as a DS enjoys the simultaneous advantages of high water flux and low solute flux, an ideal combination for FO applications. In the absence of membrane fouling, $MgCl_2$ may be preferred over NaCl as a potential draw solution, especially when a loose FO membrane (e.g., with a nanofiltration-like rejection layer) is to be used.

4.3.2 FO fouling behaviour

4.3.2.1 Effect of physical parameters

The effect of physical parameters (flux level, membrane orientation, and cross flow velocity) on FO fouling by microalgae is reported in this section. Figure 4-1(a) shows the FO fouling behavior at various initial flux levels (achieved by using different DS concentrations) for the Al-facing-DS orientation. As discussed in Section 4.3.1, higher initial flux levels were achieved at greater DS concentrations. The baseline flux had some slight decline over time, which was likely due to 1) the reduced bulk DS concentration and 2) the increase in

FW concentration as pure water was extracted from the FW to the DS (C. Y. Tang et al., 2010). Fouling can be evaluated by comparing a fouling curve to

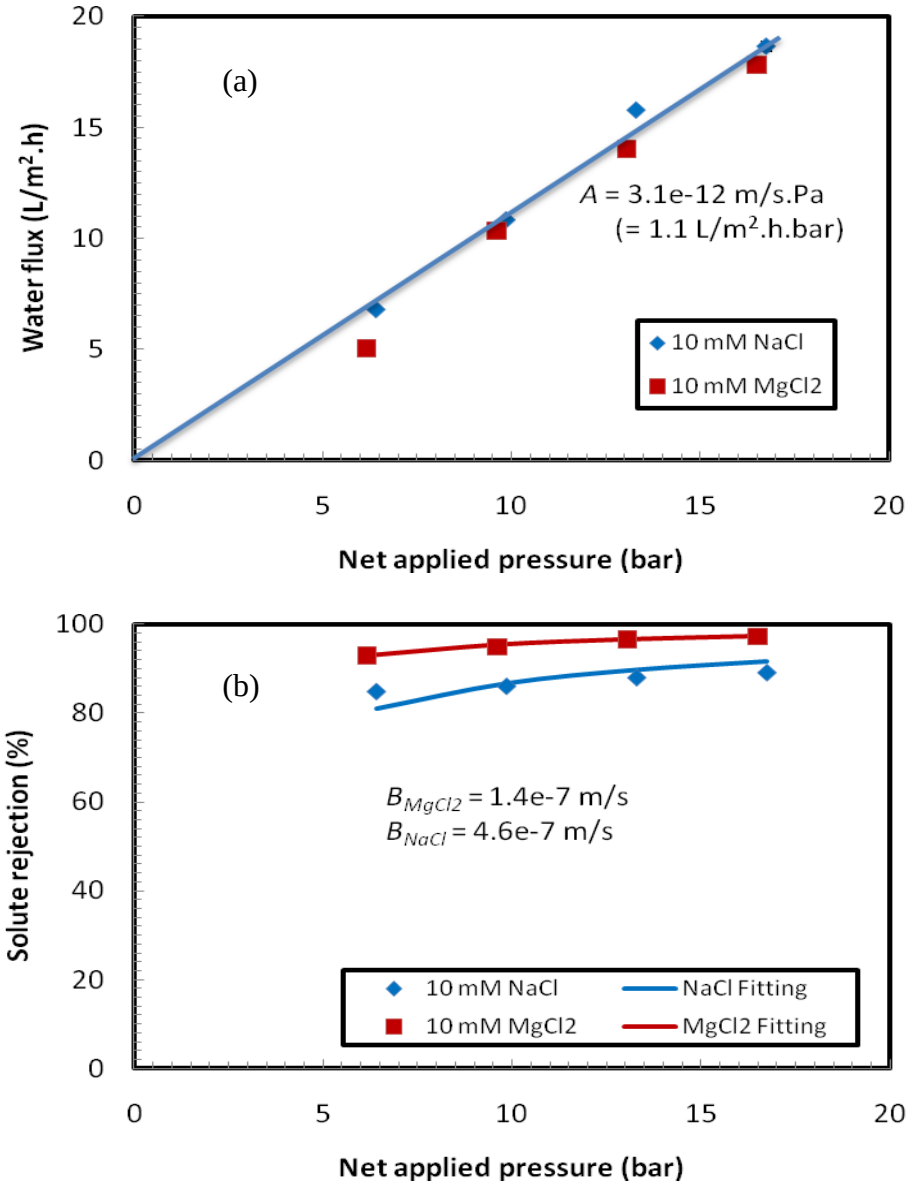

Figure 4-1 Water flux (a) and solute rejection (b) as a function of applied pressure for the HTI membrane tested in RO mode. The feed water contained either 10 mM NaCl or 10 mM $MgCl_2$

the corresponding baseline, with a great flux reduction relative the baseline indicating more severe membrane fouling (C. Y. Tang et al., 2010; Mi and Elimelech, 2008). In Figure 4-1(a), the fouling curves were nearly identical to

the respective baselines when the initial flux ≤ 36 L/m^2.h (C_{ds} ≤ 2 M), suggesting that minimal FO fouling had occurred. However, further increase in the initial flux (C_{ds} at 4 and 5 M) resulted in severe flux reduction with respect to the baseline, which might be explained by the greater permeate drag force experienced by the foulant at increased flux (Bacchin et al., 2006; Tang and Leckie, 2007). Similar flux-dependence of membrane fouling has been well documented for pressure driven membranes (e.g., RO) (Bacchin et al., 2006; Tang and Leckie, 2007), and has also been previously reported for the concentration driven FO membrane (C. Y. Tang et al., 2010; Mi and Elimelech, 2008). Indeed, the current study may suggest that the critical flux concept, which was originally developed for pressure driven membranes and which states that significant membrane fouling occurs only if the flux is above some critical value (i.e., the critical flux) (Bacchin et al., 2006), may also be applicable to the concentration driven FO membrane.

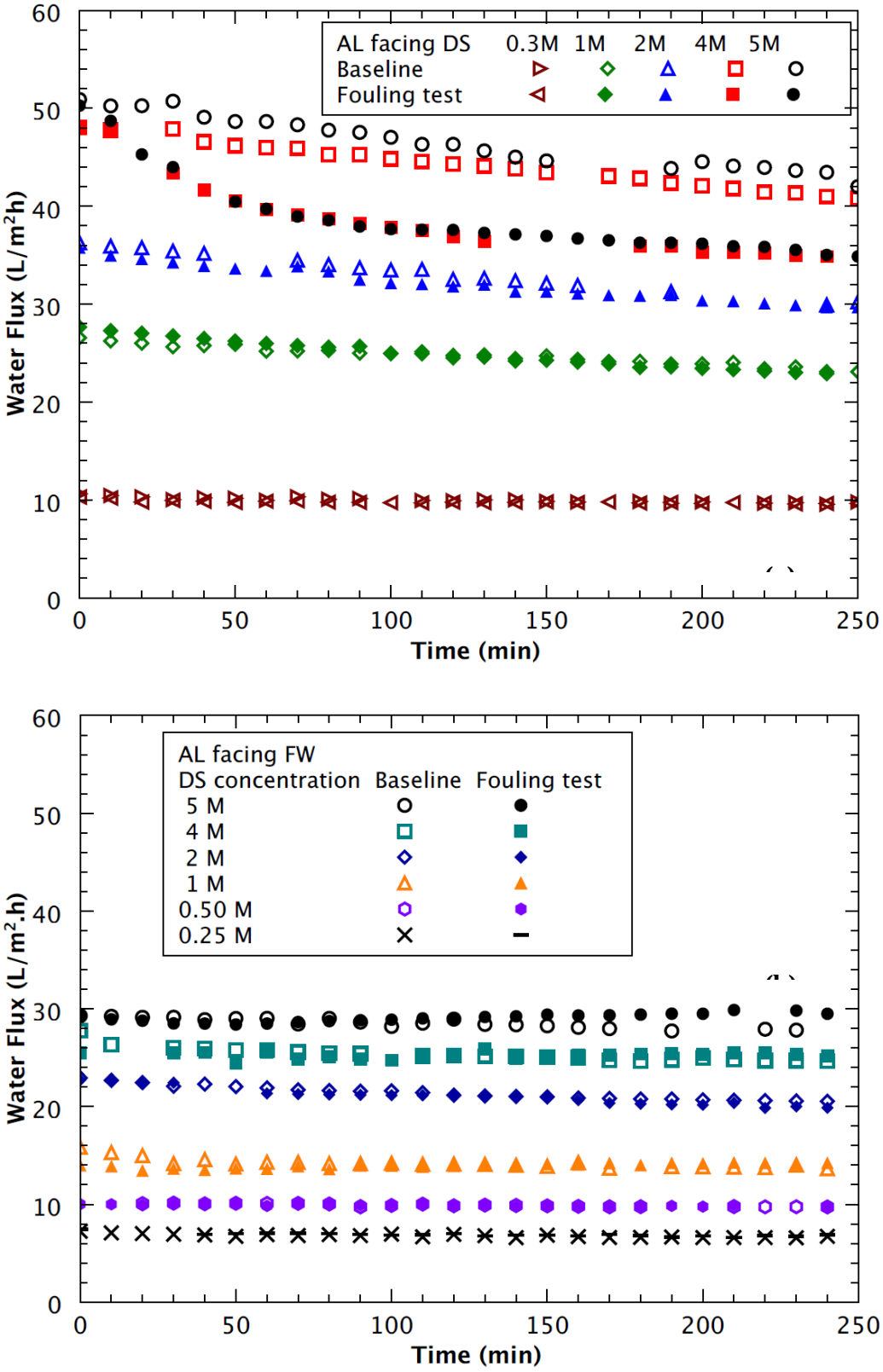

Figure 4-3 Effect of initial flux level and membrane orientation on FO fouling.

Figure 4-3(b) shows the FO flux behavior in the AL-facing-FW orientation. Compared to the alternative orientation, the baselines in AL-facing-FW showed remarkable stability. Tang et al. (C. Y. Tang et al., 2010) attributed such flux stability to the much more severe initial ICP in this orientation (see Table 4-1 and Section 4.3.1). A slight reduction in flux (say, due to the dilution of bulk DS concentration) may lead to significantly reduced ICP level (which has an exponential dependence on flux) to compensate the original cause for the flux reduction, a phenomenon referred as the ICP-compensation effect (C. Y. Tang et al., 2010). Similar to the baseline cases, FO flux in the presence of microalgae was also very stable for DS concentration ranging from 0.25 – 5 M NaCl in AL-facing-FW, which may be partially attributed to such ICP-compensation effect. In addition, the low fouling potential in this membrane orientation is also consistent with the critical flux concept, since the initial flux level in AL-facing-FW was relatively low (up to 30 L/m^2.h at 5 M NaCl) as a result of its more severe ICP (Table 4-1). In comparison, the critical flux in the AL-facing-DS was greater than 36 L/m^2.h (Figure 4.1(a)). The current studies convincingly demonstrate that stable flux operation can be achieved during FO algae filtration in the AL-facing-FW orientation, however, at the expense of more severe ICP compared to the alternative orientation. Using seawater as a potential DS (~ 0.6 M NaCl), a stable flux of more than 10 L/m^2.h may be maintained during algae separation, which makes FO potentially applicable for such applications.

The effect of cross-flow velocity on FO flux behavior is shown in Figure 4-3. While a baseline flux of ~ 25 L/m^2.h was maintained at a cross flow velocity of 22.5 cm/s, the baseline value was nearly 40% lower at a cross flow velocity of 2.3 cm/s. The reduced flux efficiency suggests that the external concentration

polarization (ECP) was likely important at the lower cross flow velocity. According to McCutcheon et al. (2006), both ECP and ICP can adversely affect the FO water flux. A lower cross flow velocity increases the boundary layer thickness and thus the extent of ECP. When microalgae were present in the feed water, the fouling curves were nearly identical to the respective baselines. While reduced cross flow usually tends to promote fouling (Bacchin et al., 2006) we observed a dramatically reduced FO baseline water flux, which has the effect to reduce fouling tendency. As a net result, no significant FO fouling was observed even at the low cross flow velocity of 2.3 cm/s, though at the expense of a low baseline flux.

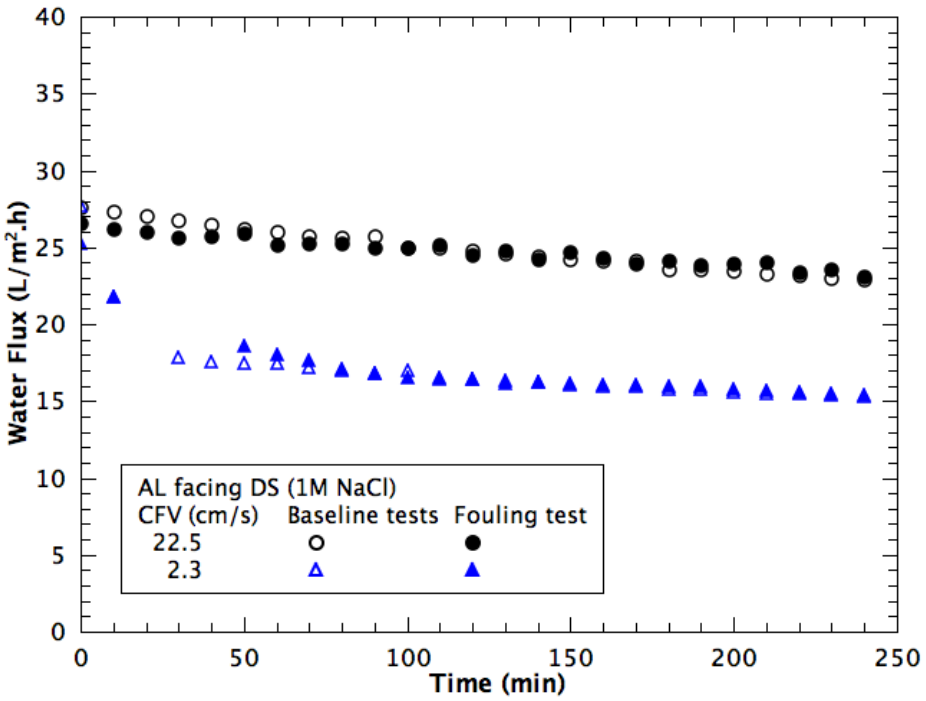

Figure 4-4 Effect of cross-flow velocity on FO flux behaviour.

4.3.2.2 Effect of chemical parameters

The dependence of FO fouling by algae on feed water chemistry (pH and [Mg^{2+}]) as well as draw solution chemistry (type of draw solutes) is presented in the current section. The feed water pH did not seem to play a significant role on FO flux behavior over the experimental pH range (pH 4.0 – 7.3, Figure 4-5). Membrane fouling was minimal for all the three pH values tested (pH 4.0, 5.8, and 7.3), which might be attributed to the relatively low flux level in the current study.

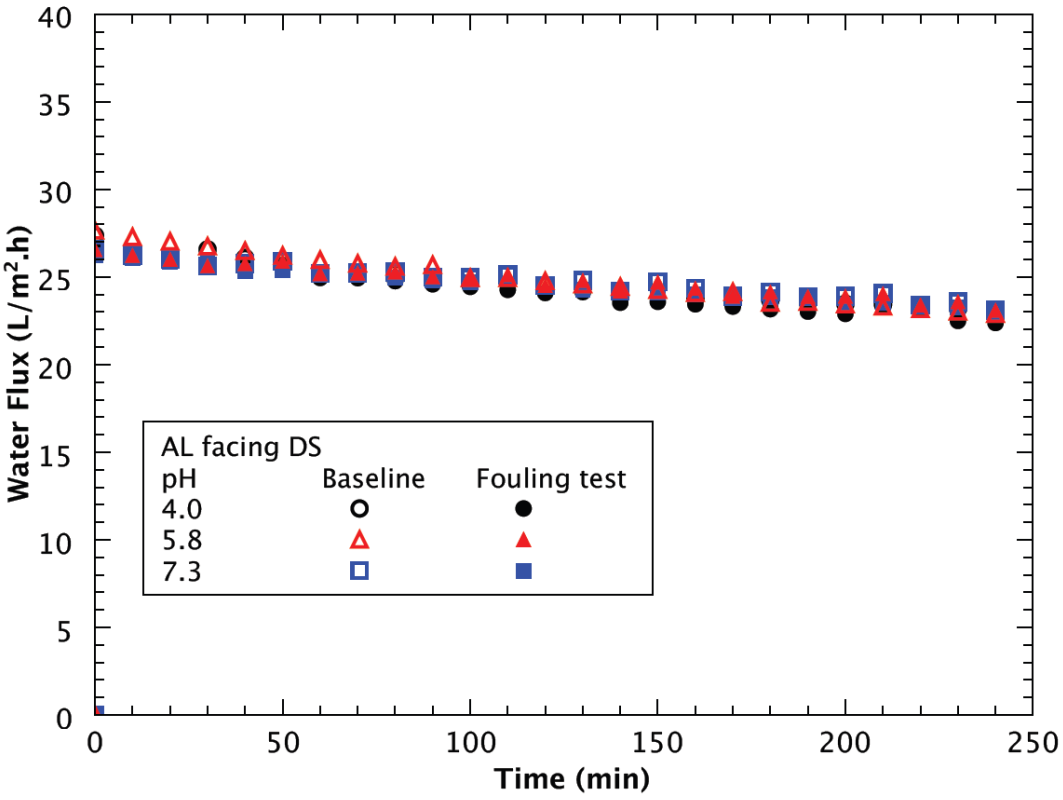

Figure 4-5 Effect of pH on FO flux behaviour.

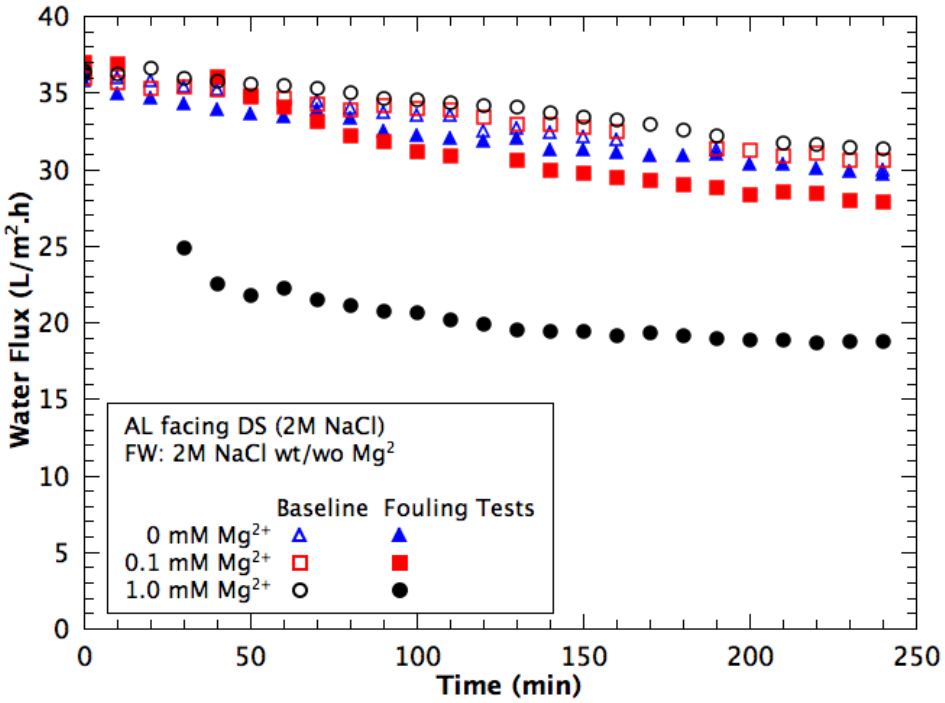

Figure 4-6 Effect of magnesium ion in the feed water on FO fouling.

Figure 4-6 presents the effect of magnesium ions in the feed water on FO flux behavior. The baseline flux was nearly unaffected by the presence of Mg^{2+} in the feed water (0 – 1.0 mM). In contrast, increased FW Mg^{2+} concentration had detrimental effect on FO fouling by microalgae. When the feed water had no Mg^{2+}, the flux reduction with respect to the baseline was minimal. The relative flux drop became noticeable (~ 10% reduction) at a 0.1 mM [Mg^{2+}]. Severe membrane fouling was observed at 1 mM [Mg^{2+}], with the fouled membrane flux was reduced to ~ 19 L/m^2.h compared to the baseline flux of 31 L/m^2.h at the end of the 4-h tests. Similar effect of divalent cations (Ca^{2+} and Mg^{2+}) has been well documented for reverse osmosis and nanofiltration membrane fouling (Li and Elimelech, 2004; Tang et al., 2009) and has also been reported for FO fouling by organic foulants (C. Y. Tang et al., 2010; Mi and Elimelech, 2008). These studies suggested that divalent ions may affect membrane fouling

by forming complex with certain functional groups such as carboxylate groups. In the current study, Mg^{2+} will likely interact with the microalgae cells and their EPSs, resulting in charge neutralization of and cation bridging between cells and EPS matrices (Arabi and Nakhla, 2009).

The effect of draw solutes type (NaCl vs. $MgCl_2$) on FO fouling is presented in Figure 4-7. The FO membrane experienced severe fouling for a 2 M $MgCl_2$ DS. In contrast, nearly no relative flux reduction was observed with respect to the baseline for a 2 M NaCl DS. The more severe fouling using the 2 M $MgCl_2$ DS may be partially attributed to its much higher initial FO flux compared to that using the 2 M NaCl DS, since a higher flux level tends to promote membrane fouling. Interestingly, the 0.5 M $MgCl_2$ DS also resulted significant flux reduction, despite that its initial flux (22 $L/m^2.h$) was ~ 30% lower than that at 2 M NaCl. Thus, flux level alone does not fully explain the more severe fouling when $MgCl_2$ was used as DS. In the current study, the severe fouling may also be partially attributed to the back diffusion of Mg^{2+} into the feed water when $MgCl_2$ was used as DS (Section 4.3.1 and Table 4-1). Based on inductively coupled plasma mass spectrometry measurements, the Mg^{2+} concentration in the feed water reached 0.05 mM at the end of the fouling test for the 0.5 M $MgCl_2$ DS, and it was 0.08 mM for 2.0M DS, even though Mg^{2+} was not present in the original feed water. Once diffused through the membrane, Mg^{2+} may interact with the foulant in the FW in an unfavorable manner (e.g., charge neutralization or bridging) to cause severe FO fouling (in a fashion similar to that in Figure 4-6).

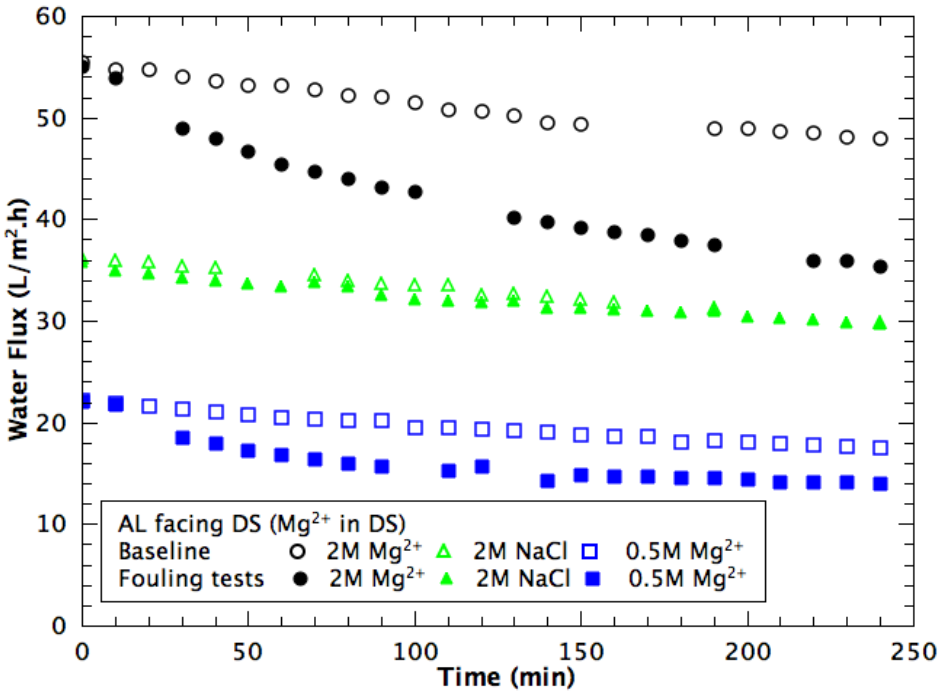

Figure 4-7 Effect of draw solution type (NaCl vs. $MgCl_2$) on FO fouling.

This is the study to demonstrate the detrimental effect of back diffusion of divalent ions on FO membrane fouling. Despite that $MgCl_2$ as draw solution perform superiorly over NaCl in terms of higher water flux and lower solute flux, it may lead to severe membrane fouling for feed waters containing foulants that are sensitive to divalent cations. Similar drawbacks may also be expected for other magnesium and calcium based draw solutes. The risk of such back-diffusion-induced-fouling shall be evaluated when selecting DS for a specific FO application.

Figure 4-8 summarizes the effect of flux and solution chemistry on FO fouling, where the fouled water flux at the end of a fouling test is plotted against the corresponding baseline flux. A 45° line is also included in the figure to

represent conditions where there was no relative flux reduction and thus negligible membrane fouling. Data points below this line correspond to tests with significant fouling. The further away from this line, the more severe the membrane fouling. Clearly, FO fouling was affected by both permeate flux level as well as solution chemistry. Fouling was more severe at higher flux levels, higher feed water [Mg^{2+}], and when $MgCl_2$ was used as a draw solution. A critical flux behavior can be observed, but its value was likely dependent on the DS type. When NaCl was used as DS and no Mg^{2+} was present in the original FW, relative flux reduction was not observed at fluxes as high as 30 $L/m^2.h$. In contrast, significant flux was already observed for a 0.5 $MgCl_2$ DS (critical flux < 18 $L/m^2.h$). The strong dependence of the critical flux value on draw solution chemistry is a unique feature for FO fouling. In this regard, a concept of DS-type-dependent "critical concentration" may also be of practical interest. When there was no Mg^{2+} in the original feed water, the critical concentration of $MgCl_2$ was below 0.5 M while that for NaCl was between 2-4 M for algae fouling in the present case. The current study suggests a strong interplay between membrane flux and DS solution chemistry on FO fouling in addition to the well documented interplay between flux and FW solution chemistry.

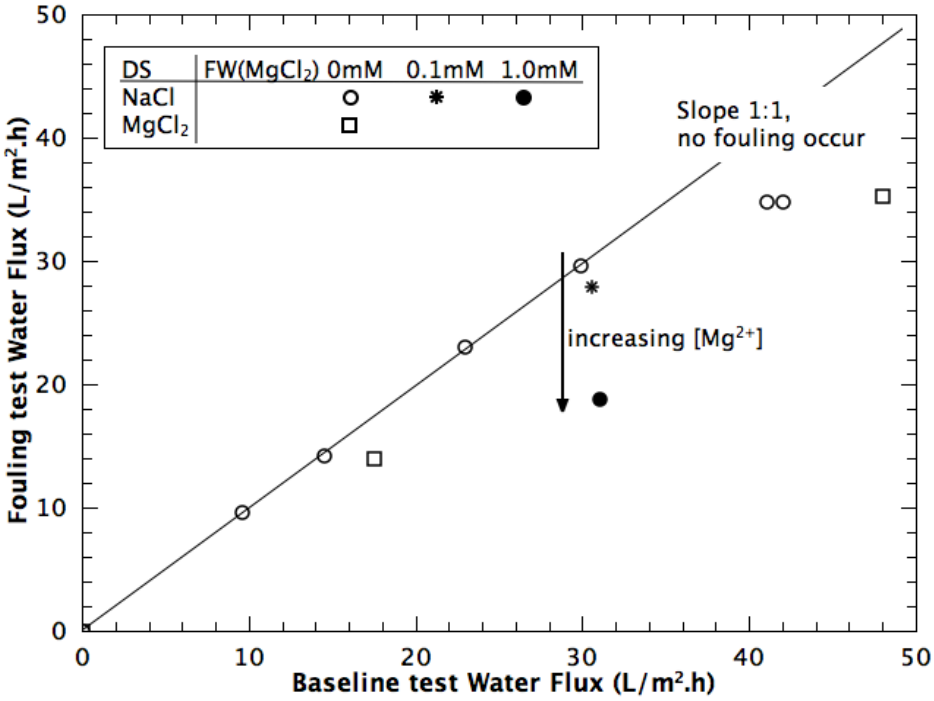

Figure 4-8 The interplay of flux and solution chemistry (Mg^{2+} in feed water as well as in draw solution) on FO fouling.

4.4 Conclusions

FO fouling during microalgae separation was investigated in the current study:

- A critical flux phenomenon was observed for the concentration-driven FO process, and more rapid FO fouling was observed at higher flux levels.

- The AL-facing-FW orientation had relatively stable water flux, but it had much lower initial flux compared to that for the AL-facing-DS orientation.

- FO fouling by microalgae was more severe at greater Mg^{2+} concentration in the feed water.

- In the absence of foulant, $MgCl_2$ as a draw solution had higher water flux and lower solute flux compared to NaCl as draw solution.

- However, the use of $MgCl_2$ as a draw solution caused severe fouling as a result of the reverse diffusion of Mg^{2+} from the draw solution into the feed water when microalgae was present in the feed water.

Chapter 5 Direct Microscopic Observation on Microalgae Fouling of Forward Osmosis Membrane

5.1 Introduction

Forward osmosis (FO) has attracted significant attention in the membrane research community for its potential applications in seawater and brackish water desalination (McCutcheon et al. 2006), wastewater treatment (Cornelissen et al. 2008), biomass concentration (Chapter 4), food processing (Petrotos et al. 1998), etc. In FO, water permeate through a semi-permeable membrane from a feed solution (FS) of low osmotic pressure to a draw solution (DS) of high osmotic pressure under the chemical potential gradient across the membrane (Cath et al. 2006). A potential advantage of FO is its low energy consumption due to the lack of applied mechanical pressure, provided that a suitable draw solution is available (e.g., seawater or other brines) or it can be easily regenerated in an energy efficient manner.

Membrane fouling can be an important issue limiting the performance of FO. In contrast to the vast literature on fouling of pressure-driven membranes such as reverse osmosis (RO) membranes, there have been only a handful of studies on the fouling of FO membranes (Mi and Elimelech 2008; Cornelissen et al. 2008; Mi and Elimelech 2010; Tang et al. 2010; Wang et al. 2010b; Zou et al. 2011). Most of these existing studies focused on the FO water flux behavior under various operational conditions. In a recent studies, it has been revealed that FO fouling tends to be more complicated compared to RO fouling due to the unique phenomena such as internal concentration polarization (ICP) and solute reverse diffusion in FO (Tang et al. 2010; Zou et al. 2011). For example, ICP can either enhance or reduce the water flux depending on the membrane

orientation (Tang et al. 2010). When the active layer faces the draw solution (AL-DS), foulants in the feed water can clog the porous support layer of the membrane and results in more severe ICP (and thus enhanced water flux loss). However, in the active-layer-facing-the-feed-solution (AL-FS) orientation, a small reduction in the water flux will drastically reduce the ICP level, which in turn tends to stabilize the water flux. Due to the presence of these complicated phenomena, methods complementary to flux measurement can be highly valuable to better understand FO fouling.

Recently, Wang et al. (2010b) developed a direct microscopic observation method to study FO fouling by latex particles. This study provides a real-time visualization of the progress of particle deposition on FO membranes. Similar method has also been previously used to investigate fouling of pressure-driven membranes and has been proven valuable for studying their critical flux behavior (Li et al., 1998; Wang et al., 2005; Zhang et al., 2006). To the author's best knowledge, the systematic application of direct microscopic observation method for FO critical flux determination is not yet available in the literature.

The objective of the research was to utilize the microscopic method to characterize the FO membrane fouling during microalgae filtration. The microscopic observation results were compared to the FO water flux performance to reveal the critical flux behavior in the FO process.

5.2 Materials and methods

5.2.1 Chemicals and materials

Analytical grade chemicals included NaCl (VWR, Singapore) and $MgCl_2$ (Merck, USA). Ultrapure water (Millipore Integral 10 Water Purification

System) was used for the preparation of working solutions throughout all the experiments.

Microalgae species Chlorella Sorokiniana (C.S) with an average cell diameter of ～5 μm was used as model algae foulant. C.S is a unique unicellular blue green microalgae with high content of chlorophyll. C.S has also been used extensively as a model algae to remove ammonium in wastewater treatment and biodiesel production (de-Bashan et al., 2008b; Mata et al., 2010). In this study, the micro-algae was cultivated using a 25-L photobioreactor in BG11 medium (Allen and Stanier, 1968) with 97～99% O_2 and 1% CO_2 injection for around 7~12 days to achieve a high concentration of around 2.5 g/L.

The cellulose triacetate (CTA) flash-sheet FO membrane used in the current study was supplied by Hydration Technology Inc. (Hydrowell Filter, HTI). This FO membrane has been characterized by some previous studies (Cath et al., 2006; Gray et al., 2006; McCutcheon and Elimelech, 2006; Wang et al., 2010b). HTI membrane is made with a minimized overall thickness (i.e., from 30 to 50 μm) in order to reduce the impact of internal concentration polarization (ICP) (Tang et al., 2010). The pores were likely to have a smaller diameter as approaching to the rejection surface, and the pore size approximately ranged 20~40 μm in the support layer of the membrane. In my study, the overall membrane thickness was around 50 μm. The configuration of the membrane was presented by Tang et al. (Tang et al., 2010)in Figure 5-1 The reported water permeability varies mildly for different batch experiments (Gray et al., 2006; Tang et al., 2010). For this study, the water permeability coefficient was determined to be 1.1L/m^2 .h.bar (Zou et al., 2011).

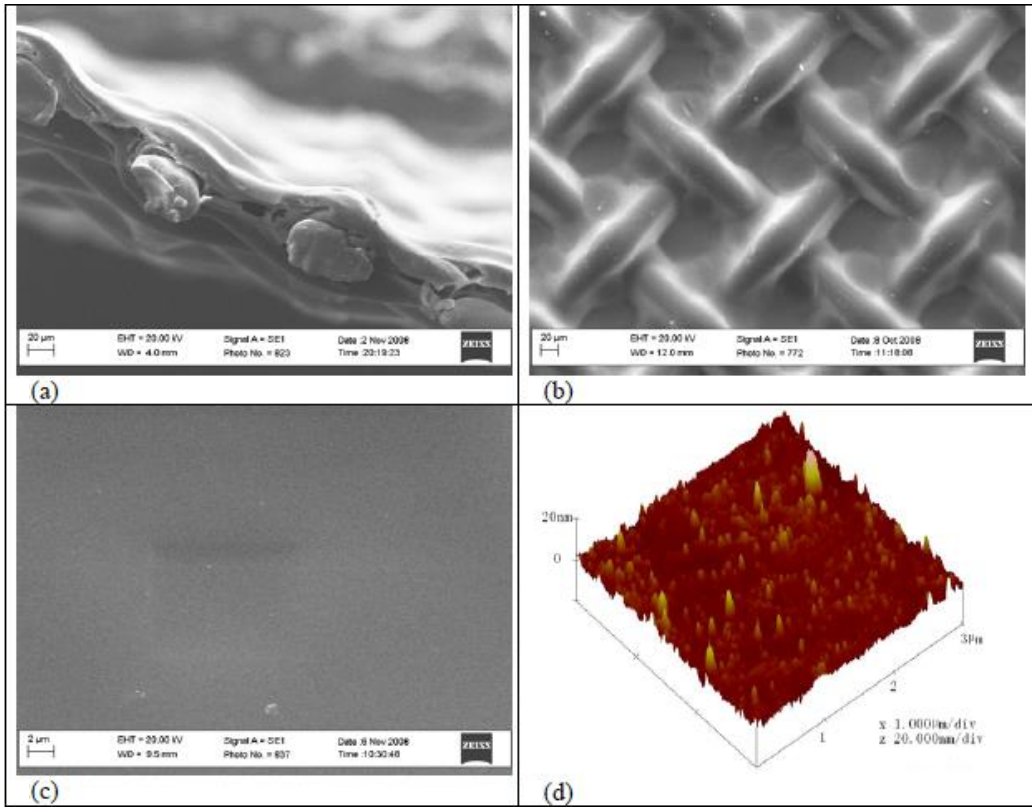

Figure 5-1 SEM and AFM micrographs of the HTI Hydrowell® FO membrane. (a) SEM image of membrane cross-section, (b) SEM image of the back (support) side of the membrane, (c) SEM image of the active surface, and (d) AFM image of the active surface (Tang et al., 2010).

5.2.2 Algae fouling test

The FO setup equipped with a direct optical microscope system has been described the study by Wang et al., (2010b). Briefly, the crossflow FO membrane cell (effective area ~ 29.2 cm^2) was made of perspex to allow the transmission of light through the cell. To avoid the interference from the pore structure of the FO membrane, the objective lens of the microscope (x10 magnification, Axiolab, Carl Zeiss) was placed at the feed water side and the focus was adjusted to the membrane-FS interface (Wang et al., 2010b). Microscopic images were captured by a high-resolution color CCD camera (JVC, model TK-C921BEG) at 30 frames/second.

For a typical test, an FO membrane coupon was placed in the test cell, and the crossflow velocities of the DS and FS were independently controlled by two peristaltic pumps. In addition to the microscopic observation, the flux data was obtained by monitoring the weight change of the feed water using a digital balance (Mettler-Toledo) connected with a computer data logging system (LabVIEW). For each test, the following two stages were involved: (1) baseline evaluation (without microalgae addition) and (2) fouling evaluation where a 100 mg/L microalgae was present in the feed. For both stages, the DS concentration was increased in predefined steps with a stepping duration of 30 minutes for each concentration level. The feed solution ionic composition during the fouling evaluation was identical to that used in the baseline evaluation. This is to ensure that the difference in flux behavior between the baseline and fouling stages can be directly attributed to membrane fouling. Upon the completion of fouling stage, the fouling reversibility was also evaluated in some tests by replacing the algae-containing feed water with the background electrolyte solution used in the baseline evaluation and simultaneous reducing the DS concentration to a lower level. The purpose of the reversibility test was to check if hydraulic flushing due to cross flow was sufficient for removing the microalgae deposited on the FO membrane.

The key parameters investigated in the study included the types and concentrations of draw solution, the feed solution ionic composition, the membrane orientation, the use of feed spacer, and the crossflow velocity. The effect of each parameter was studied by fixing the other parameters at constant. Unless otherwise specified, the following reference testing conditions were adopted:

- DS: either NaCl or $MgCl_2$, DS concentration was stepped up at 30-min time interval

- FS: either (1) 10 mM NaCl or (2) the mixture of 7 mM NaCl and 1 mM $MgCl_2$; pH 5.8
- AL-DS orientation
- Diamond shaped spacer in the DS channel only (expect where the effect of feed spacer was investigated)
- Crossflow velocity fixed at 22.3 cm/s for both DS and FS
- Room temperature (23 ± 1 ℃)

5.2.3 Image analysis

The image analysis was adapted from Wang et al. (2010b). The microscopic images captured by the computer were saved in the format of TIFF (Tagged-Image File Format). By using the MediaCybernetics image analysis software, the TIFF images were first converted to a grey-scale and then to binary type. After reducing the background noise, the ratio of the area occupied by the algal cells and the total area of the membrane was estimated to determine the membrane surface coverage.

5.3 Results and discussions

5.3.1 Visualization of FO membrane

Some preliminary characterization of the FO membrane which was utilized in this study had been done in a previous study (Wang et al., 2010b). Both of the active and support layers of the membrane were imaged by SEM test. Based on Wang and his coworkers' results (2005), there were some small bump and depression areas that crisscross the membrane surface regularly. Similar observation had also been found by Mi et.al (2008). It was believed that the roughness of the FO membrane was primarily generated by the polyester mesh

embedded.

The clean membrane surface images for the microscope facing support layer and active layer are presented in Figure 5-2(a) and (b) respectively. In active layer facing draw solution (AL-DS) orientation, FW side contacted with support layer. Since the objective microscopic lens focused on the FW side, the extruded woven mesh layer was much clearly captured in this orientation than in the other one. Similarly, the macro-pores near the support layer, appeared as bubbles in Figure 5-2(a), were bigger and clearer than showed in Figure 5-2(b). This is consistent with the SEM observations by Mi et al, (2008) and Wang et al, (2005), which validates the microscopic method as a useful tool for charactering FO membrane structure.

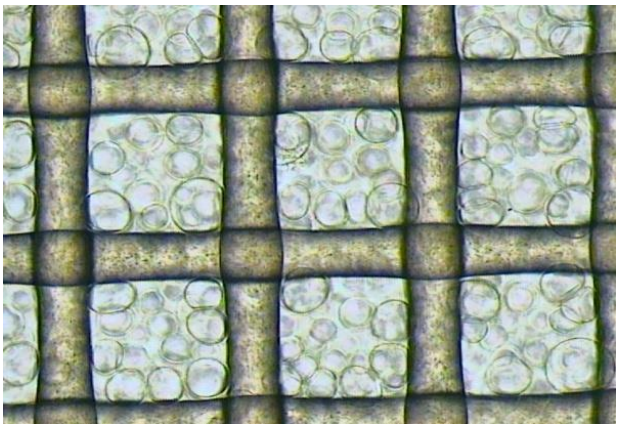

(a)

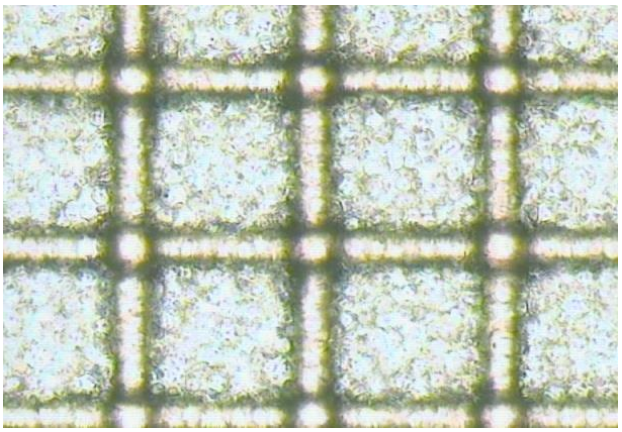

(b)

Figure 5-2 Optical microscopic images of HTI FO membrane. (a) A clean FO membrane with its support layer facing the optical microscope, (b) A clean FO membrane with its active layer facing the optical microscope.

5.3.2 Macroscopic observation of algae fouling

5.3.2.1 FO fouling without magnesium ion affection

In a typical batch mode close-loop cross flow FO experiment, the dilution of DS and the concentration of FW leads to effective osmotic pressure difference decreasing across the membrane active layer and thus a continuous flux decline. Therefore, Stage I baseline tests were conducted to differentiate the flux reduction caused by the decreasing osmotic driving force and fouling, followed by Stage II fouling tests with the same protocol as that for the baseline tests except adding foulant into the FW. The membrane surface images and videos were taken to capture the process of the algae cells deposition and the foulant layer formation throughout the filtration.

Figure 5-3(i) shows the FO flux results during Stage I~III tests using microalgae cells as foulant in AL-DS orientation, and the microscopic images of the membrane surface at the end of each concentration step are presented in Figure 5-3(II). When the DS concentration was as low as 0.25M, flux curve of fouling test overlapped very well with the baseline result, indicating that there were likely no severe fouling occurred in this step. In contrast, the membrane surface picture in Figure 5-3(ii)a shows that there was already a small amount of microalgal cells on the membrane (corresponding to ~5% surface coverage). This disagreement between the flux data and the direct observation revealed the different sensitivity of the two methods in characterizing FO fouling. While the microscopic method was highly sensitive to monitor the small amount of foulant deposition, the flux measurement was able to show any significant difference in flux after fouling likely due to the high membrane resistance of the FO membrane. This is in good agreement with previous studies on that microscopic observation is more sensitive for examining particles deposition or

cake layer formation (Li et al., 1998; Wang et al., 2005; Wang et al., 2010b). The current study may have a significant implication in the critical flux measurement for FO processes – the evaluation of the critical flux can be strongly affected by the measurement method due to their different sensitivity, with the microscopic method giving a lower critical value (DS < 0.25 M or critical flux < 10 L/m^2.h).

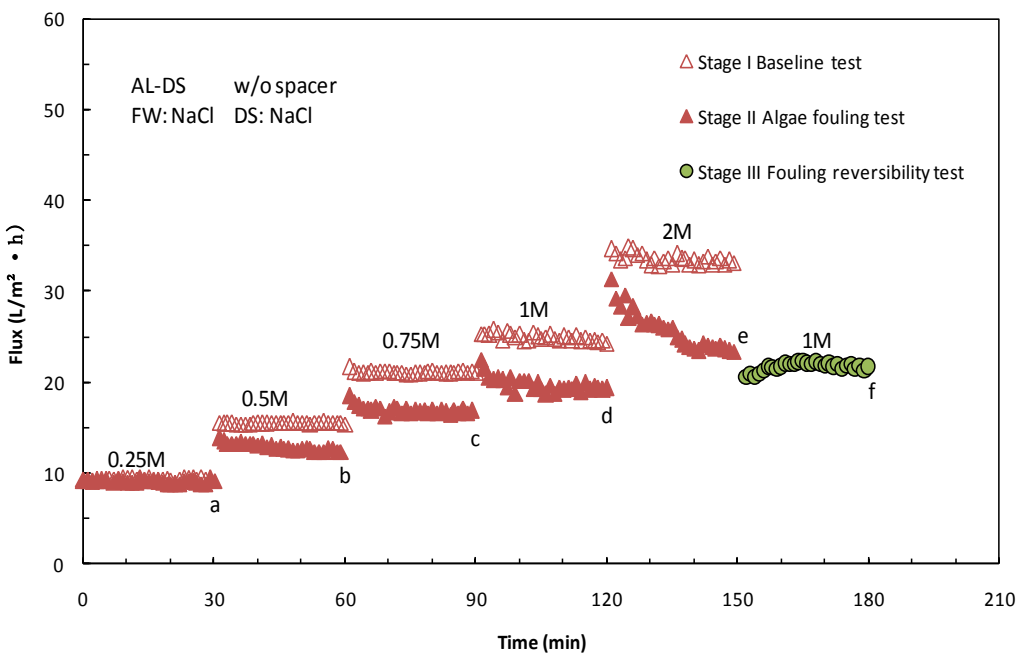

(i)

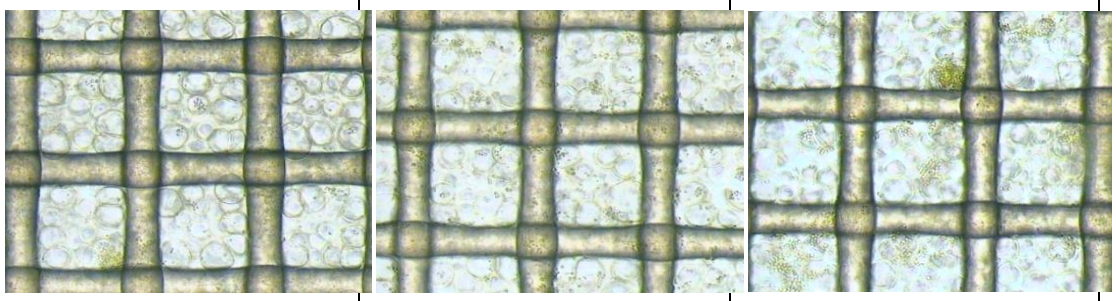

a 0.25M | b 0.5M | c 0.75M

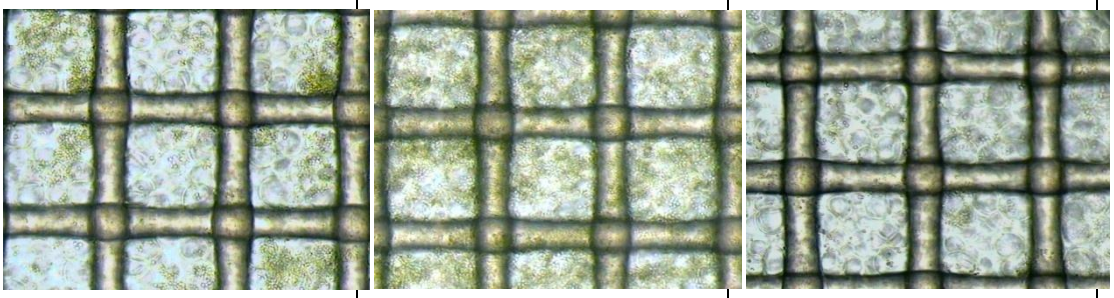

d 1M | e 2M | f 1M

(ii)

Figure 5-3 The FO flux performance during the three-stage flux stepping tests, and the images of the algae cells deposition at the end (or the middle) of different flux-stepping stages.

When the DS concentration stepped up from 0.50 M to 2 M, the fouling flux curve as well started to deviate from the baseline. The deviation gap become wider as a function of time within each step, and the overall gap distance was greater at a higher DS concentration, suggesting an aggravating fouling state. Similar growing fouling tendency by longer filtration duration and DS concentration increment were found in the corresponding microscopic images. The surface coverage of algal cells expanded from 7.5% at 0.5 M DS, 16% at 0.75 M DS, to 31.3% at 1 M DS, and reached 86% at 2 M DS. Besides, the algae cells deposition pattern transition was observed through the Stage II test. At a low DS concentration below 0.75 M, the algal cells deposition was relative randomly located and quite uniformly distributed on the membrane surface, as shown in Figure 5-3(ii) a, b. From 0.75 M DS step, the particles seemed more likely to be stopped around the embedded mesh fibre and inside of the macropore "bubbles". This is in line with other studies reporting the mesh causing local hydrodynamic condition varying that the bumpy roughness of the membrane surface reduced shear force over the depression area (Elimelech et al., 1997; Wang et al., 2010b). Other than that, the cells had a tendency to accumulate and stick to each other forming bigger cell-groups in

three-dimension suggesting a rudimental cake layer formation. At 2 M DS concentration, the membrane surface was almost fully covered by the algal cells with a 86% surface coverage. This observation was mainly attributable to the increasing drag force toward to the membrane. Within the hydrodynamic interactions, the foulant molecules deposition and accumulation situation were influenced by the drag force vertical to the membrane created by the convective flow, as well as the shear force parallel to the membrane resulting from the cross flow. Consequently, the effect of DS concentration on fouling is considered the same as the effect of initial flux since greater osmotic driving force generates higher flux causing increasing drag force.

The stage III reversibility test was conducted and shown in Figure 5-3(i), after 30 minutes filtration with 2M DS concentration. The FO membrane with a 84% surface coverage by algal cells was tested without foulant at 1M DS concentration. Interestingly, the flux curve displayed in an arch shape, and the flux level was all above that of previous 1 M DS step in Stage II fouling test. Under the microscopic lens, when the FW of algae solution was changed to 10mM NaCl and the DS concentration decreased from 2 M to 1 M, the initial flush of the cross-flow provided a very strong shear force scrapping over the membrane surface. During the early phase of the Stage III step, the aggregated cell-groups started trembling, segregating and successively swept away from the surface, inducing a great break down of the cake layer structure. These observations in microscopic videos provide explanation to the initial upwards arch-shape flux curve. The surface coverage decreased to as low as 18%. Hence, the algae fouling in this experiment was mainly due to reversible particle deposition and cake layer formation.

5.3.2.2 FO fouling with the effect of magnesium ion

The Figure 5-4(a) shows the final flux reduction compared with the associated baseline result on the effect of Mg^{2+}. The test using Mg^{2+} as DS (FW:Na-DS:Mg) and the test with Mg^{2+} in FW (Mg-Na) encountered more severe flux decline than that of no Mg^{2+} presented test (Na-Na), suggesting intensified fouling by microalgae in the presence of Mg^{2+}. Greater algae fouling propensity with addition of Mg^{2+} was as well proved by the surface coverage data represented in Figure 5-4(b). Additional, the average flux values of Stage III with the existence of Mg^{2+} were far away below those for Stage II fouling test under the same DS condition. The algae fouling in these cases appeared to be irreversible instead of reversible ones for pure algae filtration, revealing the enhanced irreversible organic fouling occurring. The algae fouling mechanism was likely changed by Mg^{2+}. When Mg^{2+} was added into FW, it is generally assumed that algae fouling was enhanced by more powerful intermolecular interactions and bridging induced by the existence of Mg^{2+} (section 4.3.2). As described by others' work (Detlef R. U.Knappe, 2004; Rosenhahn et al., 2009), unicellular algae tend to be negatively charged and this is usually attributed to the presence at the surface of polysaccharide materials with associated negatively charged carboxyl. In the meantime, some divalence ions such as Ca^{2+} and Mg^{2+} have a tendency to interact more easily with some functional groups like carboxylic and aldehyde groups of the negatively charged foulants and neutralizes the charge on the membrane (Arabi and Nakhla, 2009; Jermann et al., 2007), . Subsequently, the stronger adhesion force between the Mg^{2+} and algal EPS matrix derived from the greater

intermolecular interactions, would further develop the fouling growing by forming magnesium-binding complexes. Figure 5-4 (b) reflects the surface coverage increasing as a function of filtration duration with or without Mg^{2+}. Obviously, the surface coverage grew sharply at the early phase of this step (0-10 mins) in the presence of Mg^{2+}. However, from 10 to 20 mins, the coverage increasing rate seemed to be flatter than the ones of fouling test in the absence of Mg^{2+}.

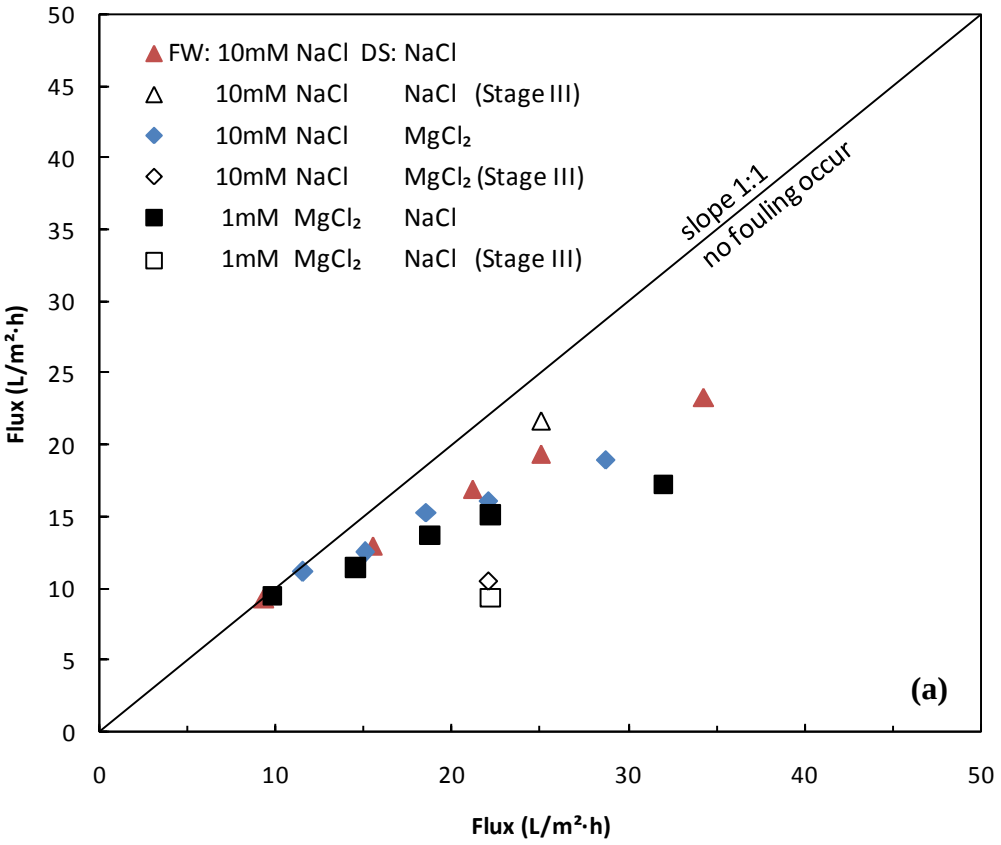

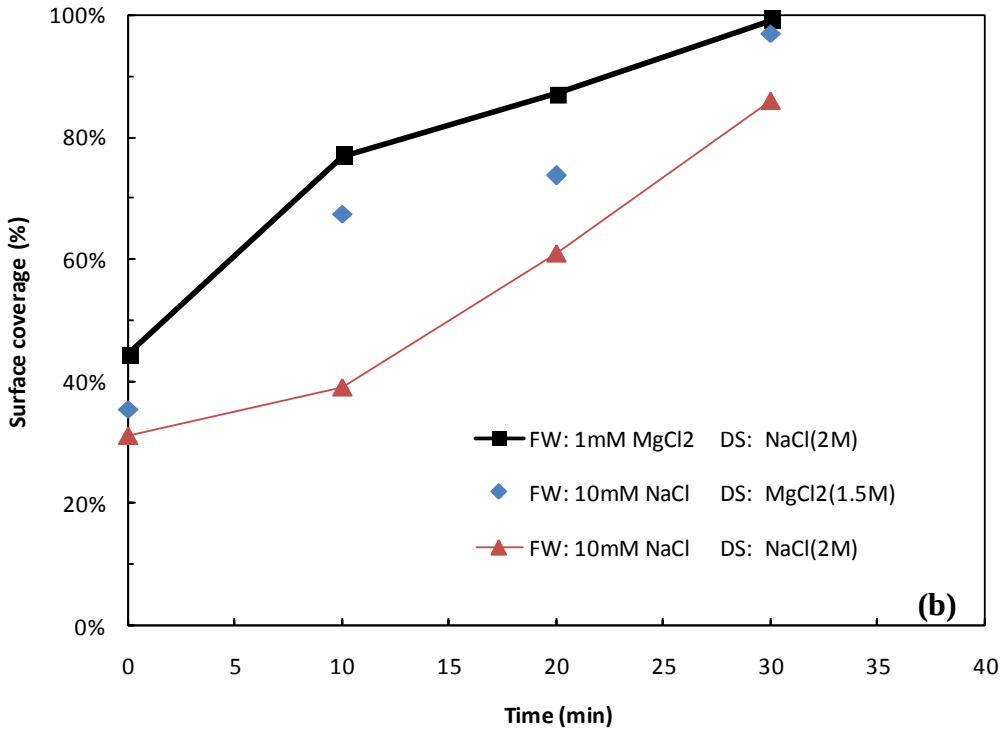
100%
80%
60%
40%
20%
0%
Surface coverage (%)
0
5
10
15
20
25
30
35
40
Time (min)
FW: 1mM MgCl2 DS: NaCl(2M)
FW: 10mM NaCl DS: MgCl2(1.5M)
FW: 10mM NaCl DS: NaCl(2M)
(b)

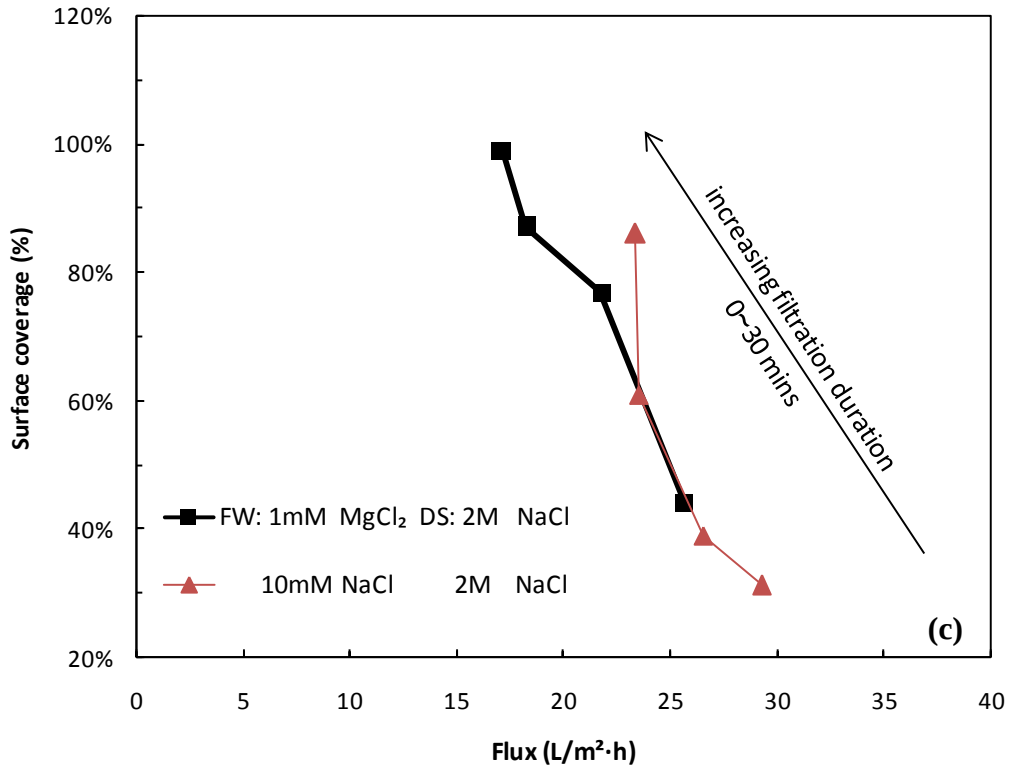

Figure 5-4 Effect of magnesium ion on flux reduction and the surface fouling exacerbation. (a) Final flux data of fouling tests (Stage II) versus final flux of baseline tests (Stage I); (b) Surface coverage as a function of time during fouling test; (c) Surface coverage as a function of flux during fouling test.

The early stage rapid coverage rising was mainly attributed to more dramatic flux decline speed for Mg^{2+} included fouling test. Initially, within the same filtration duration, the increased intermolecular interactions by Mg^{2+} caused more irreversible particles deposition, associated with remarkable flux reduction and significant surface coverage. It can be assumed that these Mg^{2+} strengthened molecular interactions not only led to the deposition of particles onto the membrane, but also onto the deposited particles forming a cake layer. When the interactions between the foulant molecules was stronger than that

between the foulant with membrane surface, the foulant would be prone to reside onto the fouled membrane rather than deposit on the clean membrane surface. This phenomenon led to a decreased acceleration of the surface coverage, and thus a comparatively tighter and less permeate cake layer structure. This possible explanation was further demonstrated by the results as in Figure 5-4(c), that Mg^{2+} included fouling had a flatter slope for the surface coverage curve at the later phase of the step.

The effect of Mg^{2+} as DS was akin to that in FW. Generally, $MgCl_2$ as DS could generate greater driving osmotic force and higher permeate flux thus making it a seemly prior choice for specific FO application. However, based on our previous work (section 4.3.2), the salt Mg^{2+} can reversely diffuse from the DS side to the FW side through the FO membrane. In the presence of Mg^{2+} in FW, these divalence ions may interact with carboxylic functional group of the algal EPS and mucilage molecules, consistently with the microscopic observation as can be seen in Figure 5-4 (b).

5.3.2.3 Effect of membrane orientation

The clean membrane microscopic images for the two orientation were stated in Figure 5-2. Unfortunately, identifiability of the pictures for the AL-FW was far worse than the AL-DS picture. Even though there were no algal cells presented, the micropores adjacent to the support/active layer interface were faintly visible, captured as small black bubbles throughout the whole membrane surface. With the difficulties of the microscopic observation posted by the fine structure of membrane, in the real algae fouling test in AL-FW orientation, it was almost impossible to quantify the smaller dark-green algal cells deposited

on the surface. Luckily, the general difference between the degrees of algae fouling in the two orientations can be observed.

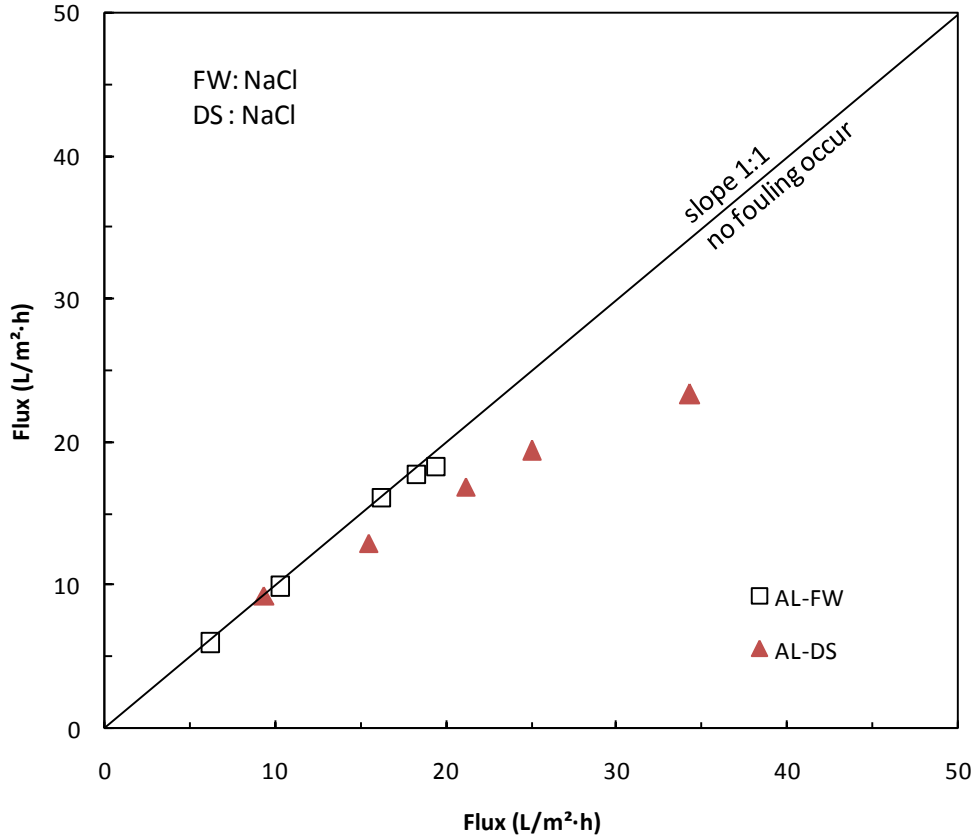

Figure 5-5 The effect of membrane orientation on flux deviation extent of the fouling test final flux from its corresponding baseline test data.

Figure 5-5 shows the FO flux behavior in both of the two orientations. As for AL-FW, the fouling flux didn't start to deviate from the baseline data until the flux level increased to 20 L/m² ·h, compared to the alternative orientation that fouling occurred when the flux was only around 15 L/m² ·h. The lower fouling potential for AL-FW orientation had been observed in the study of humic acid fouling by Tang et.al (Tang et al., 2010), and latex particles deposition on

FO membrane by Wang and coworkers (Wang et al., 2010b). The reasons of the phenomenon were summarized here as 1)smoother dense rejection layer facing FW meaning no foulant entrance into the support layer; 2)ICP self-compensation effect due to the severe ICP in this configuration. The microscopic images of the fouling test for different orientations with the same initial flux as showed in Figure 5-6(a) and 5-5 (c), represented that much fewer particles deposition for the AL-FW orientation, once again convincingly demonstrating the better sustainability in this configuration.

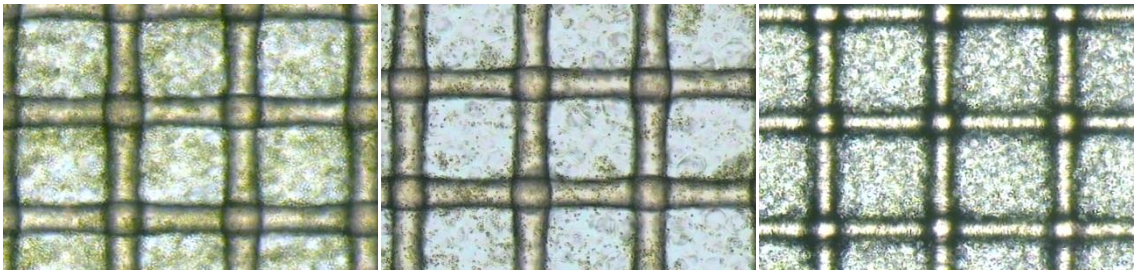

(a) AL-DS w/o spacer **(b) AL-DS wt spacer** **(c) AL-FW w/o spacer**

Figure 5-6 The microscopic observation results of the two orientation in presence or absence of spacer.

5.3.2.4 Effect of spacer and cross-flow velocity

The effect of spacer was evaluated by repeating the AL-DS pure algae fouling experiment and placing the spacer in both of the DS and FW channels in this test. The microscopic images of with or without spacer tests at the end of 2 M DS concentration step are showed in Figure 5-6 (a) and (b). Figure 5-7(a) shows the surface coverage for Stage II and Stage III tests as a function of DS

concentration. It is clear that the FO membrane was fouled more slowly with the placement of spacer on FW side. Since less particles deposited onto the clean membrane, the surface coverage rate was far less compared to that of experiment without FW side spacer. The effect of spacer on a pressure driven filtration gained numerous efforts (Gray et al., 2006; Schwinge et al., 2004). It is concluded that the plastic spacer supports the membrane, and also serves to increase turbulence and reduce external concentration polarization (ECP) which are all beneficial to the mass transfer through the membrane. Since ECP is also governed by the parallel shear force induced by cross-flow, it might be interesting to investigate the coupled effect of spacer and cross-flow velocity (CFV). The initial fluxes of the pure algae fouling tests with or without spacer on FW side with different cfv are summarized in Figure 5-7(b).

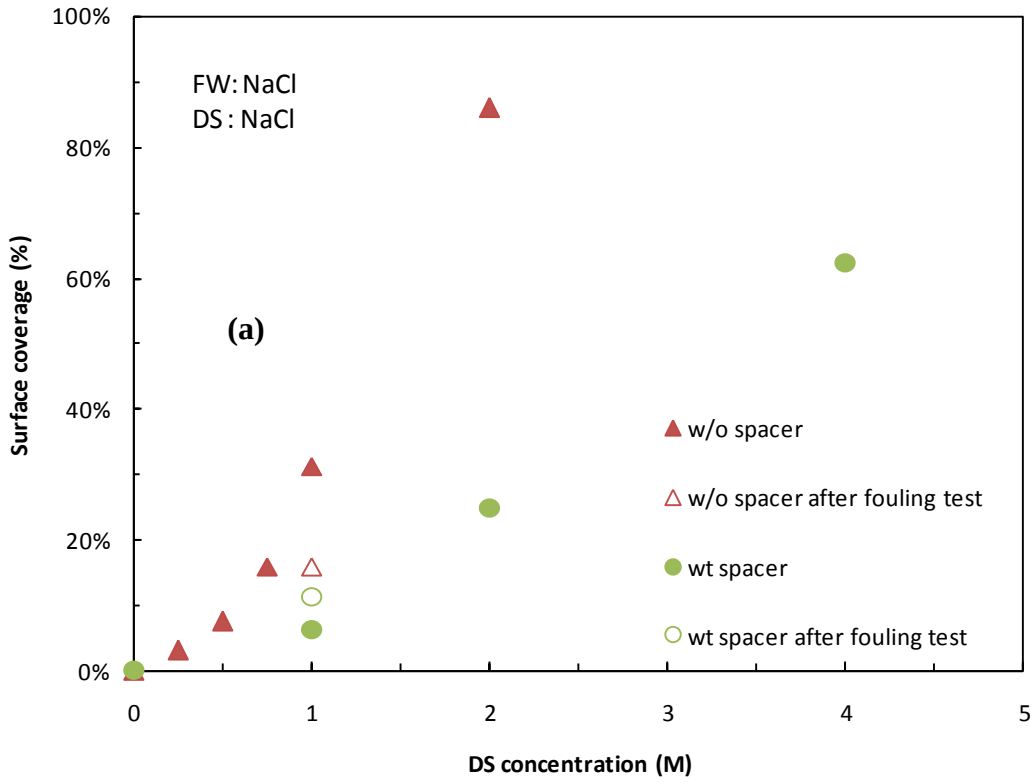

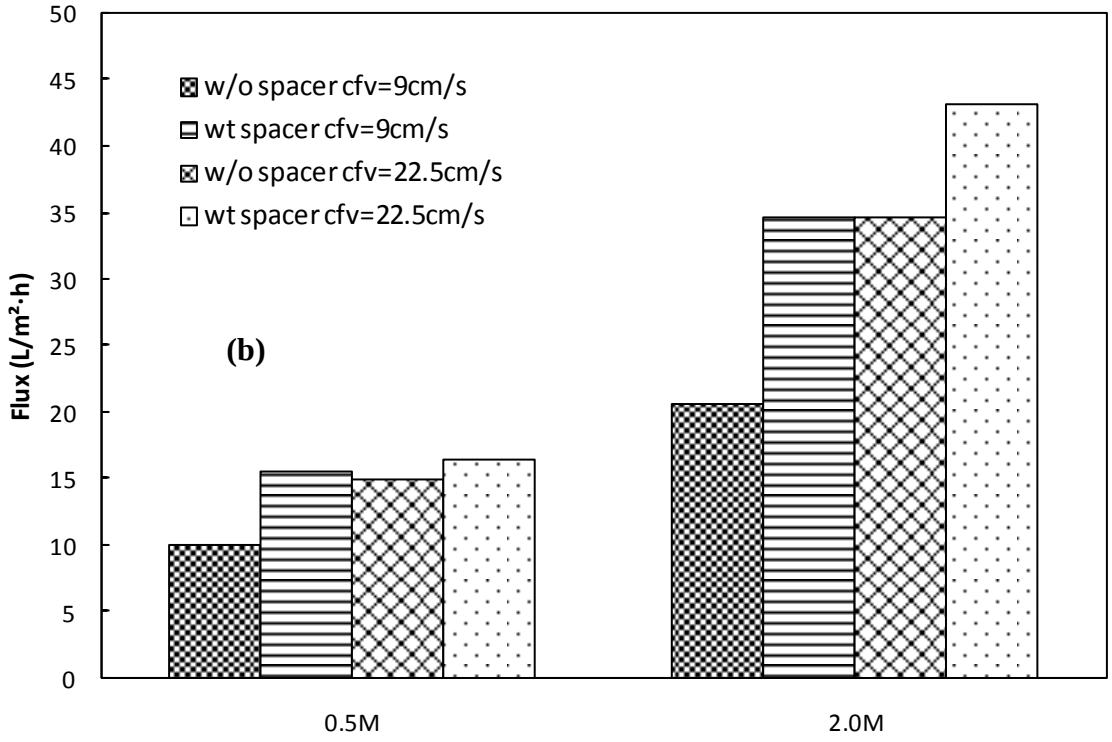

Figure 5-7 Effect of spacer and cross-flow velocity on algae filtration performance. (a) Surface coverage rate during Stage II under different DS concentration with or without spacer presented in FW channel. (b) Bar chart of Stage I initial flux level at two sets of DS concentration and crossflow velocity.

With spacer, the initial flux was improved by 55% from around 10 L/m² ·h up to 15.5 L/m² ·h at 0.5M DS with a cfv of 9 cm/s. However, when the cfv value increased to 22.5 cm/s under the same DS condition, although without spacer, the flux still get almost identical to that previous spacer improved value. In addition, the initial flux improvement by spacer was negligible at this higher cfv condition, suggesting a vanished spacer effect. Interestingly, as for a higher DS concentration, when increasing the cfv, the existence of spacer still plays an important role to influence the initial flux. This indicates the different degrees of spacer/cfv effects on the membrane fouling. With a weaker ECP effect level, the ECP decrease by cross-flow shear force prevail the decrease by spacer turbulence. But with a stronger ECP resulted by higher DS concentration,

convective flow is enhanced and thus the turbulence provided by spacer shall be stronger. Since the higher cfv is achieved at the expense of more energy consumption, the coupled effect by the spacer and cfv shall be optimized for a more energy saving FO operation.

5.4 Conclusions

In this study, the direct microscopic observation technique demonstrated good potential for further understanding FO fouling and the membrane structure. The existence of critical flux phenomenon was proved in FO process again. DOTM method is likely to be more precise on the particles deposition or cake layer formation investigation. In this study, it was obvious that particle deposition type of fouling was prior to the organic fouling based on the integrated analysis of images and flux data. With a low DS concentration, the algal cells deposition was relative randomly located and quite uniformly distributed on the membrane surface. As the concentration stepping forward, the particles seemed more likely to be stopped around the embedded mesh fibre and inside of the macropore “bubbles”. The greater FO fouling induced by the Mg^{2+} ions present in FW or DS was verified by the surface coverage analysis as direct evidence.

Chapter 6 Conclusions and Recommendations

6.1 Conclusions

6.1.1 Characterization of flux performance in MF-MBR system

Short-term experiments showed that the determination of critical flux using pressure cycling method could be considered as a more accurate measurement to determine the strong form and the weak form critical flux in that it could provide more information about the reversibility of the membrane fouling. When using a concentrated mixed liquor during MF process and the stepping time interval was set constant as 10 min, the critical flux value derived by the pressure stepping method was 17.2 $L/m^2.h$, a little higher than the value determined by cycling method which is 16.22 $L/m^2.h$.

With the regard of timescale, a proper time interval for the critical flux determination should be chosen to avoid any ignorance of irreversible fouling since some macro-fouling could only be observed to a certain extent of accumulation. Generally, a longer time interval would result in a lower critical flux result. When using a diluted mixed liquor for pressure stepping method, the critical flux with a 30 min stepping interval was 6.28 $L/m^2.h$, while the result was increased to 7.4 $L/m^2.h$ when setting the interval as 10 min.

The initial flux reduction at the start-up phase of the filtration test was characterized based on simple modelling analysis. The reasons of the flux loss relied on an extremely rapid membrane fouling resulted from the finest membrane pores blockage.

In the sub-critical flux operation which is defined as sustainable flux operation, the membrane fouling was very limited, while in the sub-critical flux operation during which the initial flux was beyond the critical flux, a greater initial flux tended to lead to a faster flux reduction but finally giving a pseudo stable flux-limiting flux (around 4 $L/m^2.h$) for two types of MF membranes with different pore size (0.1 and 0.2 μm). Limiting flux is independent on membrane pore size or initial flux level, but dependent on the mixed liquor composition that a higher mixed liquor suspended solids (MLSS) could decrease the limiting flux value. For conventional activated sludge with a MLSS value of around 2,200 mg/L, the limiting flux was observed as around 7 $L/m^2.h$, however, for MBR sludge which is more concentrated in MLSS (around 3805 mg/L), the limiting flux was decreased to around 4 $L/m^2.h$.

6.1.2 FO fouling and flux performance for algae harvesting

For the FO process for microalgae harvesting, the concept of critical flux was applied successfully as for the pressure-driven membrane, in that there is a critical flux level that below which the membrane fouling is neglectable. More rapid FO fouling was observed at higher flux levels above the critical flux.

Under the active layer (AL)-facing-feedwater (FW) orientation, it had relatively stable water flux, but it had much lower initial flux compared to that for the AL-facing-draw solution (DS) orientation.

FO fouling by microalgae was more severe at greater $[Mg^{2+}]$ in the feed water. While in the absence of foulant, $MgCl_2$ as a draw solution had higher water flux and lower solute flux compared to NaCl as draw solution. However, the use of $MgCl_2$ as a draw solution caused severe fouling as a result of the reverse

diffusion of Mg^{2+} from the draw solution into the feed water when microalgae was present in the feed water. In this study, Mg^{2+} would likely interact with the microalgae cells and their extracellular polysaccharides (EPSs), resulting in charge neutralization of and cation bridging between cells and EPS matrices

6.1.3 FO fouling for algae filtration observation by direct microscopic observation

Direct microscopic observation technique was applied to directly observe the algae particles deposition and accumulation on a micro-scale. Images were analyzed and characterized as an immediate evidence of the algae fouling along with the integration of flux reduction data for baseline tests, fouling tests and fouling reversibility tests. For the coupled membrane fouling mechanism, the different fouling starting points determined by microscopic observation and flux data respectively were used to analyze the different fouling occurring condition and growing speed of the two fouling types. In this test, it was obvious that particle deposition type of fouling was prior to the organic fouling. With a low DS concentration, the algal cells deposition was relative randomly located and quite uniformly distributed on the membrane surface. As the concentration stepping forward, the particles seemed more likely to be stopped around the embedded mesh fibre and inside of the macropore “bubbles”. The greater FO fouling induced by the Mg^{2+} ions present in FW or DS was verified by the surface coverage analysis as direct evidence.

6.2 Recommendations

6.2.1 Further Critical flux characterization for FO filtration by short-term experiments

As it is obvious that the stability of solution is hardly controllable in filtration plants and is highly dependent on the preparation of the fluid, the development of material and of a systematic method to measure critical flux appears essential. Those procedures should be able ones in an industrial operation to choose the operating parameters in order to better control the fouling of membranes. As the critical flux concept can be applied in FO membrane, a further characterization work is needed. A new determination strategy for FO critical flux is recommended to be established. The possible determination methods include DS concentration stepping and cycling. The physical factors controlling the results of critical flux determination measurement, such as concentration stepping interval and the timescale, and the mechanisms behind could be studied profoundly. The research on the impact of critical flux in the long-term sub-critical flux filtration operation and the mechanisms leading to different fouling behaviours during the operation is meaningful and urgent work. The impact of chemical factors such as FW and DS composition would also help pursuing the fouling mechanisms.

The present study showed the existence of limiting flux in MF-MBR system and its basic properties which is a further reference for the possible conceptual model demonstration for both of pressure-driven membrane and concentration-driven FO membrane.

6.2.2 Membrane fouling under sustainable flux (sub-critical) operation in long-term FO experiments

It has become evident through a number of studies that even at very low fluxes some fouling occurs in pressure-driven membrane processes, such that the original definition of critical flux where there is a flux below which no fouling (or permeability decline) occur does not apply in practice. A more suitable indicator and definition would be "transitional flux," thus representing the change from relatively low and stable fouling to higher fouling rate at the onset of significant fouling. This value is often used as a guide to establish an operating flux for a given system. The future study could investigate further the changes in low-flux (sustainable flux) fouling during long-term operation.

In summary, this study sheds lights into the development of a novel notion of sustainable flux. However, there are many unclear and uncertain corners in the fouling mechanisms and practical performance of the membrane technology.

Appendix

Section A

The experiment protocol was described previously in Section 3.3.3.

For mixed liquor test, $J_m = \frac{\Delta P - \Delta \pi}{\mu_w (R_m + R_f)}$ 3.1

where J_m is the mixed liquor flux, ΔP is the pressure difference between the mixed liquor side and the permeate side, $\Delta \pi$ is an osmotic pressure term reducing efficiency of the transmembrane pressure which is caused by the concentration gradients across the membrane, μ_m is the solution viscosity of mixed liquor, R_m is the resistance caused by the membrane material, and R_f is the fouling resistance caused by membrane fouling during filtration;

based on the film theory, we can modify the Eq3.1 to:

$$J_m = \frac{\Delta P - \pi_{F,b} \cdot \exp(\frac{J_m}{k})}{\mu_m (R_m + R_f)} \quad 3.2$$

where $\pi_{F,b}$ is the osmotic pressure of the bulk feed solution, k is the mass transfer coefficient.

for secondary water test in this study, $J_w = \frac{\Delta P}{\mu_w (R_m + R_f)}$ 3.3

where J_w is the secondary water flux value, μ_w is pure water viscosity, R_f represent the fouling resistance caused by earlier mixed liquor test.

Thus the ratio of mixed liquor flux and fake water flux with the same ΔP is:

$$J_m / J_w = \frac{\mu_w}{\mu_m}\left(1-\frac{\Delta\pi}{\Delta P}\right) = \frac{\mu_w}{\mu_m}\left(1-\frac{\pi_{F,b}\cdot\exp\left(\frac{J_m}{k}\right)}{\Delta P}\right) \qquad 3.4$$

when there is no concentration polarization, $\Delta\pi = 0$, $J_m / J_w = \frac{\mu_w}{\mu_m}$, then the ratio should be constant; when the concentration polarization exists, since J_m is proportional to the value of ΔP, and the term $\pi_{F,b}\cdot\exp\left(\frac{J_m}{k}\right)$ grows exponentially as a function of J_m, so $\pi_{F,b}\cdot\exp\left(\frac{J_m}{k}\right)$ also grows exponentially as a function of ΔP. As a result, theoretically the value of J_m / J_w decreases with increasing ΔP.

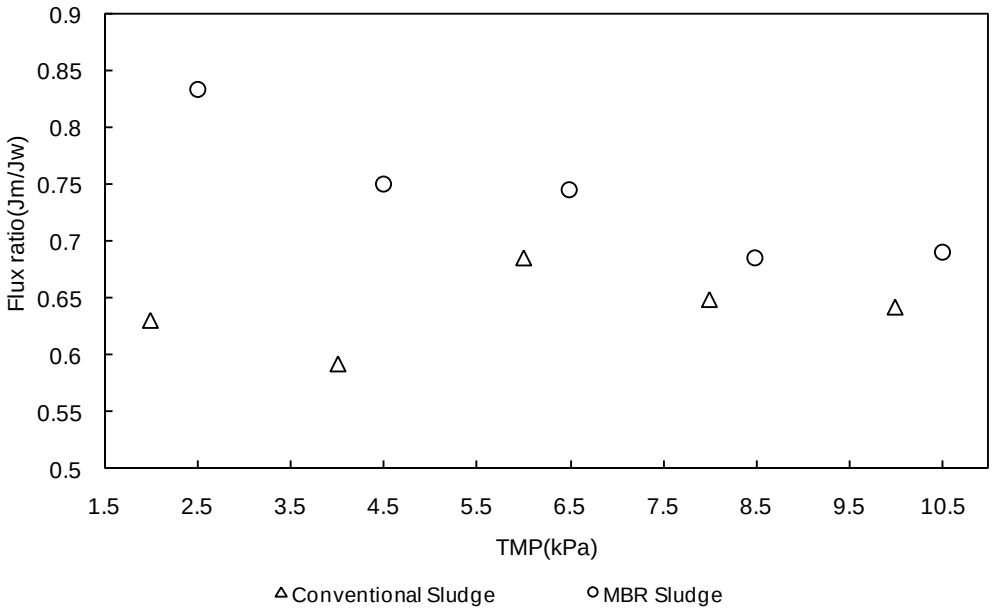

Figure A 2 The ratio of mixed liquor flux and fake water flux with the same ΔP for activated sludge and MBR sludge.

As shown in Figure A 1, the ratios were not constant for conventional sludge and MBR sludge either, which means in current study, except for rapid membrane fouling, concentration polarization might be partially responsible for the initial flux decline compared with pure water flux. It is also moteworthy that for MBR sludge, the relationship of J_m / J_w and ΔP doesn't follow our previous mathematical prediction - the curve has a sudden rise when TMP = 6kPa. The experimental system limitation and the digital pressure sensor reading error should be considered.

References

Achilli, A., Cath, T.Y., Marchand, E.A., Childress, A.E., 2009. The forward osmosis membrane bioreactor: A low fouling alternative to MBR processes. Desalination 238, 10-21.

Aimar, P., Sanchez, V., 1986. A novel approach to transfer limiting phenomena during ultrafiltration of macromolecules. Industrial and Engineering Chemistry Fundamentals 25, 789-798.

Allen, M.M., Stanier, R.Y., 1968. Growth and division of some unicellular blue-green algae. Journal of General Microbiology 51, 199-202.

Amin, S., 2009. Review on biofuel oil and gas production processes from microalgae. Energy Conversion and Management 50, 1834-1840.

Arabi, S., Nakhla, G., 2009. Impact of magnesium on membrane fouling in membrane bioreactors. Separation and Purification Technology 67, 319-325.

Arora, N., Davis, R.H., 1994. Yeast cake layers as secondary membranes in dead-end microfiltration of bovine serum albumin. Journal of Membrane Science 92, 247-256.

Bacchin, P., 1994. Formation et résistance au transfert d'un dépôt de colloïdes sur une membrane d'ultrafiltration, University Paul Sabatier.

Bacchin, P., Aimar, P., Field, R.W., 2006. Critical and sustainable fluxes: Theory, experiments and applications. Journal of Membrane Science 281, 42-69.

Bacchin, P., Aimar, P., Sanchez, V., 1995. Model for colloidal fouling of membranes. AIChE Journal 41, 368-376.

Bacchin, P., Aimar, P., Sanchez, V., 1996. Influence of surface interaction on transfer during colloid ultrafiltration. Journal of Membrane Science 115, 49-63.

Bacchin, P., Meireles, M., Aimar, P., 2002. Modelling of filtration: From the polarised layer to deposit formation and compaction. Desalination 145, 139-146.

Belfort, G., Davis, R.H., Zydney, A.L., 1994. The behavior of suspensions and macromolecular solutions in crossflow microfiltration. Journal of Membrane Science 96, 1-58.

Bessiere, Y., Abidine, N., Bacchin, P., 2005. Low fouling conditions in dead-end filtration: Evidence for a critical filtered volume and interpretation using critical osmotic pressure. Journal of Membrane Science 264, 37-47.

Bin, C., Xiaochang, W., Enrang, W., 2004. Effects of TMP, MLSS concentration and intermittent membrane permeation on a hybrid submerged MBR fouling. Proceedings of the Water Environment-Membrane Technology Conference.

Bordel, S., Guieysse, B., Munoz, R., 2009. Mechanistic model for the reclamation of industrial wastewaters using algal-bacterial photobioreactors. Environmental Science and Technology 43, 3200-3207.

Bouhabila, E.H., Ben A ïm, R., Buisson, H., 2001. Fouling characterisation in membrane bioreactors. Separation and Purification Technology 22-23, 123-132.

Bowen, W.R., Calvo, J.I., Hernandez, A., 1995. Steps of membrane blocking in flux decline during protein microfiltration. Journal of Membrane Science 101, 153-153.

Brites, A.M., Depinho, M.N., 1993. New approach to the evaluation of the effects of protein adsorption onto a polysulfone membrane. Journal of Membrane Science 78, 265.

Brune, D.E., Lundquist, T.J., Benemann, J.R., 2009. Microalgal biomass for

greenhouse gas reductions: Potential for replacement of fossil fuels and animal feeds. Journal of Environmental Engineering 135, 1136-1144.

C. Y. Tang, Q. She, W.C.L. Lay, R. Wang, Fane, A.G., 2010. Coupled effects of internal concentration polarization and fouling on flux behavior of forward osmosis membranes during humic acid filtration. Journal of Membrane Science 354, 123-133.

Cath, T.Y., Childress, A.E., Elimelech, M., 2006. Forward osmosis: Principles, applications, and recent developments. Journal of Membrane Science 281, 70-87.

Causserand, C., Jover, K., Aimar, P., Meireles, M., 1997. Modification of clay cake permeability by adsorption of protein. Journal of Membrane Science 137, 31-44.

Causserand, C., Kara, Y., Aimar, P., 2001. Protein fractionation using selective adsorption on clay surface before filtration. Journal of Membrane Science 186, 165-181.

Chang, I.-S., Clech, P.L., Jefferson, B., Judd, S., 2002. Membrane fouling in membrane bioreactors for wastewater treatment. Journal of Environmental Engineering 128, 1018-1029.

Chang, I.-S., Kim, S.-N., 2005. Wastewater treatment using membrane filtration - Effect of biosolids concentration on cake resistance. Process Biochemistry 40, 1307-1314.

Chang, I.S., Bag, S.O., Lee, C.H., 2001. Effects of membrane fouling on solute rejection during membrane filtration of activated sludge. Process Biochemistry 36, 855-860.

Chang, I.S., Lee, C.H., 1998. Membrane filtration characteristics in membrane-coupled activated sludge system - The effect of physiological states of activated sludge on membrane fouling. Desalination 120, 221-233.

Chen, V., Fane, A.G., Madaeni, S., Wenten, I.G., 1997. Particle deposition

during membrane filtration of colloids: Transition between concentration polarization and cake formation. Journal of Membrane Science 125, 109-122.

Chong, T.H., Wong, F.S., Fane, A.G., 2007. Fouling in reverse osmosis: Detection by non-invasive techniques. Desalination 204, 148-154.

Chudacek, M.W., Fane, A.G., 1984. The dynamics of polarisation in unstirred and stirred ultrafiltration. Journal of Membrane Science 21, 145-160.

Clarens, A.F., Resurreccion, E.P., White, M.A., Colosi, L.M., 2010. Environmental life cycle comparison of algae to other bioenergy feedstocks. Environmental Science and Technology 44, 1813-1819.

Clark, W.M., Bansal, A., Sontakke, M., Ma, Y.H., 1991. PROTEIN ADSORPTION AND FOULING IN CERAMIC ULTRAFILTRATION MEMBRANES. Journal of Membrane Science 55, 21.

Cornelissen, E.R., Harmsen, D., de Korte, K.F., Ruiken, C.J., Qin, J.J., Oo, H., Wessels, L.P., 2008. Membrane fouling and process performance of forward osmosis membranes on activated sludge. Journal of Membrane Science 319, 158-168.

Cui, Z.F., Chang, S., Fane, A.G., 2003. The use of gas bubbling to enhance membrane processes. Journal of Membrane Science 221, 1-35.

de-Bashan, L.E., Trejo, A., Huss, V.A.R., Hernandez, J.-P., Bashan, Y., 2008a. Chlorella sorokiniana UTEX 2805, a heat and intense, sunlight-tolerant microalga with potential for removing ammonium from wastewater. Bioresource Technology 99, 4980-4989.

de-Bashan, L.E., Trejo, A., Huss, V.A.R., Hernandez, J.P., Bashan, Y., 2008b. Chlorella sorokiniana UTEX 2805, a heat and intense, sunlight-tolerant microalga with potential for removing ammonium from wastewater. Bioresource Technology 99, 4980-4989.

Defrance, L., Jaffrin, M.Y., Gupta, B., Paullier, P., Geaugey, V., 2000. Contribution of various constituents of activated sludge to membrane

bioreactor fouling. Bioresource Technology 73, 105-112.

Detlef R. U.Knappe, R.C.B., 2004. Algae detection and removal strategies for drinking water treatment plants. AWWA Research Foundation,Water Resources Research Institute.

Elimelech, M., Zhu, X., Childress, A.E., Hong, S., 1997. Role of membrane surface morphology in colloidal fouling of cellulose acetate and composite aromatic polyamide reverse osmosis membranes. Journal of Membrane Science 127, 101-109.

Enegess, D., Togna, A.P., Sutton, P.M., 2003. Membrane separation applications to biosystems for wastewater treatment. Filtration and Separation 40, 14-17.

Espinasse, B., Bacchin, P., Aimar, P., 2002. On an experimental method to measure critical flux in ultrafiltration. Desalination 146, 91-96.

Fane, A.G., Fell, C.J.D., Waters, A.G., 1983. Ultrafiltration of protein solutions through partially permeable membranes - the effect of adsorption and solution environment. Journal of Membrane Science 16, 211-224.

Fane, A.G., Fell, C. J. D., and Nor, M. T., 1981. Ultrafiltration/Activated sludge system—development of a predictive model. Polymer Science Technology 13, 631-658.

Fane, A.G., Tang, C.Y., Wang, R., 2011. Membrane Technology for Water: Microfiltration, Ultrafiltration, Nanofiltration, and Reverse Osmosis, in: Wilderer, P. (Ed.), Treatise on Water Science. Academic Press, Oxford, pp. 301-335.

Fane, A.G., Wei, X., Wang, R., 2006. Membrane Filtration Processes and Fouling, in: Newcombe, G., Dixon, D. (Eds.), Interface Science in Drinking Water Treatment: Fundamentals and Applications. Academic Press.

Field, R.W., Wu, D., Howell, J.A., Gupta, B.B., 1995. Critical flux concept for microfiltration fouling. Journal of Membrane Science 100, 259-272.

Freger, V., 2005. Diffusion impedance and equivalent circuit of a multilayer film. Electrochemistry Communications 7, 957.

Güell, C., Czekaj, P., Davis, R.H., 1999. Microfiltration of protein mixtures and the effects of yeast on membrane fouling. Journal of Membrane Science 155, 113-122.

Gésan-Guiziou, G., Daufin, G., Boyaval, E., 2000. Critical stability conditions in skimmed milk crossflow microfiltration: Impact on operating modes. Lait 80, 129-138.

Gésan-Guiziou, G., Wakeman, R.J., Daufin, G., 2002. Stability of latex crossflow filtration: Cake properties and critical conditions of deposition. Chemical Engineering Journal 85, 27-34.

Gao, D.W., Zhang, T., Tang, C.Y., Wu, W.M., Wong, C.Y., Lee, Y.H., Yeh, D.H., Criddle, C.S., 2010. Membrane fouling in an anaerobic membrane bioreactor: Differences in relative abundance of bacterial species in the membrane foulant layer and in suspension. Journal of Membrane Science 364, 331-338.

Goosen, M.F.A., Sablani, S.S., Ai-Hinai, H., Ai-Obeidani, S., Al-Belushi, R., Jackson, D., 2004. Fouling of reverse osmosis and ultrafiltration membranes: A critical review. Separation Science and Technology 39, 2261.

Gray, G.T., McCutcheon, J.R., Elimelech, M., 2006. Internal concentration polarization in forward osmosis: role of membrane orientation. Desalination 197, 1-8.

Harmant, P., Aimar, P., 1998. Coagulation of colloids in a boundary layer during cross-flow filtration. Colloids and Surfaces A: Physicochemical and Engineering Aspects 138, 217-230.

Henderson, R., Chips, M., Cornwell, N., Hitchins, P., Holden, B., Hurley, S., Parsons, S.A., Wetherill, A., Jefferson, B., 2008. Experiences of algae in UK waters: A treatment perspective. Water and Environment Journal 22, 184-192.

Jermann, D., Pronk, W., Meylan, S., Boller, M., 2007. Interplay of different

NOM fouling mechanisms during ultrafiltration for drinking water production. Water Research 41, 1713-1722.

Judd, S., 2006. The MBR Book: Principles and Applications of Membrane Bioreactors in Water and Wastewater Treatment. The MBR Book: Principles and Applications of Membrane Bioreactors in Water and Wastewater Treatment.

Judd, S.J., 2004. A review of fouling of membrane bioreactors in sewage treatment. Water Science and Technology 49, 229-235.

Kang, S.T., Subramani, A., Hoek, E.M.V., Deshusses, M.A., Matsumoto, M.R., 2004. Direct observation of biofouling in cross-flow microfiltration: Mechanisms of deposition and release. Journal of Membrane Science 244, 151-165.

Karner, D.A., Standridge, J.H., Harrington, G.W., Barnum, R.P., 2001. Microcystin algal toxins in source and finished drinking water. Journal / American Water Works Association 93, 72-81+16.

Kuberkar, V.T., Davis, R.H., 1999. Effects of added yeast on protein transmission and flux in cross-flow membrane microfiltration. Biotechnology Progress 15, 472-479.

Kuiper, S., Van Rijn, C.J.M., Nijdam, W., Krijnen, G.J.M., Elwenspoek, M.C., 2000. Determination of particle-release conditions in microfiltration: A simple single-particle model tested on a model membrane. Journal of Membrane Science 180, 15-28.

Kwon, B., Park, N., Cho, J., 2005. Effect of algae on fouling and efficiency of UF membranes. Desalination 179, 203-214.

Kwon, D.Y., Vigneswaran, S., Fane, A.G., Aim, R.B., 2000. Experimental determination of critical flux in cross-flow microfiltration. Separation and Purification Technology 19, 169-181.

Lay, W.C.L., Chong, T.H., Tang, C.Y., Fane, A.G., Zhang, J., Liu, Y., 2010.

Fouling propensity of forward osmosis: Investigation of the slower flux decline phenomenon. Water Science and Technology 61, 927-936.

Le-Clech, P., Chen, V., Fane, T.A.G., 2006. Fouling in membrane bioreactors used in wastewater treatment. Journal of Membrane Science 284, 17-53.

Lee, K.L., Baker, R.W., Lonsdale, H.K., 1981. Membranes for power generation by pressure-retarded osmosis. Journal of Membrane Science 8, 141-171.

Lee, W., Kang, S., Shin, H., 2003. Sludge characteristics and their contribution to microfiltration in submerged membrane bioreactors. Journal of Membrane Science 216, 217-227.

Leiknes, T., Odegaard, H., Myklebust, H., 2004. Removal of natural organic matter (NOM) in drinking water treatment by coagulation-microfiltration using metal membranes. Journal of Membrane Science 242, 47-55.

Li, H., Fane, A.G., Coster, H.G.L., Vigneswaran, S., 1998. Direct observation of particle deposition on the membrane surface during crossflow microfiltration. Journal of Membrane Science 149, 83-97.

Li, H., Fane, A.G., Coster, H.G.L., Vigneswaran, S., 2000. An assessment of depolarisation models of crossflow microfiltration by direct observation through the membrane. Journal of Membrane Science 172, 135-147.

Li, Q.L., Elimelech, M., 2004. Organic fouling and chemical cleaning of nanofiltration membranes: Measurements and mechanisms. Environmental Science & Technology 38, 4683.

Loeb, S., 2002. Large-scale power production by pressure-retarded osmosis, using river water and sea water passing through spiral modules. Desalination 143, 115-122.

Mänttäri, M., Nyström, M., 2000. Critical flux in NF of high molar mass polysaccharides and effluents from the paper industry. Journal of Membrane Science 170, 257-273.

Madaeni, S.S., Fane, A.G., Wiley, D.E., 1999. Factors influencing critical flux in membrane filtration of activated sludge. Journal of Chemical Technology and Biotechnology 74, 539-543.

Marlaire, R.D., 2009a. NASA Envisions "Clean Energy" From Algae Grown in Waste Water.

Marlaire, R.D., 2009b. NASA Envisions "Clean Energy" From Algae Grown in Waste Water.

Mata, T.M., Martins, A.A., Caetano, N.S., 2010. Microalgae for biodiesel production and other applications: A review. Renewable and Sustainable Energy Reviews 14, 217-232.

McCutcheon, J.R., Elimelech, M., 2006. Influence of concentrative and dilutive internal concentration polarization on flux behavior in forward osmosis. Journal of Membrane Science 284, 237-247.

McCutcheon, J.R., McGinnis, R.L., Elimelech, M., 2006. Desalination by ammonia-carbon dioxide forward osmosis: Influence of draw and feed solution concentrations on process performance. Journal of Membrane Science 278, 114-123.

McDonogh, R.M., Gruber, T., Stroh, N., Bauser, H., Walitza, E., Chmiel, H., Strathmann, H., 1992. Criteria for fouling layer disengagement during filtration of feeds containing a wide range of solutes. Journal of Membrane Science 73, 181-189.

Mi, B., Elimelech, M., 2008. Chemical and physical aspects of organic fouling of forward osmosis membranes. Journal of Membrane Science 320, 292-302.

Mi, B., Elimelech, M., 2010. Organic fouling of forward osmosis membranes: Fouling reversibility and cleaning without chemical reagents. Journal of Membrane Science 348, 337-345.

Molina Grima, E., Belarbi, E.H., Acien Fernandez, F.G., Robles Medina, A., Chisti, Y., 2003. Recovery of microalgal biomass and metabolites: Process

options and economics. Biotechnology Advances 20, 491-515.

Muñoz, R., Guieysse, B., 2006. Algal-bacterial processes for the treatment of hazardous contaminants: A review. Water Research 40, 2799-2815.

Mulder, M., 1991. Basic principles of membrane technology.

Mulder, M., 1996. Basic principles of membrane technology. Kluwer Academic Publishers.

Ognier, S., Wisniewski, C., Grasmick, A., 2002. Characterisation and modelling of fouling in membrane bioreactors. Desalination 146, 141-147.

Packer, M., 2009. Algal capture of carbon dioxide; biomass generation as a tool for greenhouse gas mitigation with reference to New Zealand energy strategy and policy. Energy Policy 37, 3428-3437.

Panpanit, S., Visvanathan, C., 2001. The role of bentonite addition in UF flux enhancement mechanisms for oil/water emulsion. Journal of Membrane Science 184, 59-68.

Park, H., Choo, K.H., Lee, C.H., 1999. Flux enhancement with powdered activated carbon addition in the membrane anaerobic bioreactor. Separation Science and Technology 34, 2781-2792.

Persson, A., Jönsson, A.S., Zacchi, G., 2001. Separation of lactic acid-producing bacteria from fermentation broth using a ceramic microfiltration membrane with constant permeate flow. Biotechnology and Bioengineering 72, 269-277.

Petrotos, K.B., Quantick, P., Petropakis, H., 1998. A study of the direct osmotic concentration of tomato juice in tubular membrane - Module configuration. I. The effect of certain basic process parameters on the process performance. Journal of Membrane Science 150, 99-110.

Petsev, D.N., Starov, V.M., Ivanov, I.B., 1993. Concentrated dispersions of

charged colloidal particles: Sedimentation, ultrafiltration and diffusion. Colloids and Surfaces A: Physicochemical and Engineering Aspects 81, 65-81.

Pillay, V.L., Buckley, C.A., 1992. Cake formation in cross-flow microfiltration systems. Water Science and Technology 25, 149-162.

Rosenberger, S., Evenblij, H., Te Poele, S., Wintgens, T., Laabs, C., 2005. The importance of liquid phase analyses to understand fouling in membrane assisted activated sludge processes - Six case studies of different European research groups. Journal of Membrane Science 263, 113-126.

Rosenhahn, A., Finlay, J.A., Pettit, M.E., Ward, A., Wirges, W., Gerhard, R., Callow, M.E., Grunze, M., Callow, J.A., 2009. Zeta potential of motile spores of the green alga Ulva linza and the influence of electrostatic interactions on spore settlement and adhesion strength. Biointerphases 4, 7-11.

Schwinge, J., Neal, P.R., Wiley, D.E., Fletcher, D.F., Fane, A.G., 2004. Spiral wound modules and spacers: Review and analysis. Journal of Membrane Science 242, 129-153.

Shimizu, Y., Shimodera, K.I., Watanabe, A., 1993. Cross-flow microfiltration of bacterial cells. Journal of Fermentation and Bioengineering 76, 493-500.

Smith, C.W., Di Gregorio, D., Talcott, R.M., 1969. The use of ultrafiltration membrane for activated sludge separation. Proc. 24th Annual Purdue Industrial Waste Conference, 1300-1310.

Soderman, 2010. Offshore Membrane Enclosure for Growing Algae (OMEGA).

Stephenson, T., Judd, S., Jefferson, B., Brindle, K., 2000. Membrane Bioreactors for Wastewater Treatment. Membrane Bioreactors for Wastewater Treatment.

Tang, C.Y., Chong, T.H., Fane, A.G., 2011. Colloidal interactions and fouling of NF and RO membranes: A review. Advances in Colloid and Interface Science 164, 126-143.

Tang, C.Y., Kwon, Y.N., Leckie, J.O., 2009. The role of foulant-foulant electrostatic interaction on limiting flux for RO and NF membranes during humic acid fouling-Theoretical basis, experimental evidence, and AFM interaction force measurement. Journal of Membrane Science 326, 526-532.

Tang, C.Y., Leckie, J.O., 2007. Membrane independent limiting flux for RO and NF membranes fouled by humic acid. Environmental Science and Technology 41, 4767-4773.

Tang, C.Y., She, Q., Lay, W.C.L., Wang, R., Fane, A.G., 2010. Coupled effects of internal concentration polarization and fouling on flux behavior of forward osmosis membranes during humic acid filtration. Journal of Membrane Science 354, 123-133.

Timmer, J.M.K., Van Der Horst, H.C., Labbé, J.P., 1997. Cross-flow microfiltration of β-lactoglobulin solutions and the influence of silicates on the flow resistance. Journal of Membrane Science 136, 41-56.

Van Der Bruggen, B., Vandecasteele, C., Van Gestel, T., Doyen, W., Leysen, R., 2003. A review of pressure-driven membrane processes in wastewater treatment and drinking water production. Environmental Progress 22, 46-56.

van der Waal, M.J., Racz, I.G., 1989. Mass transfer in corrugated-plate membrane modules. I. Hyperfiltration experiments. Journal of Membrane Science 40, 243-260.

Van Reis, R., Gadam, S., Frautschy, L.N., Orlando, S., Goodrich, E.M., Saksena, S., Kuriyel, R., Simpson, C.M., Pearl, S., Zydney, A.L., 1997. High performance tangential flow filtration. Biotechnology and Bioengineering 56, 71-82.

Visvanathan, C., Ben Aim, R., 1989. Studies on colloidal membrane fouling mechanisms in crossflow microfiltration. Journal of Membrane Science 45, 3-15.

W. C. L. Lay, T. H. Chong, C. Y. Tang, A. G. Fane, Zhang, J., Liu, Y., 2010. Fouling propensity of Forward Osmosis: investigation of the slower flux

decline phenomenon. Water Science and Technology 61, 927-936.

Wang, R., Shi, L., Tang, C.Y., Chou, S., Qiu, C., Fane, A.G., 2010a. Characterization of novel forward osmosis hollow fiber membranes. Journal of Membrane Science 355, 158–167.

Wang, S., Guillen, G., Hoek, E.M.V., 2005. Direct observation of microbial adhesion to membranes. Environmental Science and Technology 39, 6461-6469.

Wang, Y., Wicaksana, F., Tang, C.Y., Fane, A.G., 2010b. Direct microscopic observation of forward osmosis membrane fouling. Environmental Science and Technology 44, 7102-7109.

WERF, 2006.

Wisniewski, C., Grasmick, A., 1998. Floc size distribution in a membrane bioreactor and consequences for membrane fouling. Colloids and Surfaces A: Physicochemical and Engineering Aspects 138, 403-411.

Wu, D., Howell, J.A., Field, R.W., 1999. Critical flux measurement for model colloids. Journal of Membrane Science 152, 89-98.

Xu, Y., Peng, X., Tang, C.Y., Fu, Q.S., Nie, S., 2010. Effect of draw solution concentration and operating conditions on forward osmosis and pressure retarded osmosis performance in a spiral wound module. Journal of Membrane Science 348, 298-309.

Yamamoto, K., Hiasa, M., Mahmood, T., Matsuo, T., 1989. Direct solid-liquid separation using hollow fiber membrane in an activated sludge aeration tank. Water Science and Technology 21, 43-54.

Yang, W., Cicek, N., Ilg, J., 2006. State-of-the-art of membrane bioreactors: Worldwide research and commercial applications in North America. Journal of Membrane Science 270, 201-211.

Ye, Y., Chen, V., 2005. Reversibility of heterogeneous deposits formed from yeast and proteins during microfiltration. Journal of Membrane Science 265, 20-28.

Youravong, W., Grandison, A.S., Lewis, M.J., 2002. Effect of hydrodynamic and physicochemical changes on critical flux of milk protein suspensions. Journal of Dairy Research 69, 443-455.

Zeman, L.J., Zydney, A.L., 1996. Microfiltration and Ultrafiltration: Principles and Applications.

Zhang, X., Hu, Q., Sommerfeld, M., Puruhito, E., Chen, Y., 2010a. Harvesting algal biomass for biofuels using ultrafiltration membranes. Bioresource Technology 101, 5297-5304.

Zhang, X., Hu, Q., Sommerfeld, M., Puruhito, E., Chen, Y., 2010b. Harvesting algal biomass for biofuels using ultrafiltration membranes. Bioresource Technology 101, 5297-5304.

Zhang, Y.P., Fane, A.G., Law, A.W.K., 2006. Critical flux and particle deposition of bidisperse suspensions during crossflow microfiltration. Journal of Membrane Science 282, 189-197.

Zhao, S., Zou, L., Tang, C.Y., Mulcahy, D., 2012. Recent developments in forward osmosis: Opportunities and challenges. Journal of Membrane Science 396, 1-21.

Zou, S., Gu, Y., Xiao, D., Tang, C.Y., 2011. The role of physical and chemical parameters on forward osmosis membrane fouling during algae separation. Journal of Membrane Science 366, 356-362.